Dissertation zur Erlangung des Doktorgrades
der Fakultät für Biologie
der Ludwig-Maximilians-Universität München

Genome-Wide Identification of Nucleosome Positioning Determinants
in *Schizosaccharomyces pombe*

Julia Pointner
München

18. Juli 2013

Eingereicht am 18. Juli 2013

Mündliche Prüfung am 12. November 2013

1. Gutachter: Prof. Dr. Peter B. Becker
2. Gutachter: Prof. Dr. Stefan Jentsch
3. Gutachter: Prof. Dr. Heinrich Leonhardt
4. Gutachter: Prof. Dr. Bettina Kempkes
5. Gutachter: Prof. Dr. Michael Boshart
6. Gutachter: Prof. Dr. Kirsten Jung

Ehrenwörtliche Versicherung

Ich versichere hiermit ehrenwörtlich, dass die vorgelegte Dissertation von mir selbständig und ohne unerlaubte Hilfe angefertigt wurde.

München, den ………………………….   ………………………………………

(Julia Pointner)

Erklärung

Hiermit erkläre ich, dass ich mich nicht anderweitig einer Doktorprüfung ohne Erfolg unterzogen habe.

München, den …………………………. ………………………………………

(Julia Pointner)

Wesentliche Teile dieser Arbeit sind in folgender Publikation veröffentlicht:

Pointner J., Persson J., Prasad P., Norman-Axelsson U., Stralfors A., Khorosjutina O., Krietenstein N., Svensson J.P., Ekwall K., Korber P. 2012. CHD1 remodelers regulate nucleosome spacing in vitro and align nucleosomal arrays over gene coding regions in *S. pombe*. *EMBO J.*, 31(23):4388-403

Acknowledgements

I would like to thank the following people:

First of all, Dr. Philipp Korber for giving me the opportunity to join his group and work on this project, for his advice and support, and for the pleasant atmosphere in his lab.

Prof. Dr. Peter Becker for his role as my official PhD supervisor and for providing a great, collegial and scientific stimulating atmosphere in the department.

Prof. Dr. Stefan Jentsch, Dr. Dietmar Martin and Dr. Tobias Straub for being members of my thesis advisory committee.

Dr. Dietmar Martin for giving me the opportunity to use the Affymetrix microarray facility, Kerstin Maier for facility booking and advice.

Prof. Dr. Karl Ekwall, Jenna Persson, Dr. Punit Prasad, Ulrika Norman-Axelsson and Dr. Peter Svensson for a great collaboration.

Prof. Dr. Jürg Bähler, Dr. Samuel Marguerat and Sophie Atkinson for a great collaboration.

Prof. Dr. Frank Pugh and Megha Wal for Illumina Sequencing.

Dr. Tobias Straub for his support on microarray data analysis.

Nils, Corinna, Sebastian and Dorle for being great lab mates.

The whole molecular biology department for a great atmosphere.

My family and friends

My special thanks goes to Michi

Content

Content I

Summary 1

Zusammenfassung 2

1 Introduction 4

1.1 General aspects of chromatin 4

1.1.1 Nucleosome structure 4

1.1.2 Higher order chromatin structure 5

1.2 Regulation of chromatin structure 6

1.2.1 Histone variants 7

1.2.2 Posttranslational modifications of histones and DNA methylation 8

1.2.3 Chromatin remodeler 9

1.3 Nucleosome positioning 11

1.3.1 How to map nucleosome positions 12

1.3.1.1 Mapping of nucleosome positions at single loci 12

1.3.1.2 Mapping of nucleosome positions genome-wide by microarrays or high throughput sequencing 13

1.3.1.3 Chemical mapping 13

1.3.2 Candidates for nucleosome positioning determinants 14

1.3.2.1 DNA sequence features 14

1.3.2.2 General regulatory factors 16

1.3.2.3 Chromatin remodeler 17

1.3.2.3.1 SWI/SNF family 17

1.3.2.3.2 ISWI family 18

1.3.2.3.3 CHD family 20

1.3.2.3.4 INO80 family 22

1.3.3 Histone variant H2A.Z 23

1.3.4 RNA Polymerase II and the transcriptional process 24

1.4 Objective ... 25

2 Material and Methods ... 26

2.1 Materials ... 26

2.1.1.1 Chemicals ... 26

2.1.1.2 Enzymes ... 27

2.1.1.3 Other ... 28

2.1.1.4 Media, buffers and solutions ... 28

2.1.1.4.1 Media for *E. coli* ... 28

2.1.1.4.2 Media for *S. pombe* ... 29

2.1.1.4.3 Buffers and solutions ... 30

2.1.1.5 Oligonucleotids and plasmids ... 34

2.1.1.5.1 Oligonucleotids ... 34

Oligonucleotids (Sigma) used for probe generation for indirect end labelling experiments: ... 34

2.1.1.5.2 Strains ... 34

2.2 Methods ... 35

2.2.1 General molecular biological methods ... 35

2.2.1.1 Generation of competent *E. coli* cells ... 35

2.2.1.2 Transformation of *E. coli* ... 36

2.2.1.3 Isolation of plasmids from *E. coli* ... 36

2.2.1.4 Polymerase Chain Reaction (PCR) ... 36

2.2.1.5 DNA purification by phenol/chloroform extraction ... 36

2.2.1.6 DNA precipitation ... 36

2.2.1.7 DNA quantification ... 37

2.2.1.8 Horizontal and vertical agarose gel electrophoresis ... 37

2.2.1.9 Southern blot, preparation of radioactively labelled probes and hybridization ... 37

2.2.1.10 DNA extraction from agarose gel ... 38

2.2.2 General methods for working with *S. pombe* ... 38

2.2.2.1 Growth of *S. pombe* strains ... 38

2.2.2.1.1 Nitrogen starvation ... 38

2.2.2.2 Viability assay ... 39

2.2.2.3 Spotting assay ... 39
2.2.2.4 Microscopy ... 39
2.2.2.5 Isolation of genomic DNA ... 39
2.2.3 Nucleosome mapping by MNase-chip ... 40
2.2.3.1 Preparation of mononucleosomal DNA ... 40
2.2.3.2 Sample fragmentation and hybridization to Affymetrix tiling arrays 40
2.2.3.3 Data processing ... 41
2.2.4 Nucleosome mapping by MNase-ChIP-seq ... 41
2.2.5 Nucleosome mapping by indirect end labelling ... 42
2.2.5.1 Preparation of chromatin, MNase digest and DNA purification ... 42
2.2.5.2 MNase digest of free DNA ... 42
2.2.5.3 Secondary cleavage ... 42
2.2.5.4 Generation of markers ... 43
2.2.5.5 Generation of probe DNA ... 43
2.2.6 Generation of *in vitro* chromatin ... 43
2.2.6.1 Expansion of libraries ... 43
2.2.6.2 Purification of histone octamers from *D. melanogaster* embryos ... 43
2.2.6.3 Chromatin assembly via salt gradient dialysis ... 44
2.2.6.4 MNase-ChIP-seq of *in vitro* chromatin ... 44
3 Results ... 46
3.1 Improvement of methodology ... 46
3.2 Comparison of nucleosome occupancy maps generated by microarray hybridization (MNase-chip) and Illumina sequencing (MNase-ChIP-seq) ... 48
3.3 Effect of MNase digestion degree on nucleosome occupancy patterns ... 49
3.4 Annotation of bidirectional and tandem promoters ... 51
3.5 Comparison of TSS annotations by RNA-chip, RNA-seq and RNA-CAGE-seq 54
3.6 Nucleosome occupancy patterns of strains carrying mutations in genes coding for chromatin-related factors ... 56
3.6.1 The histone variant H2A.Z and the remodeler ATPase Swr1 do not play a major role in nucleosome positioning around TSSs ... 56

3.6.2 The RSC remodeling complex seems not to be involved in nucleosome positioning around TSSs 59

3.6.3 The Mi-2 remodeler ATPase Mit1 does not substantially participate in nucleosome positioning around TSSs 62

3.6.4 The CHD1 remodeler ATPases Hrp1 and Hrp3 are crucial for regular nucleosomal array formation downstream of the +1 nucleosome 63

3.6.4.1 Nucleosome occupancy of all genes aligned at TSSs and spectral analysis 64

3.6.4.2 Hrp1 and Hrp3 binding-targets 66

3.6.4.3 Transcriptional responders of Hrp1 and/or Hrp3 depletions......... 67

3.6.4.4 Bulk MNase ladders were not much disturbed in Hrp mutants 71

3.6.4.5 Confirmation of chromatin changes at single loci by indirect end-labelling 71

3.6.4.6 The *hrp1Δ hrp3Δ* mutant shows increased sensitivity to 6-azauracil 73

3.6.5 The histone deacetylase Clr6 and the histone lysine methyltransferase Set2 are not substantially involved in nucleosome positioning around TSSs 74

3.7 The role of transcription in nucleosome positioning 76

3.7.1 Relation between RNA synthesis rate and promoter nucleosome occupancy... 76

3.7.2 Nucleosome positioning patterns around TSSs do not significantly change in a *rpb7-ts* mutant under restrictive conditions................................... 77

3.7.3 The impact of changes in the transcriptional program on chromatin structure 78

3.8 Chromatin assembled by salt gradient dialysis *in vitro* has a nucleosome occupancy pattern around TSSs that is very different from the *in vivo* pattern 81

4 Discussion.. 84

4.1 The role of H2A.Z in nucleosome positioning 84

4.2 The role of RSC in nucleosome positioning.. 86

4.3 The role of CHD1 remodelers in nucleosome positioning 86

4.4 What positions the +1 nucleosome?.. 88

4.5 Why are nucleosomes so well-positioned at gene bodies?........................ 90

4.6 Factors involved in prevention of cryptic transcription 91

4.7 Models of nucleosome positioning at promoters and gene bodies............ 94

4.7.1 Statistical positioning 95

4.7.2 Barrier/organising centre packing model 96

4.7.3 Transcription 96

4.7.4 Combined nucleosome positioning model 97

4.8 Relationship of transcriptional changes and chromatin changes 98

4.9 Outlook 99

4.9.1 Involvement of remodelers and transcription in nucleosome positioning around TSSs 99

4.9.2 Histone exchange 100

4.9.3 Transcriptome mapping by CAGE and annotation of TSSs 101

4.9.4 Annotation of bidirectional and tandem promoters 101

References 102

Abbreviations 118

Curriculum vitae 122

Summary

The view that nucleosomes just store DNA in the nucleus has been abandoned quite a long time ago and it is known today that nucleosomes play a regulatory role in DNA-related processes. Especially the role of nucleosomes in transcriptional regulation is of outstanding interest and investigated by a large number of researchers in various organisms. Interestingly, nucleosomes show stereotypic occupancy patterns at promoters and in gene bodies, namely a nucleosome depleted region (NDR) just upstream of the transcriptional start site (TSS) followed by a regular nucleosomal array. Our research focuses on the identification of factors that set up these stereotypic patterns. We chose the fission yeast *S. pombe* as a model organism as it is as easy to handle and to manipulate as *S. cerevisiae*, the best-studied and traditional model yeast, but many aspects of its chromatin biology are more similar to higher eukaryotes. In addition, the far evolutionary divergence between *S. cerevisiae* and *S. pombe* allows to uncover conserved mechanisms. In general, besides intrinsic DNA sequence features in *cis*, several factors in *trans* are discussed as potential candidates for nucleosome positioning determinants, e.g. histone variants, sequence specific DNA-binding proteins, chromatin remodelers and transcription. In order to identify factors involved in nucleosome positioning around TSSs, we compared nucleosome occupancy in wildtype cells and cells depleted for candidate factors. The histone variant H2A.Z is enriched at the best-positioned nucleosome just downstream of the TSS. However, comparison of nucleosome occupancy of a mutant strain depleted for H2A.Z and SWR1, the remodeler responsible for H2A.Z incorporation, and wildtype revealed no significant differences arguing against a role for H2A.Z in nucleosome positioning around TSSs. Furthermore, nucleosome patterns did not majorly change upon depletion of the RNA-polymerase II subunit Rpb7, the histone methyltransferase Set2 or the histone deacetylase Clr6. In *S. cerevisiae*, the RSC remodeler complex is involved in NDR formation. Surprisingly, this seems not to be the case in *S. pombe*. Nucleosomal arrays were impaired in CHD1 remodeler Hrp1 and Hrp3 single and double mutants. While the single *hrp1Δ* and *hrp3Δ* mutants exhibited nucleosomal arrays with diminished amplitudes in comparison to wildtype, the nucleosomal array from the +3 nucleosome onwards was completely abolished in the *hrp1Δ hrp3Δ* double mutant. However, bulk MNase ladders were not significantly affected. Thus, Hrp1 and Hrp3 might not be responsible for spacing nucleosomes in gene bodies but for linking nucleosomal arrays to TSSs. As cryptic antisense transcription was upregulated in the *hrp1Δ hrp3Δ* mutant in comparison to wildtype, we suppose that regular nucleosomal arrays over gene bodies prevent initiation of cryptic transcription.

Zusammenfassung

Die Ansicht, dass Nukleosomen nur der Aufbewahrung der DNA im Zellkern dienen ist längst veraltet und man weiß heute, dass Nukleosomen eine regulatorische Rolle in DNA-bezogenen Prozessen spielen. Vor allem die Rolle von Nukleosomen in Regulation der Transkription ist von außerordentlichem Interesse und wird von vielen Wissenschaftlern in verschiedenen Organismen untersucht. Interessanterweise weisen Nukleosomen stereotype Muster an Promotoren und in Genen auf, nämlich eine nukleosomenarme Region (NDR) in 5' Richtung direkt neben der Transkriptions-Start-Stelle gefolgt von einer regelmäßigen Nukleosomen-Anordnung. Wir haben die Spalthefe *S. pombe* als Modelorganismus gewählt, da sie ähnlich leicht gehandhabt und manipuliert werden kann wie *S. cerevisiae*, die am besten untersuchte und herkömmliche Modellhefe, aber bezüglich ihrer Chromatinbiologie höheren Eukaryoten ähnlicher ist. Zusätzlich erlaubt der weite evolutionäre Unterschied zwischen *S. cerevisiae* und *S. pombe* die Aufdeckung konservierter Mechanismen. Generell werden neben intrinsischen Eigenschaften der DNA in *cis*, mehrere *trans*-Faktoren als potentielle Nukleosom-Positionierungs-Kandidaten diskutiert, wie zum Beispiel Histon-Varianten, sequenzspezifische DNA-Bindeproteine, Chromatin Remodeler und Transkription. Um Faktoren zu identifizieren, die in das Positionieren von Nukleosomen um die TSS herum involviert sind, haben wir Nukleosomen-Muster in Wildtyp-Zellen und in Zellen, denen bestimmte Kandidaten-Faktoren fehlen, verglichen. Die Histon-Variante H2A.Z ist im am besten positioniertem Nukleosom angereichert, welches in 5' Richtung direkt neben der TSS liegt. Allerdings waren Nukleosomen-Muster eines Stammes, dem H2A.Z und der Remodeler SWR1, der H2A.Z in das Chromatin einbaut, fehlen, und eines Wildtyp-Stammes nicht signifikant unterschiedlich. Dies spricht gegen eine Rolle von H2A.Z in Nukleosom-Positionierung. Außerdem wiesen Nukleosomen-Muster von Stämmen ohne der RNA-Polymerase II Untereinheit Rpb7, der Histon-Methyltransferase Set2 oder der Histon-Deacetylase Clr6 keine signifikanten Unterschiede zu Nukleosomen-Mustern eines Wildtyp-Stammes auf. In *S. cerevisiae* ist der RSC Remodeler-Komplex an der Bildung der NDR beteiligt. Überraschenderweise, scheint das in *S. pombe* nicht der Fall zu sein. Die reguläre Nukleosomen-Anordnung war in Zellen, denen die CHD1 Remodeler Hrp1 und/oder Hrp3 fehlen, gestört. Während die *hrp1Δ* und *hrp3Δ* Einzelmutanten im Vergleich zum Wildtyp Nukleosomen-Muster mit verminderter Amplitude aufwiesen, waren die Nukleosomen-Muster in der *hrp1Δ hrp3Δ* Doppelmutante vom +3 Nukleosom an komplett verschwunden. Allerdings waren „bulk“ MNase Leitern nicht signifikant betroffen. Deshalb sind Hrp1 und Hrp3 vermutlich nicht für die Generierung von gleichmäßigen Abständen zwischen den Nukleosomen verantwortlich, sondern knüpfen reguläre Nukleosomen-Anordnungen

an die TSS. Da kryptische Gegenstrang-Transkripte in der *hrp1Δ hrp3Δ* Doppelmutante hochgeregelt waren, vermuten wir, dass reguläre Nukleosomen-Anordnungen in Genen die Initiation von kryptischer Transkription verhindern.

1 Introduction

1.1 General aspects of chromatin

1.1.1 Nucleosome structure

In eukaryotic cells DNA forms repeating complexes with basic, highly conserved proteins called histones. These nucleoprotein complexes bear the name nucleosome and have two very important functions in the nucleus. First, positively charged histones balance the negative charges of the DNA backbone and hence allow folding of DNA. Second, nucleosomes limit access of other factors to DNA and therefore they play important regulatory roles in all DNA-related processes such as transcription, replication and repair. Already in 1973, it was shown that digestion of rat liver nuclei with a Ca-Mg-endonuclease led to generation of DNA fragments of regular size distributions, namely multiples of the smallest DNA fragments [12]. Around the same time, the appearance of the 10 nm chromatin fibre as “particles/beads on a string” in electron microscopy was observed [13, 14]. In 1977, the first –even though low resolution- crystal structure of a nucleosome was published [15]. In course of time, methodologies were improved and crystal structures of nucleosomal particles with increasing resolution were generated [16-18]. We learned from these nucleosome structures and other experiments that a canonical nucleosome core particle consists of 147 bp of DNA wrapped around a histone octamer in 1.65 turns of a left-handed superhelix [17]. A histone octamer was found to be composed of a histone $(H3\text{-}H4)_2$ tetramer and two histone H2A-H2B dimers [16]. Histones consist of well-ordered histone-fold domains and poorly ordered N-terminal tails [18]. The histone-fold domains mediate interactions with other histones in a characteristic “handshake” motif [16] and with DNA [18]. Interactions of histones and DNA occur at 14 sites in the minor grooves of the DNA [18]. The N-terminal tails protrude from the nucleosome core and are targets for posttranslational modification. Nucleosome core particles are connected by linker DNA, and nucleosome core particle plus linker DNA are defined as a nucleosome. The nucleosome repeat length (NRL) defined as the average distance between the midpoints of the two linkers flanking a nucleosome [19], varies from organism to organism or in multicellular organisms even from cell type to cell type [20, 21]. For instance, the fission yeast *S. pombe* exhibits a rather short NRL of only 154 bp, while for the budding yeast *S. cerevisiae* a NRL of 167 bp was determined [8, 22-24]. In most eukaryotes another protein of the histone family, the linker histone H1 exists

[25, 26]. H1 is not part of the nucleosome itself, but can bind on each side of the nucleosome occupying about 20 bp of DNA. Such a complex is called chromatosome. H1 and its subtypes are implicated in various processes like chromatin condensation and regulation of chromatin function.

1.1.2 Higher order chromatin structure

For a long time, it was common textbook knowledge that the 10 nm fibre folds progressively into certain higher order structures. Already in the 1970s the folding of nucleosomes into fibres with a diameter of 30 nm was proposed [7, 27]. Further evidence for the existence of such 30 nm fibres was shown *in vivo* in starfish sperm by electron microscopy (EM) [28] and in chicken erythrocytes by EM [28] and small-angle X-ray scattering (SAXS) [29]. Furthermore, several *in vitro* studies revealed clear evidence for a 30 nm higher order chromatin structure by applying various visualisation techniques like EM [30], high- resolution cryo-EM [31] or crystallization and subsequent X-ray [32]. Several models for the exact shape of the 30 nm fibre were proposed with the “solenoid” or “one-start helix” and the “zigzag” or “two-start helix” being the two most prominent [7, 27, 33-35]. In the solenoid model, nucleosomes are packed around a central axis of symmetry with consecutive nucleosomes lying next to each other. In the zigzag model, nucleosomes interact with the second neighbour building up a helical conformation via a zigzag structure. Experimental evidence for both, the solenoid model, e.g. [31, 33, 36], and the zigzag model, e.g. [30, 32, 33] exists. However, in the recent past the existence of 30 nm fibres in interphase cells as well as mitotic cells was called into question. Kazuhiro Maeshima and Co-workers could show by cryo-EM, SAXS and ultrasmall-angle X-ray scattering (USAXS) that mitotic chromosomes [29] and interphase nuclei of HeLa cells [10] do not contain periodic structures with diameters of > 11 nm after removal of contaminating ribosome aggregates. The authors proposed a dynamic irregular folding of the nucleosome fibre [10] (Fig. 1). This arrangement is achieved through inter-fibre contacts, while a 30 nm fibre could only be build up through intra-fibre contacts. Furthermore, they suggest that areas of interdigitated nucleosome fibres constitute chromatin domains, which are folded together during mitosis. Presumably, those chromatin domains exist also in interphase nuclei and genes lying in such domains are transcriptionally silenced, while genes looped out of those domains can be transcriptionally active. Now of course the question arises why so many groups were able to detect 30 nm fibres before. *In vivo* evidence for the 30 nm fibre was only found in rather special cell types, namely transcriptionally silent chicken erythrocytes and starfish spermatozides [37]. The formation of 30 nm structures in *in vitro* experiments can be explained by the presence of nucleosomes in very dilute conditions compared to the presence of high nucleosome concentrations *in vivo*. Under such dilute conditions nucleosomes form rather intra-fibre contacts. However, it is still possible that also *in vivo* short stretches of 10 nm fibres make intra-fibre connections and hence, built up 30 nm structures.

A further model of chromatin organization, the fractal globule model, which is fundamentally similar to the chromatin domain model was suggested and experimentally supported by Lieberman-Aiden et al. [38]. They mapped chromatin interactions genome-wide in a human lymphoblastoid cell line by Hi-C and were able to delineate chromosome territories and compartmentalisation of open and closed chromatin. Their observations led them suggest chromatin organisation in fractal globules [38, 39]. Fractal globules are flexible and dynamic structures, which lack knots, can easily unfold and refold and have a territorial organisation. Hence, such a chromatin structure would be suitable for all kinds of dynamic processes taking place in the nucleus like gene activation and gene repression.

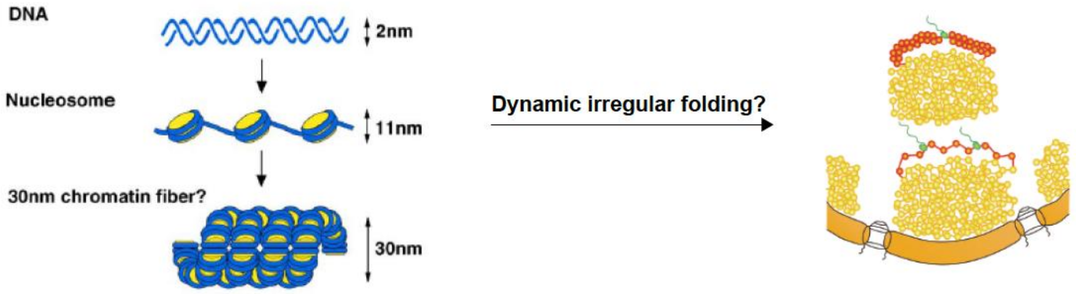

Figure 1 Higher order chromatin structure: 30 nm fibre versus dynamic irregular folding. The folding of nucleosomes into 30 nm chromatin fibres was called in question and dynamic irregular folding was proposed instead. In this model chromatin forms domains (yellow nucleosomes). Chromatin looping out of these domains can be actively transcribed (red nucleosomes, green RNA-polymerase and nascent RNA). However, parts of chromatin might form 30 nm structures (upper red nucleosomes). Images adapted from Maeshima et al. [7] and Joti et al [10].

1.2 Regulation of chromatin structure

Nucleosomes compete for DNA binding with factors involved in all kinds of DNA-related processes and thus have an impact on all those processes. Therefore, chromatin structure must be tightly regulated and highly dynamic to ensure an accurate function of all DNA-dependent processes. In general, chromatin structure is regulated via incorporation of histone variants, posttranslational modifications of histones and DNA, non-coding RNAs and chromatin remodeling.

1.2.1 Histone variants

Histone variants are non-allelic isoforms of canonical histones with a different primary structure compared to the canonical isoform, which causes in some cases differences in stability. Canonical histones are mainly expressed during S-phase while most histone variants are expressed in other cell cycle phases [40]. Variants of the core histones H2A and H3 were described in most eukaryotic organisms, while for H2B only some tissue-specific variants [41] and for H4 only variants in tetrahymena, trypanosomes and an urochordate [42] were described. In mammals the histone H2A variants H2A.Z, H2A.X, macroH2A and H2ABbd have been reported [41]. For H2A.Z, involvement in all kinds of cellular processes like transcription regulation, heterochromatin formation, DNA repair, chromosome segregation and mitosis were found [42]. Besides some cell-type specific functions, one major role of H2A.X is its involvement in DNA double strand repair. In *S. cerevisiae* and *S. pombe*, H2A.Z is the only H2A variant. Interestingly, H2A proteins in *S. cerevisiae* and *S. pombe* resemble mammalian H2A.X proteins rather than mammalian H2A proteins [43]. The only H3 variant common to all eukaryotes is the centromere specific variant CENP-A [41]. CENP-A is next to other kinetochore-specific proteins crucial for establishment and maintenance of a functional centromere and kinetochore, and therefore ensures proper chromosome segregation. The structure of CENP-A-containing nucleosomes is highly debated and ranges from the conventional octasome (two copies of H2A, H2B, CENP-A and H4) over a hexasome (two copies of the CENP-A specific *S. cerevisiae* chaperone Scm3, CENP- A and H4) to a tetrasome (two copies of CENP-A and H4) or hemisome (one copy of H2A, H2B, CENP-A and H4 with DNA wrapped in a right-handed orientation) [41]. Mammalian genomes code for several other H3 histone variants like H3.1, H3.2 and H3.3. H3.3 is ubiquitously expressed, replication-independently incorporated into chromatin and enriched at transcriptionally active regions, telomeres and pericentromeric regions. *S. cerevisiae* and *S. pombe* harbour besides CENP-A only the canonical histone H3 protein. The amino-acid sequence of *S. cerevisiae* H3 is very similar to mammalian H3.3, while *S. pombe* H3 is a hybrid of H3.3 and H3.2 [44]. Several histone variants are brought to specific sites and loaded onto chromatin by distinct histone chaperones and chromatin remodeling factors. For example, in humans, the chaperone HJURP is involved in loading CENP-A onto centromeric chromatin [41]. Furthermore, a role for the chaperone FACT and the remodeler CHD1 in CENP-A loading was demonstrated in chicken cells [45]. In yeast, exchange of H2A-H2B dimers against H2A.Z-H2B dimers requires the histone chaperones Nap1 and Chz1 and the chromatin remodeler Swr1 [46-49].

1.2.2 Posttranslational modifications of histones and DNA methylation

Histones can be posttranscriptionally modified in various ways [50]. Acetylation and deacetylation are catalysed by histone acetyltransferases (HATs) and histone deacetylases (HDACs), respectively. Methylation marks are set by histone methyltransferases (HMTs) and removed by arginine deiminases, arginine demethylases or lysine demethylases. Interestingly, over the last years in addition to histone targets more and more non-histone targets of these enzymes were found [51, 52], and therefore the nomenclature was changed to a more general one like for example lysine methyltransferase (KMT) instead of HMT. Phosphorylation and dephosphorylation are carried out by kinases and phosphatases, respectively. Further histone modifications are ubiquitination, sumoylation and poly(ADP-ribose)ylation (PARylation). Posttranslational modifications (PTMs) are mainly set at the unstructured, flexible N-terminal tails of the histones, but PTMs at several amino acids in the nucleosomal core were discovered, too [53]. Distinct PTMs at distinct histone residues are associated with distinct chromatin functions [50]. For example, H3K36 methylation, H3K4 methylation and H3/H4 acetylation, are associated with actively transcribed chromatin, while H3K9 methylation, H4K20 methylation and low levels of acetylation are associated with silent chromatin. As histone tails are necessary for secondary and tertiary chromatin structure and mediate nucleosome-nucleosome attraction [54], it was discussed if the main read-out of histone tail modifications is their influence on higher order chromatin structure [55]. So far, such a role was shown only for acetylated lysine 16 on histone H4 (H4K16ac) *in vitro* and *in vivo*. For example, *in vitro* reconstituted nucleosomal arrays containing H4K16ac or histone H4 lacking the N-terminal tail, respectively, showed similar defects in $MgCl_2$ dependent chromatin compaction and in inter-fibre interactions [56]. Another level of function of PTMs came into play when so called chromatin reader proteins were discovered [57]. Chromatin readers contain domains that specifically bind certain types of modifications, e.g. bromodomains bind acetylated histones or PHD fingers bind methylated lysines. In 2000, Strahl and Allis proposed the histone code hypothesis [55]. This hypothesis implies that combinations of several histone modifications at one or multiple histone tails result in specific downstream effects. Considering the large amount of posttranslational histone modifications and the resulting combinatorial possibilities, such a histone code would lead to a new dimension of chromatin regulation. However, during the last years, genome-wide mapping of histone modifications suggested that the histone code hypothesis is - if at all - only in a quite bare bone version true [58]. Studies of such type in various model organisms revealed that the observed combinatorial complexity of histone marks is rather limited. For example genome-wide analysis of 53 chromatin components and four histone marks in Drosophila cells revealed only five distinct chromatin states [58, 59].

Methylation of DNA at cytosines is common in vertebrates, several invertebrates and plants, however, absent in *S. cerevisiae* and *S. pombe* [60]. In mammals, particularly cytosines followed by guanins (CpG) are methylated to 5-methylcytosine (5mC). Regions with high frequency of CpG sequences are called CpG islands (CGIs) and are found at more than half of the gene promoters in vertebrates. Only promoter CGIs of long-term repressed genes are methylated, e.g. genes on the inactive X-chromosome or imprinted genes. Methylation of CpG outside of CGIs is more dynamic and promoter methylation inhibits transcription initiation while methylation in gene bodies is positively correlated with expression. Regulation and read-out of DNA methylation is connected to the binding of 5mC reader proteins, e.g. MECP2, to the presence or absence of nucleosomes, to histone modifications and to histone variants. De novo DNA methylation is catalysed by the DNA methyltransferases DNMT3A and DNMT3B and plays, for example, an important role in early mammalian development. DNMT1 in cooperation with DNMT3A and DNMT3B maintains methylation patterns [60]. Demethylation of 5mC is achieved through oxidation catalysed by the methylcytosine dioxygenase TET (ten-eleven translocation) [61]. The product of the oxidation reaction is 5-hydroxymethylcytosine (5hmC) and evidence increases that 5hmC is not only an intermediate of demethylating 5mC but a regulatory modification mark itself. It is for example involved in regulating pluripotency and differentiation of embryonic stem cells. In this sense, there are not only four, but six bases in mammalian DNA: A, C, G, T, 5mC and 5hmC. Maybe the further oxidation products 5-formyl-C and 5-carboxy-C are not just intermediates but have biological functions as well.

1.2.3 Chromatin remodelers

Chromatin remodeling complexes usually consist of an ATPase domain containing protein and various accessory proteins. Remodeling complexes can slide nucleosomes along the DNA, disassemble nucleosomes, generate non-canonical altered nucleosomal states and/or exchange canonical histones with histone variants or vice versa [62, 63] (Fig. 2). Most chromatin remodeler ATPases belong to the Snf2 family of helicases that can be further divided into subfamilies based on the sequence homology of their ATPase subunits: the SWI/SNF (switch/sucrose-nonfermenting), ISWI (imitation switch), CHD (chromo-helicase/ATPase-DNA-binding) and INO80 (inositol-requiring) subfamily [11, 64, 65]. Oversimplified, the respective remodeler subfamilies can fulfil certain of the just mentioned tasks [5]. SWI/SNF family remodelers move or disassemble nucleosomes and are for example involved in transcriptional activation. Some of the ISWI family members are able to evenly space nucleosomes. Members of the CHD family of remodelers slide or disassemble nucleosomes. Moreover, the *D. melanogaster* ISWI remodeler ACF and certain *D. melanogaster* and both *S. pombe* CHD remodeler were shown to assemble nucleosomes onto DNA *in vitro* [66]. Members of the INO80 family have the ability to restructure chromatin [5].

Chromatin remodeling complexes were found to function in all kind of processes in which DNA accessibility must be regulated like DNA repair, DNA replication or transcription. Recently, the mobility of the two ISWI remodelers Snf2H and Snf2L was analysed in living cells by fluorescence microscopy [64, 67]. In G1/2 phase both ISWI remodelers were rather mobile and binding to chromatin was only transient, while tightly bound remodelers were observed at replication foci and DNA repair sites. Those results led the authors to the hypothesis that ISWI remodelers rapidly translocate through the nucleus via diffusion and continuously sample nucleosomes until they find their target location. Chromatin remodelers find their specific targets in the nucleus with the help of DNA sequence features [68], recognition of histone modifications [69-72] and/or histone variants [73] and interaction with chromatin-associated proteins [64, 74].

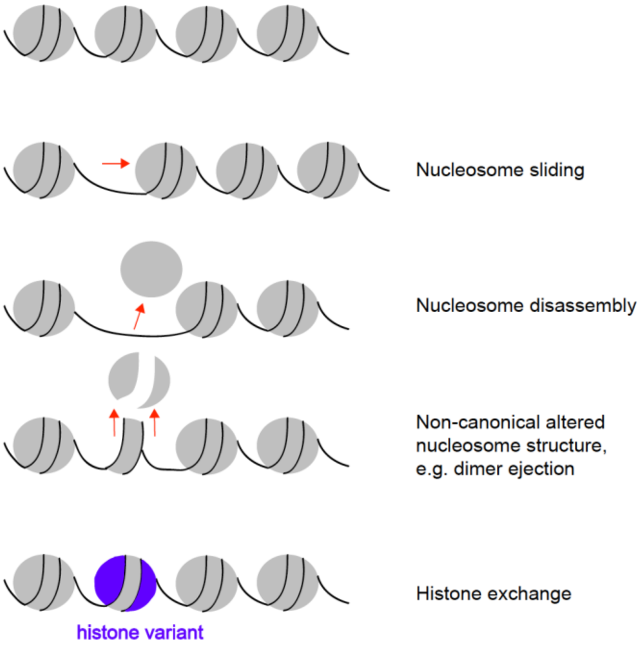

Figure 2 Functionalities of chromatin remodelers. Chromatin remodelers can slide nucleosomes, disassemble nucleosomes, create non-canonical altered nucleosome structures or exchange canonical histones against histone variants or vice versa. (adapted from Clapier and Cairns [5])

1.3 Nucleosome positioning

How does the structure of the 10 nm fibre that is so tightly regulated by the mechanisms described above, look like? Strikingly, it was shown in various organisms from yeast to human that nucleosomes adopt stereotypic positions at the 5`ends of genes relative to the transcription start site (TSS) [8, 75-79] (Fig. 3). In yeast, just upstream of the TSS, a nucleosome depleted region (NDR) is found which is flanked by two well-positioned nucleosomes, the -1 and the +1 nucleosome. The +1 nucleosome is the first nucleosome of an array of positioned nucleosomes extending into the gene body. However, the degree of positioning decreases the further the array runs into the gene body. What does the term positioned or well-positioned nucleosome denote at all? A nucleosome consists of 147 bp of DNA wrapped around a histone octamer. These 147 bp define the position of a nucleosome and a specific nucleosome position can be described by the nucleosome's start, dyad or end position [19]. "Nucleosome positioning" describes the probability of a given base pair to serve as start, dyad or end position of a nucleosome in a population of cells at a specific locus or in a population of cells at various loci relative to fixed points, e.g. TSSs. A well-positioned nucleosome has a high probability to have its start, dyad or end position at the same or a close-by base pair position in a population of cells [80]. A less well-positioned or better fuzzy nucleosome has a low probability to have its start, dyad or end position at the same or a close-by base pair position in a population of cells. Another way of defining the localization of a nucleosome is "nucleosome occupancy". Nucleosome occupancy describes the probability with which a certain base pair is covered by a nucleosome [19, 80]. It does not matter which part of the nucleosome the very position covers, and thus, nucleosome occupancy is a much less stringent way of describing the localization of a nucleosome compared to nucleosome positioning.

If the term nucleosome positioning is used in the just described way, it is also referred to as "translational nucleosome positioning". Furthermore, there exists the term "rotational nucleosome positioning" that describes the local orientation of the DNA helix on the histone surface [6]. Rotational nucleosome positioning will be discussed in more detail in section 1.3.2.1.

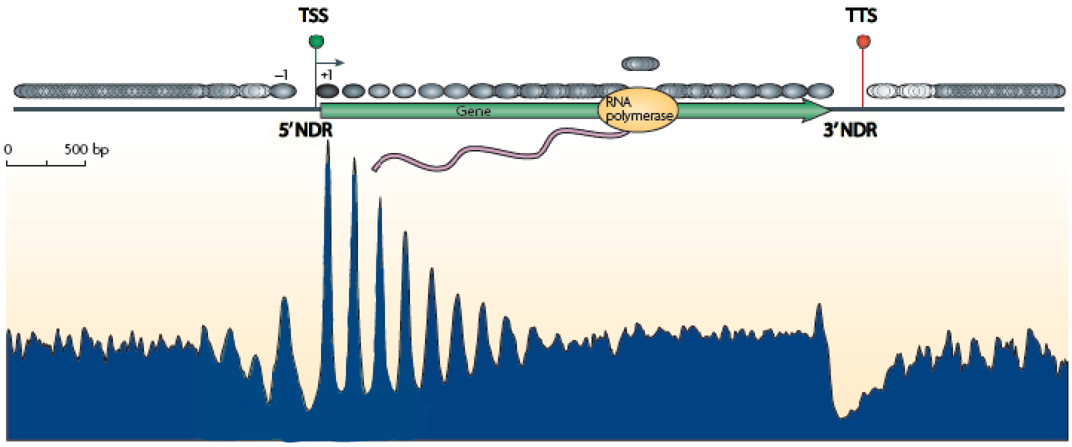

Figure 3 Stereotypic nucleosome patterns at *S. cerevisiae* genes. Consensus distribution of nucleosomes of all yeast genes aligned at the transcriptional start site (TSS) or the transcription termination site (TTS) is shown as drawing (upper part, grey circles represent nucleosomes) and as composite plot (lower part) (adapted from Jiang and Pugh [6]).

1.3.1 How to map nucleosome positions

1.3.1.1 Mapping of nucleosome positions at single loci

The observation that nucleases like DNase I or micrococcal nuclease (MNase) cut preferentially at DNA sites that are not occluded by proteins is quite old [81]. Since then, this capacity of DNase I or MNase has been exploited to map locations that are digested by nucleases, so-called hypersensitive sites, and locations that are protected from digestion. In 1980, Carl Wu, the inventor of hypersensitive site mapping, found hypersensitive sites at the 5`ends of heat shock genes in Drosophila [82, 83]. Limited digest of chromatin with DNase I or MNase followed by the indirect end labelling technique can also be applied to map nucleosome positions at specific loci. After digestion of chromatin with a nuclease, DNA is purified and cleaved with a restriction enzyme cutting close to the genomic region of interest to obtain a reference point. Samples are gel electrophoresed, blotted onto a membrane, and hybridized with a radioactively labelled probe complementary to a part of the region of interest. On the basis of the length of the bands, distances between nuclease cuts and the reference point can be calculated, and thus, the chromatin structure can be determined [84, 85].

1.3.1.2 Mapping of nucleosome positions genome-wide by microarrays or high throughput sequencing

The property of MNase to preferentially cut linker DNA while nucleosome covered sequences are protected from digestion, can also be exploited to map nucleosome positions genome-wide. In general, chromatin is isolated from the organism or cell-type of interest and treated with MNase. Careful titration of MNase is very critical in order to obtain mostly mononucleosomes without overdigestion. If desired, a chromatin immunoprecipitation step (ChIP) with an antibody against specific histones, histone modifications or nucleosome-associated factors can be conducted. Subsequently, DNA is purified, loaded on an agarose gel and bands corresponding to mononucleosomal DNA are purified. Mononucleosomal DNA can be analysed by microarray hybridization (MNase-chip) or high-throughput sequencing (MNase-seq). In 2005, the Rando laboratory mapped nucleosome positions over 482 kb of the *S. cerevisiae* genome applying tiled microarrays with 20 bp resolution [76]. This map revealed for the first time that a large subset of genes is organized in the stereotypic way described above. Only a couple of years later, a genome-wide nucleosome occupancy map with 4 bp resolution [75] and a occupancy map generated by high-throughput sequencing [86] were published for *S. cerevisiae* confirming the key findings of the lower resolution data set. Nucleosome occupancy maps for *Drosophila melanogaster* [78], *C. elegans* [77], *S. pombe* [8], human CD4$^+$ T-cells [20, 79, 87], human CD8$^+$ T-cells, human granulocytes [20], *Arabidopsis thaliana* [88] and mouse liver [89] followed.

1.3.1.3 Chemical mapping

MNase is commonly used for genome-wide mapping of nucleosome occupancy. However, MNase does not cut all sequences with the same probability but preferentially cuts at AT base pairs, and, in addition, it does not exclusively cut linker DNA but also –at least under certain circumstances, e.g. depending on the digestion degree- nucleosomal DNA. It was first in 1983 [90] and later repeatedly called into question if MNase is the right choice to appropriately map nucleosome positions as its sequence preference might heavily bias or even distort the results. For example, digestion of chromatin or naked DNA and subsequent sequencing of recovered fragments approximately 150 bp in size resulted in similar coverage profiles for both samples [91]. However, recently Allan et al. [92] compared recovered DNA fragments from in vitro chromatin either digested with MNase or with caspase-activated DNase (CAD). CAD has different sequence preferences compared to MNase and its structure does not allow digestion of nucleosomal DNA. Interestingly, DNA fragments recovered with both methods were highly similar, and thus, MNase biases in genome-wide nucleosome occupancy data should be negligible.

The Widom laboratory applied for genome-wide mapping of nucleosome positions *in vivo* a very sophisticated nuclease-independent method, which was originally developed by the Richmond group for analysis of *in vitro* chromatin [93, 94]. In this chemical method a unique cysteine is introduced into histone H4 at sites, which in a nucleosome are located in very close proximity to the DNA backbone and symmetrically flank the nucleosome dyad. A copper-chelating phenanthroline label can attach covalently to cysteines in histone H4. Upon addition of copper and hydrogen, peroxide hydroxyl radicals are formed that cleave the nearby DNA backbone close to the nucleosome dyad at specific sites. Subsequently, the fragmented DNA is purified and DNA fragments corresponding to linker DNA flanked by two half nucleosomes are selected and sequenced. Strikingly, such chemically mapped nucleosome dyad positions corresponded well with MNase-seq mapped nucleosome dyad positions. Thus, chemical mapping represents a valuable method to map nucleosome-positions genome-wide with high resolution, and it confirms that nucleosome positions can be mapped confidently with MNase-based techniques [94].

1.3.2 Candidates for nucleosome positioning determinants

As we are especially interested in the role of nucleosomes in transcriptional regulation the question of which factors are responsible for the arrangement of nucleosomes in such well-defined patterns at promoters and 5’ ends of genes is a very intriguing one. Potential candidate factors determining nucleosome positioning are DNA sequence features, general regulatory factors, chromatin remodelers, histone variants, and RNA polymerase or the transcription process. While the DNA sequence acts in *cis*, all other factors act in *trans*.

1.3.2.1 DNA sequence features

Nucleosomes are formed without any base-specific interactions and any DNA can be accommodated in a nucleosome. Nevertheless, intrinsic DNA sequence features can influence nucleosome formation. DNA needs to bend sharply every DNA helical repeat (~10 bp), when the minor groove points inwards towards the histone octamer, and offset by 5 bp when the minor groove points outwards [95]. Certain dinucleotides can support this bending of DNA: while AA/TT dinucleotides slightly narrow the minor groove, GC dinucleotides slightly expand it. Indeed, such dinucleotide periodicities in phase with the DNA curvature around the histone octamer can be found in DNA assembled into nucleosomes *in vivo* and *in vitro* [4, 96-98]. Rotational nucleosome positioning is probably caused by this dinucleotide periodicity. Physical properties of DNA sequences could also have the ability to influence translational positioning. For example, homopolymeric (dA:dT) tracts are rather stiff and have a low average nucleosome occupancy *in vivo* and *in vitro* [4, 97, 99]. How large the influence of histone octamer binding sequence preferences on *in vivo* nucleosome positioning really is was heavily debated during the last couple of years. In 2006, Segal et al. [97] proposed a genomic code for nucleosome positioning based on a combination of experimental *in vivo* and *in vitro* approaches in *S. cerevisiae* and computational modelling. The authors claimed that ~50% of the *in vivo* nucleosome positions are intrinsically determined. Critical evaluation of their data by others and poor correlation between their predictions and genome-wide *in vivo* data, weakened the positioning code hypothesis [100]. Also others endeavoured to computationally predict nucleosome positions or occupancy from DNA sequence alone for different organisms; some agreed -at least to some extend- and others disagreed with the concept of a positioning code [8, 101-105]. Furthermore, two studies were published applying similar techniques but drawing opposing conclusions [4, 96]. Both groups assembled histones genome-wide on yeast DNA by salt gradient dialysis and mapped *in vitro* nucleosome positions or occupancy and compared *in vitro* nucleosome positions to *in vivo* nucleosome positions. While the groups of Widom and Segal concluded that DNA sequence plays a central role in determining nucleosome positions [4], Struhl and coworkers concluded that a genomic code for nucleosome positioning does not exist [96]. Experimental differences and different data analysis probably account for several discrepancies in the data. First, the Struhl group used a histone:DNA mass ratio of 1, while the Widom and Segal groups used limiting amounts of histones (histone:DNA mass ratio of 0.4). With limiting histone concentrations most of the DNA does not form chromatin, histones compete less with each other and rather bind to intrinsically preferred nucleosome positions. Second, the Zhang group really compared nucleosome positioning of the *in vivo* and *in vitro* data sets, while the others used the much less stringent criteria of histone density or nucleosome occupancy. However, overall both data sets did not differ that much from each other, but the conclusions drawn were strongly conflictive. Both groups found histone depletion at promoter regions *in vitro*. In *S. cerevisiae* nucleosome disfavouring homopolymeric (dA:dT) tracts are enriched at promoters. However, depletion at promoters in the *in vitro* samples was far less prominent compared to the *in vivo* situation. Thus, the DNA sequence alone is not sufficient to keep promoters nucleosome-free. Furthermore, homopolymeric (dA:dT) tracts are not enriched at promoters of many other organisms like for example *S. pombe* [8]. Interestingly, like others before, both groups found good evidence for intrinsic determination of rotational positioning. With an increasing number of studies showing a role for *trans* factors in translational nucleosome positioning, the idea of a positioning code has more and more taken a back seat.

1.3.2.2 General regulatory factors

General regulatory factors (GRFs) are a class of sequence-specific DNA binding proteins. In simple terms, GRFs could influence and shape chromatin structure in two ways. First, they can compete with nucleosomes for DNA binding and thus, displace the very nucleosome they were competing with. Second, they could recruit other factors as for example chromatin remodeling complexes that then remodel nearby chromatin. Interestingly, binding motifs for various transcription factors can be found in NDRs. In *S. cerevisiae,* binding motifs for e.g. Rsc3, Rsc30, Abf1 and Reb1 are preferentially enriched in NDRs and ablation of any of these factors led to an increase of nucleosome occupancy at promoters containing binding sites for the respective factor [68, 106, 107]. MNase-ChIP-seq mapping of nucleosome-bound Reb1 and high resolution mapping of nucleosome-bound and -unbound Reb1 by a combination of ChIP and exonuclease digest (ChIP-exo) revealed interesting features of Reb1 binding at promoters [108, 109]. Reb1 binding could be detected at very defined positions 95 bp upstream of the TSS and at the -1 nucleosome leading to the hypothesis that Reb1 might direct positioning of the -1 nucleosome and thereby create the upstream NDR border. Strikingly, insertion of a sequence containing a Reb1 binding site and a poly(dT) tract into the body of a transcriptionally quiescent gene led to the formation of a NDR flanked by a downstream nucleosomal array [110]. Ablation of Reb1 or the ATPase subunit of the RSC complex (Sth1) prevented NDR and nucleosomal array formation suggesting a mechanism in which Reb1 might recruit the RSC complex [107]. Binding sites for Reb1 are nucleosome occupied *in vitro* [4], hence, *trans* mechanisms, probably Reb1 binding and recruitment of the RSC remodeling complex, are necessary to liberate those sites from nucleosomes *in vivo*. A comparison of GRF binding sites between 13 yeast species revealed that a transition in the repertoire of GRFs happened during evolution [111]. Those 13 yeast species evolutionary diverged before and after a whole genome duplication (WGD). While Cbf1 is the major GRF in pre-WGD yeast species, e.g. *C. albicans*, Reb1 is the major GRF in post-WGD yeast species, e.g. *S. cerevisiae*. *S. pombe* uses Sap1 as an important GRF. In mice, the Reb1-related transcription termination factor (TTF-I) is involved in repression and activation of rRNA genes via regulation of promoter chromatin structure [111, 112].

Interestingly, not only GRFs in close proximity to TSSs influence nucleosome positioning. It was shown *in vivo* in human cells that nucleosomes are well positioned around binding sites for the vertebrate-specific insulator binding protein CTCF. In contrast, *in vitro* those binding sites are occupied by a nucleosome and a nucleosomal array is absent [20, 113, 114].

1.3.2.3 Chromatin remodelers

Genome-wide *in vitro* reconstitution of *S. cerevisiae* chromatin revealed that generation of NDRs and nucleosomal arrays is dependent on the presence of whole cell extract and ATP [2]. Hence, active mechanisms must be responsible for setting up nucleosome occupancy patterns around TSSs. Prime candidates for actively regulating chromatin structure are chromatin remodeling complexes.

1.3.2.3.1 SWI/SNF family

Most eukaryotes possess two types of SWI/SNF remodelers. SWI/SNF remodelers are implicated in various nuclear processes. *S. cerevisiae* and *S. pombe* harbour two remodeler ATPases of the SWI/SNF type that are subunits of two remodeling complexes called SWI/SNF and RSC (Table 1). While RSC is essential for viability in both yeasts, SWI/SNF is not [115]. The SWI/SNF and RSC complexes of *S. cerevisiae* contain five paralog subunits including the ATPase subunits and share three subunits. *S. pombe* SWI/SNF and RSC even share six subunits which is similar to the mammalian BAF and PBAF complexes. *S. cerevisiae* and *S. pombe* RSC complexes contain several ortholog subunits, but also differ in other subunits. For example, the Rsc3 subunit that was shown to bind DNA sequence-specific is missing in the *S. pombe* RSC complex.

In *S. cerevisiae*, SWI/SNF is implicated in regulation of nucleosome occupancy and transcription at several promoters, e.g. at heat shock genes [116-120] and *PHO* promoters [121-124]. Also in *S. pombe* SWI/SNF plays a role in both, transcriptional activation and repression [115] and promotes *in vitro* transcription in the context of chromatin [125]. Strikingly, several subunits of human SWI/SNF remodelers have been found inactivated in various cancers [126].

In *in vitro* experiments the remodeling ability of purified yeast RSC complex on mono-, di- and trinucleosomal DNA assembled on 601 positioning sequences was studied applying atomic force microscopy (AFM) imaging [127, 128]. These studies revealed that RSC moves nucleosomes until it encounters a physical barrier, i.e. a DNA-end or another nucleosome, and thereby renders longer stretches of DNA nucleosome-free. While one group found that the DNA-sequence does not impose directionality on the sliding process [127], another group could show sequence dependency of sliding direction [128]. The *in vitro* data demonstrating a sequence-independent nucleosome sliding activity of RSC fit quite well with the role of RSC in promoter chromatin remodeling observed *in vivo*. Ablation of the ATPase subunit of the RSC complex, Sth1, resulted in higher nucleosome occupancy in NDRs and movement of nucleosomes towards NDRs at 55% of promoters [107]. Furthermore, rather drastic increase of histone density was observed at Polymerase III promoters in a similar mutant [129]. Similarly, higher promoter nucleosome occupancy was also seen upon loss of the RSC subunit Rsc3 [68]. The Rsc8 subunit of RSC could be mapped to the -1, +1, +2 and +3 nucleosomes [130], fitting well with the effects of RSC mutants on 5`NDRs. However, RSC could also generate nucleosome free regions via nucleosome disassembly and not sliding. For example, the *PHO5* promoter is liberated from nucleosomes via nucleosome disassembly [131, 132], and RSC is able to disassemble nucleosomes via histone transfer to histone chaperons [133]. In *S. pombe*, much less is known about the functions of RSC in general and nothing about its functions in nucleosome positioning around TSSs. Similar to *S. cerevisiae* [134, 135], a role for RSC in mitosis could be shown as cells carrying a temperature-sensitive allele for the ATPase subunit Snf21 (*snf21-ts*) exhibited cell-cycle arrest at G2-M phase and chromosome segregation defects at the non-permissive temperature [136]. Furthermore, Garcia et al. [137] found that RSC might generate nucleosome free regions at some heterochromatic loci in *S. pombe* that are under normal conditions prevented by Clr3, the HDAC subunit of the SHREC complex.

1.3.2.3.2 ISWI family

The first ISWI remodeler ATPase was discovered in *Drosophila melanogaster* and the family of ISWI remodelers was named after it [138]. In flies, there exist three ISWI remodeler complexes, namely NURF, CHRAC and ACF [139-141]. All three complexes share the same ATPase subunit, ISWI, which is essential for development. Subsequently, ISWI proteins were identified in several other organisms like humans, frogs or budding yeast [142]. In *S. cerevisiae*, two ISWI proteins were found, Isw1 and Isw2 [143, 144] (Table 1). Both proteins are not essential for viability. Isw2 forms only one complex, while Isw1 forms two distinct complexes, ISW1a and ISW1b. Surprisingly, *S. pombe* does not harbour any remodelers of the ISWI family [11].

The actions of fly and budding yeast ISWI and ISWI-containing complexes on nucleosomal templates were studied extensively *in vitro*. The NURF complex was shown to disrupt regular arrays of nucleosomes when present in high amounts [139], whereas ACF and CHRAC space nucleosomes in a regular way [145]. ISW2 and ISW1a show *in vitro* nucleosome spacing activity of ~175 and ~200 bp, respectively. On the contrary, Isw1b shows only very little *in vitro* nucleosome spacing activity [143, 144].

The respective ISWI-containing complexes also show different nucleosome sliding behaviour. On mononucleosomal templates, CHRAC and ACF exhibit nucleosome sliding activity from an end position to a central position but not vice versa. NURF and ISWI ATPase alone move nucleosomes only from a central position to an end position. Moreover, ISWI remodeling complexes slide nucleosome in *cis*, but do not dis- and reassemble them in *trans* [146-148].

ISW1a is active when bound to a nucleosome with extranucleosomal DNA at only one site [149]. It then moves the nucleosome in direction of extranucleosomal DNA. Such a configuration allows binding of ISW1a to extranucleosomal DNA on both sites resulting in conformational changes and ceasing of the nucleosome sliding reaction. Extranucleosomal DNA of ~33 bp in length on both sides of the nucleosome led to efficient ceasing of the remodeling reaction. Those data fit well with the for ISW1a observed spacing activity of ~175 bp. ISW1b behaves significantly differently and mobilizes nucleosomes of substrates with extranucleosomal DNA on one or both ends equally well. Hence, ISW1a meets the requirements for a nucleosome spacing enzyme while ISW1b does not. ISW2 exhibits the same sliding directionality as ISW1a, i.e. moving nucleosomes from an end to a central position [150]. In addition, nucleosomal interaction and activity of ISW2 depend on length of extranucleosomal DNA, too. A minimal length of 20 bp is required for nucleosome mobilization [151], while the optimal length is with 70-85 bp rather long [152]. The SLIDE domain of Isw2 binds to linker DNA and is required for effective remodeling as it contributes to push linker DNA into the nucleosome and facilitates unidirectional movement of nucleosomes [153]. Furthermore, ISW1a and ISW2 are incapable of moving nucleosomes closer than 15 bp from a DNA-end, while ISW1b can do so [150].

Dependence of the sliding reaction on linker DNA was also shown for the human ACF complex harbouring the ISWI subunit SNF2h [154, 155]. Applying fluorescence resonance energy transfer (FRET) and single-particle electron microscopy on *in vitro* assembled nucleosomes, the Narlikar laboratory proposed that ACF functions as a dimer of ATPases, binding each side of a nucleosome and working in a coordinated manner. The ATPase binding to the longer linker hydrolysed ATP faster leading to DNA translocation. Hence, a dynamic equilibrium is generated and most DNA fragments harboured centered nucleosomes.

Thus, directionality of nucleosome sliding seems to be achieved by intrinsic activities of the remodeling complexes other than the ATPase subunits and binding of extranucleosomal DNA or linker DNA might regulate the spacing activity of the respective complexes.

The *in vivo* situation is of course much more complex and several other aspects like for example remodeler recruitment influence the outcome of chromatin remodeling. However, the observations made *in vitro* can at least in parts explain the ones made *in vivo*. Isw2 mainly interacts with the +1 and the terminal nucleosome, i.e. nucleosomes flanking rather large linker regions, namely the 5’ and the 3’ NDR [130]. ISW2 slides nucleosomes towards 5’ and 3’ NDRs as deletion of the gene coding for Isw2 led to nucleosome movement away from both NDR types. High resolution mapping of Isw2 by ChIP-exo indicated that orientation of Isw2 on +1 nucleosomes fits very well with movement of nucleosomes towards 5’ NDRs [130]. On one hand, ISW2 covers canonical promoters with nucleosomes acting as a transcriptional repressor, which was for example shown for early meiotic genes during mitotic growth [156]. On the other hand, ISW2 covers cryptic promoters at 3' NDRs, especially at genes with tandem orientation, thereby preventing initiation of cryptic antisense transcription [130, 157]. ISW1a was mainly found at +1, -2 and terminal nucleosomes and similar to ISW2 slides nucleosomes towards 5`and 3' NDRs [130]. ISW1b predominantly interacts with the +2, +3, +4 and the penultimate nucleosomes and shifts nucleosomes in 3' direction. Genome-wide nucleosomes positioning studies showed that deletion of the gene coding for Isw1, the remodeler ATPase subunit shared between ISW1a and ISW1b, lead to nucleosome shifts in 5' direction, increased fuzziness of nucleosomes and reduced nucleosome occupancy in gene-bodies [158]. Interestingly, nucleosome shifts upon Isw1 depletion were enriched in cryptic transcription initiation sites. Furthermore, single loci studies, implicated ISW1a in induction of promoter inactivation and ISW1b in regulation of transcriptional elongation and termination via controlling the amount of RNA- Polymerase II entering productive elongation [159]. Remarkably, combinatorial depletion of Isw1 or both Isw remodeler ATPases and Chd1, a remodeler ATPase of the CHD1 subfamily severely changed nucleosome occupancy pattern around TSSs [160]. Nucleosome occupancy of the +1 and +2 nucleosomes was reduced and nucleosomal arrays from the +3 nucleosome onwards were completely lost. These results were in line with the former findings that Isw1 and Isw2 genetically interact with Chd1 [143].

Also in fly, the ISWI machine and its complexes are involved in both positive and negative regulation of transcription. NURF and ACF facilitated *in vitro* transcription of a chromatin template by chromatin remodeling prior to transcription [141, 161]. A hint of a repressive role of the ISWI remodeler in transcription gave the observation that the distributions of ISWI and RNA-Polymerase II on salivary gland polytene chromosomes did not overlap [162]. Furthermore, ISWI repressed wingless target genes in wing imaginal discs [163].

1.3.2.3.3 CHD family

Chd1, the founding member of the CHD family was discovered in mouse lymphoid cells [164]. The protein was named CHD as it contained three different domains, a chromo domain, an ATPase/helicase domain and a DNA binding domain. The CHD remodeler family is subdivided into CHD1, Mi-2 and CHD7 subfamilies. As remodelers of the CHD7 subfamily are neither present in *S. cerevisiae* nor in *S. pombe*, they will not be discussed here. Chd1 is conserved from yeast to human. Interestingly, Chd1 does not form a complex, but acts as a monomer. An ortholog Chd1 protein was identified in *S. cerevisiae* [165] and two orthologs were identified in *S. pombe*, Hrp1 and Hrp3 [166, 167] (Table 1). In *in vitro* experiments, *S. cerevisiae* Chd1 moved nucleosomes from end to central positions similar to ISW1a and ISW2 [150]. The DNA-binding domain of Chd1 was shown to be necessary for nucleosome centring, but not for the nucleosome sliding activity itself. To prove more directly that the DNA-binding domain determines the directionality of the sliding reaction, a sequence-specific DNA-binding domain was fused to Chd1 lacking its original DNA-binding domain [168]. Strikingly, on a sequence containing the binding motif for the fusion construct, nucleosome sliding was directed toward the DNA-binding motif. The like was observed when fusing Chd1 lacking the DNA-binding domain to streptavidin and using biotinylated DNA as a template for the sliding reaction [169]. Remarkably, when tethering Chd1-streptavidin to biotinylated histones, Chd1-streptavidin was able to slide histones off of DNA-ends and to disrupt canonical histone-DNA contacts. Usually these are properties of SWI/SNF remodelers.

Fly Chd1 exhibited nucleosome assembly ability both *in vitro* and *in vivo*. Recombinant Chd1 in collaboration with the chaperone Nap1 could assemble and regularly space fly histones on plasmid DNA [170]. *In vivo*, Chd1 is necessary for de novo chromatin assembly during very early embryonic development [171]. After fertilization, Chd1 in concert with the chaperone HIRA loads the histone variant H3.3 replication-independently onto chromatin of the male pronucleus. Maternal Chd1 deletion resulted in formation of haploid embryos containing maternal chromosomes only.

Several findings suggest a role for CHD1 remodelers in activating or facilitating transcription. Fly Chd1 bound to lowly compacted transcriptional active regions on polytene chromosomes [172]. In *S. cerevisiae*, Chd1 interacted with subunits of three complexes involved in transcriptional elongation, namely Rtf1 (PAF complex), Spt5 (DSIF complex) and Pob3 (FACT complex) [173]. In addition, Rtf1, Spt5 and Chd1 associated with coding regions of actively transcribed genes. Findings in *S. pombe* also support the hypothesis that CHD1 remodelers influence transcription positively. The CHD1 remodelers Hrp1 and Hrp3 together with the chaperone Nap1 decreased histone density at promoter regions [174]. Furthermore, both, *S. cerevisiae* Chd1 and *S. pombe* Hrp1 play a role in transcriptional termination [166]. Hrp1 is also implicated in transcriptional silencing of the mating type locus and centromeric regions [175, 176]. In line with the deregulation of centromeric chromatin, Hrp1 depletion resulted in reduced CENP-A levels, anaphase decondensation and loss of minichromosomes. Interestingly, the decondensation and minichromosome loss phenotype was even stronger in cells overexpressing Hrp1.

S. cerevisiae does not harbour any remodelers of the Mi-2 subfamily while *S. pombe* harbours one, Mit1. Mit1 is the ATPase subunit of the SHREC complex which is involved in transcriptional silencing of heterochromatic regions [177]. The SHREC complex contains in addition to the remodeling activity also a HDAC activity and is in this regard similar to the NuRD complex, which is present in higher eukaryotes like fly or humans [178].

1.3.2.3.4 INO80 family

The family of INO80 (inositol auxotroph 80) chromatin remodelers was discovered in *S. cerevisiae* in a screen for mutants defective in ICRE (inositol/choline responsive element)-dependent gene activation [179]. Later, INO80 complexes were also identified in other organisms like human [180] and *D. melanogaster* [181]. In addition, SWR1, a complex containing an ATPase subunit related to Ino80 was identified in *S. cerevisiae* [48] and other organisms [182]. Several subunits of the respective complexes are conserved from yeast to human and are characteristics of the INO80 chromatin remodeler family: An ATPase protein containing a split ATPase domain, two proteins that are related to bacterial RuvB-like helicases as well as actin and actin-related proteins (Arps). In addition, the respective complexes contain species-specific and function-specific subunits. The human INO80 complex for example can contain the transcription factor yin yang (YY1) and function in transcription activation [183]. As binding of YY1 is dependent on the activity of the INO80 complex, INO80 possibly remodels chromatin around YY1 binding-sites in order to make those sites accessible for YY1 and possibly also for the transcription machinery. A regulatory role in transcription was attributed to the INO80 complex in several other studies, e.g. microarray-based transcriptome analysis yielded a rather large number of genes with changed expression in a *S. cerevisiae* Ino80 mutant [48]. In *S. pombe*, INO80 regulates histone density and thereby transcription of genes involved in nucleotide metabolism [184]. Furthermore, the INO80 complex is involved in DNA double strand break repair, regulation of cell cycle checkpoint pathways, DNA replication, telomere regulation, centromere stability, and chromosome segregation [182].

The SWR1 complex exchanges canonical histone H2A for the histone variant H2A.Z [46-49]. It was shown recently that substrate specificity of the SWR1 complex depends on the presence or absence of a specific histone acetylation mark [185]. While an unacetylated histone H3 lysine 56 residue (H3K56) promoted incorporation of H2A.Z in H2A-containing nucleosomes, acetylation of histone H3 on lysine 56 (H3K56ac) led to incorporation of H2A in H2A.Z-containing nucleosomes. The INO80 complex was shown to fulfil the exchange of H2A.Z against H2A [73]. *In vivo*, depletion of Ino80 resulted in altered H2A.Z localisation, especially at promoters with a decrease of H2A.Z occupancy at the +1 nucleosome and gain of H2A.Z in coding regions. Interestingly, most of the mislocated H2A.Z was unacetylated. Hence, one function of the INO80 complex might be the removal of unacetylated H2A.Z. Interestingly, in *in vitro* experiments *S. cerevisiae* INO80 was shown to center end positioned nucleosomes and to regularly space di- and trinucleosomal arrays resulting in a repeat length of ~177 bp [186]. Thus, INO80 might be a good candidate for a nucleosome positioning determinant.

Table 1 Remodeler subfamilies. Listed are subfamilies of chromatin remodelers and their representatives in *S. pombe* and *S. cerevisiae* that are relevant for this thesis (according to Clapier and Cairns [5] and Flaus et al. [11])

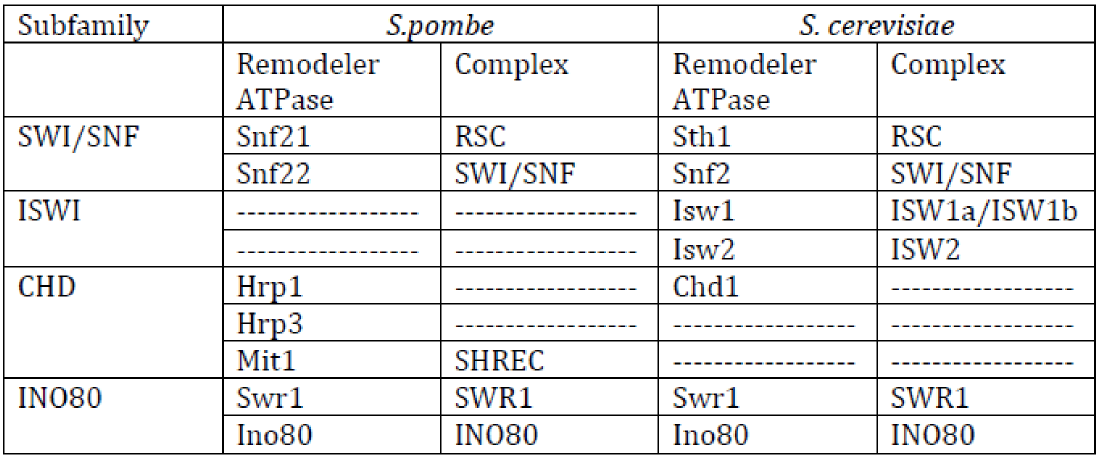

Subfamily	*S.pombe*		*S. cerevisiae*	
	Remodeler ATPase	Complex	Remodeler ATPase	Complex
SWI/SNF	Snf21	RSC	Sth1	RSC
	Snf22	SWI/SNF	Snf2	SWI/SNF
ISWI	------------------	------------------	Isw1	ISW1a/ISW1b
	------------------	------------------	Isw2	ISW2
CHD	Hrp1	------------------	Chd1	------------------
	Hrp3	------------------	------------------	------------------
	Mit1	SHREC	------------------	------------------
INO80	Swr1	SWR1	Swr1	SWR1
	Ino80	INO80	Ino80	INO80

1.3.3 Histone variant H2A.Z

The histone variant H2A.Z is conserved from yeast to human [42]. H2A.Z is essential for survival in metazoans, however, dispensable in *S. cerevisiae* and *S. pombe*. H2A.Z and the canonical histone H2A share about 60% sequence identity. The differences are mainly located in the C-terminus where H2A.Z contains an alternative docking domain and an extended specific acidic patch creating a different interface in the nucleosome [187, 188]. It is still highly debated if the presence of H2A.Z in nucleosomes leads to higher, unchanged or lower nucleosome stability [42]. The disagreement in the literature might at least partly be based on varying experimental conditions, for example, the presence of post-translational modifications on H2A.Z histone tails. H2A.Z is implicated in various nuclear processes like establishment and maintenance of chromatin boundaries, cell cycle progression and DNA repair [187]. Furthermore, a number of studies provided evidence for a role of H2A.Z in transcriptional regulation. Remarkably, H2A.Z was found enriched at nucleosomes flanking the promoter NDR in fission and budding yeast [49, 110], plant [189], fly [190] and mammalians [87]. Some studies suggest that H2A.Z influences nucleosome positioning and chromatin structure. Slight nucleosome positioning changes upon H2A.Z deletion were evident at the *GAL1* locus [191]. In *in vitro* experiments it could be shown that H2A.Z-containing nucleosomes occupy different positions compared to canonical nucleosomes. Furthermore, arrays of H2A.Z containing nucleosomes impeded the formation of inter-fibre interactions but enhanced the formation of intra-fibre interactions and folding into higher order chromatin structures [192]. However, other studies found that H2A.Z is not implicated in nucleosome positioning [107, 193].

1.3.4 RNA Polymerase II and the transcriptional process

After discussing all the factors establishing contact with nucleosomes at promoters and over coding sequences (CDS), one factor having extensive contact to nucleosomes is missing: The RNA-polymerase II (Pol II) itself. In *in vitro* experiments nucleosomes were a barrier for Pol II passage [194]. Though, addition of factors influencing chromatin structure like remodelers (RSF or ISW2) or histone chaperones (FACT) facilitated *in vitro* transcription initiation and elongation [195-197]. The fate of nucleosomes during polymerase passage has been extensively studied mostly in *in vitro* but also in *in vivo* experiments. Initially, Pol II encounters one of the two H2A-H2B dimers and probably gains access to nucleosomal DNA through DNA breathing, which takes place in very short intervals of only about 250 ms and frees about the first 20 bp of nucleosomal DNA [198]. Subsequently, nucleosomes are disassembled through the successive processes of opening of the $(H3\text{-}H4)_2$ tetramer/ (H2A-H2B) dimer interface, H2A-H2B dimer release and $(H3\text{-}H4)_2$ removal [199, 200]. In agreement with those results, during *in vitro* transcription, a single H2A- H2B dimer is removed during first passage of polymerase and the remaining hexamer is subsequently evicted during the second round of polymerase passage, thus proposing dependence of histone displacement from density of transcribing polymerase molecules [201]. The like was seen monitoring histone turnover *in vivo*. Histone H3 turnover was rather low in gene bodies and turnover rate correlated with RNA-Polymerase II occupancy [202]. On the contrary, turnover rates of H2B were high in gene bodies of active and inactive genes [203]. Employing biochemical methods, optical tweezers and AFM a looping model for Pol II passage through nucleosomes was proposed and confirmed by independent groups applying various methods [204-206]. According to this model, the formation of an intra-nucleosomal loop allows histones to contact DNA up- and downstream of transcribing polymerase, thus enabling histone transfer in *cis*. Investigating the composition of nucleosomes present after *in vitro* transcription, a dependence of histone transfer on transcription rate was suggested [206]. Possibly, slow transcription might allow transfer of the whole octamer, while fast transcription might lead to H2A-H2B disassembly and transfer of hexamers and even faster transcription might result in octamer loss before histone transfer can take place.

Passage of Pol II through chromatin is accompanied by various factors, namely chromatin remodelers, histone chaperones and histone modifying enzymes, either through direct interaction with elongating Pol II or through indirect interactions. Of course, this high complexity of the transcription process makes it rather difficult to separate the action of RNA-Polymerase itself and the action of factors implicated in the transcription process in order to assign the task of a nucleosome positioning determinant to RNA-Polymerase.

In *S. pombe* and mammalian cells, nucleosomes are only in register with the TSS as a reference point at active, but not at inactive genes [8, 79, 207]. In metazoans, polymerase pausing at TSS is a frequently observed phenomenon [78, 79]. Interestingly, also genes with paused polymerase show positioned nucleosomes over gene bodies and a downstream shift of the +1 nucleosome in human and fly. In *S. cerevisiae*, depletion of the largest RNA Polymerase subunit Rpb1 led to a shift of nucleosomes away from the NDR [208]. Recently, a clever experimental setup of the Rando and Struhl laboratories gave further indications of a connection between nucleosome positioning and transcription [209]. They used a system where *S. cerevisiae* strains carried DNA of other yeast species (*K. lactis* or *D. hanseii*) on yeast artificial chromosomes (YACs) and compared nucleosome positioning and transcription of endogenous loci and loci on YACs. Interestingly, on YACs generation of fortuitous NDRs with positioned nucleosomes and active transcription events were observed. Strikingly, the length of transcripts correlated with the length of positioned arrays. Such a correlation has also been observed for endogenous transcripts in *S. pombe* [8]. However, in all those experimental setups and observations a direct effect of Pol II on nucleosome positioning and indirect effects of other factors accompanying Pol II elongation cannot be distinguished.

1.4 Objective

Since regular positioning patterns of nucleosomes at promoters and over gene bodies were detected in budding yeast [76], research interest in the nucleosome positioning field increased immensely. Strikingly, similar nucleosome patterns were found in other organisms like *S. pombe*, *C. elegans*, *D. melanogaster* and even humans [8, 77-79]. The question of which factors those nucleosome patterns determine and which purpose regular positioned nucleosomes fulfil arose.

We decided to use the fission yeast *S. pombe* as a model organism in order to find answers to those questions as *S. pombe* is easy to manipulate and as its chromatin biology is similar to metazoans.

We aimed to screen several candidate factors for implication in setting up nucleosomal patterns around TSSs by examining chromatin patterns of strains depleted for the respective factors in comparison to wildtype. Furthermore, we wanted to shed light on the role of transcription in nucleosome positioning in *S. pombe*. For this purpose on the one hand we mapped nucleosome occupancy of a temperature-sensitive polymerase mutant at the permissive temperature and on the other hand we mapped nucleosome occupancy before and after the switch of biological conditions that is accompanied by large changes in the transcriptional program.

2 Material and Methods

2.1 Materials

2.1.1.1 Chemicals

All chemicals not listed were purchased in analytical grade from Merck.

6- Azauracil	Sigma
Adenine	Sigma
Agarose	BIO&SELL / Biozym
Amino acids	Sigma
Ammonium hydroxide	Sigma
Ampicillin	Roth
ATP	Sigma
α-P^{32}- dCTP	Hartmann Analytics
Bacto agar	Becton Dickinson
Biotin	Sigma
Boric acid	VWR
Bromophenolblue	Merck
BSA, purified	NEB
β-mercaptoethanol	Sigma
Chloroform	Merck
Complete EDTA-free protease inhibitor	Roche
Creatine phosphate	Sigma
DMSO	Sigma
dNTP-mix	NEB
DTT	Roth
EDTA	VWR
EGTA	Roth
Ethanol	VWR
Ethidiumbromide	Roth
Formaldehyde	Sigma

Glucose, D(+)	Merck
Glycogen, for molecular biology	Roche
Hepes	Roth
Hydroxylapatite resin	Biorex
Igepal	Sigma
Isoamylalcohol	Roth
Isopropanol	Honeywell
Kanamycin	Sigma
Myo-inositol	Sigma
Nicotinic acid	Sigma
Orange G	Sigma
Pantothenic acid	Sigma
Phenol	Sigma
PMSF	Sigma
Potassium hydrogen phtallate	Sigma
SDS	Serva
Spermidine	Sigma
Triton X-100	Sigma
Tween 20	Sigma
Uracil	Sigma
Vectashield with DAPI	Vector

2.1.1.2 Enzymes

Creatine Kinase	Roche
MNase	Sigma
Proteinase K	Roche
Restriction endonucleases	NEB
RNase A	Roche
Taq DNA Polymerase	NEB
Zymolyase 100T	MP Biomedicals

2.1.1.3 Other

Amicon Centrifugal Units, 50K	Millipore
2-Log DNA Ladder (0.1–10.0 kb)	NEB
Dialysis membrane Spectra/Por, MWCO: 3.500 Da	Roth
Fast PES Bottle Top Filter, 500ml, 0.2 µm Pore size	Nalgene
Freeze ‘N Squeeze Gel extraction kit	Biorad
GeneChip Hybridization, Wash and Stain Kit	Affymetrix
GeneChip Mapping 10K Xba Assay Kit, 900441	Affymetrix
GeneChip S. Pombe Tiling 1.ORF Array	Affymetrix
Miracloth	Merck
Nylon Transfer membrane, Biodyne B 0.45 µm	Pall Corporation
Pantothenic acid	Sigma
Prime-It II Random Primer Labeling Kit	Stratagene
QIAGEN Plasmid Maxi Kit	Qiagen
QIAGEN Plasmid Midi Kit	Qiagen
QIAGEN Plasmid Mini Kit	Qiagen
QIAquick Gel Extraction Kit	Qiagen
QIAquick PCR Purification Kit	Qiagen
Quantum PrepTM Freeze ‘N Squeeze DNA Gel Extraction Spin Columns	BioRad
Quick spin columns for radiolabeled DNA, Sephadex G-50 Fine	Roche
RNA 6000 nano	Agilent
Siliconised reaction tubes, 1.5 ml	Biozym
Sterile syringe filter 0.2 µm and 0.45 µm	VWR
Super RX Fuji medical X-ray film	Fuji

2.1.1.4 Media, buffers and solutions

2.1.1.4.1 Media for *E. coli*

Luria-Bertani (LB) –medium:

1.0% Bacto tryptone

1.0% NaCl

0.5% Bacto yeast extract

The pH was adjusted to 7.0 with 10 M NaOH. For preparation of plates 1.5% Bacto agar was added. Medium was autoclaved for 20 min at 120 °C.

2.1.1.4.2 Media for *S. pombe*

Yeast Extract with Supplements (YES)-medium:

0.5% Bacto yeast extract

3.0% glucose

0.7 g/l amino acid mix (adenine, leucine, histidine, uracil, lysine, arginine, glutamine)

Edinburgh Minimal Medium (EMM):

3 g/l potassium hydrogen phthallate

2.2 g/l Na_2HPO_4

5 g/l NH_4Cl

20 g/l glucose

20 ml/l 50x salt stock

1 ml/l 1000x vitamin stock

0.1 ml/l 10000x mineral stock

Edinburgh Minimal Medium w/o nitrogen (EMM-N):

3 g/l potassium hydrogen phthallate

2.2 g/l Na_2HPO_4

20 g/l glucose

20 ml/l 50x salt stock

1 ml/l 1000x vitamin stock

0.1 ml/l 10000x mineral stock

Media were sterile filtered.

For preparation of plates, glucose was at first omitted, 2.4% Bacto agar was added. Medium was autoclaved for 20 min at 120 °C and autoclaved 50% glucose solution was added before pouring plates.

50 x salt stock

52.5 g/l $MgCl_2.6H_2O$

0.735 g/l $CaCl_2.2H_2O$

50 g/l KCl

2 g/l Na_2SO_4

1000x vitamin stock

1 g/l pantothenic acid

10 g/l nicotinic acid

10 g/l inositol

10 mg/l biotin

10000x mineral stock

5 g/ boric acid

4 g/l $MnSO_4$

4 g/l $ZnSO_4.7H_2O$

2 g/l $FeCl_2.6H_2O$

0.4 g/l molybdic acid

1 g/l KI

0.4 g/l $CuSO_4$.5H2O

10 g/l citric acid

All stocks were filter sterilized and stored at 4 °C.

2.1.1.4.3 Buffers and solutions

Ampicillin stock solution	100 mg/ml Ampicillin 1000x
Denaturation buffer	0.5 M NaOH 1.5 M NaCl
Denhardt (10x)	5% (w/v) SDS 10 mM EDTA, pH 8.0 0.2% (w/v) BSA 0.2% (w/v) Ficoll 0.2% (w/v) PVP40
Dialysis buffer	20 mM Hepes/KOH, pH 7.5 20% glycerol 50 mM NaCl 1 mM EGTA, pH 8.0 5 mM DTT

	Complete protease inhibitor
DTT stock solution	1M DTT
Ex50 buffer	10 mM Hepes/NaOH, pH 7.6 50 mM NaCl 1.5 mM $MgCl_2$ 0.5 mM EGTA, pH 8.0 10% (v/v) glycerol 1 mM DTT 0.2 mM PMSF
Genomic DNA buffer 1	0.9 M sorbitol 0.1 M EDTA 50mM DTT pH 7.5
Genomic DNA buffer 2	50 mM Tris-HCl 50 mM EDTA, pH 8.0
High-salt buffer	10 mM Tris/HCl, pH 7.6 2 M NaCl 1 mM EDTA, pH 8.0 1 mM ß-mercaptoethanol 0.05% Igepal
Hydroxyurea	Sigma
Kanamycin stock solution	10 mg/ml Kanamycin 1000x
Loading buffer (6x)	0.25% Orange G 30% glycerol
Loening buffer (10x)	0.4 M Tris 0.2 M NaOAc(3 H_2O) 0.01 M EDTA, pH 8.0 2% (v/v) acetic acid
Low-salt buffer	10 mM Tris/HCl, pH 7.6 50 mM NaCl 1 mM EDTA, pH 8.0 1 mM ß-mercaptoethanol 0.05% Igepal
Lysis buffer	15 mM HEPES-KOH, pH 7.5 10 mM KCl

	5 mM $MgCl_2$ 0.1 mM EDTA 0.5 mM EGTA 17.5% (w/v) sucrose 1 mM DTT 0.2 mM PMSF 1 mM sodium metabisulfite
MNase stock solution (Sigma)	500 U MNase were resuspended in 850 µl Ex50 buffer
NP Buffer	1 M sorbitol 50 mM NaCl 10 mM Tris/HCl, pH 7.4 5 mM $MgCl_2$ 1 mM $CaCl_2$ 0.75% (v/v) Igepal 1 mM β-mercaptoethanol 0.5 mM spermidine
NP-S buffer (+10mM EDTA, $–Mg^{2+}$, $-Ca^{2+}$)	50 mM NaCl 10 mM Tris- HCl, pH 7.5 0.075 % igepal 10 mM EDTA, pH 8.0 0.5 mM spermidine
PMSF stock solution	200 mM PMSF in 2-propanol
Prehybridization buffer	2x SSC 1x Denhardt 0.1 mg/ml salmon sperm DNA
Preincubation solution	20 mM Na_2HPO_4 20 mM citric acid 40 mM EDTA, pH 8.0 28.6 mM β-mercaptoethanol
Proteinase K stock solution	20 mg/ml in 10 mM Tris/HCl, pH 8.0
RNase A stock solution	10 mg/ml in 5 mM Tris/HCl, pH 7.5 boiled for 15 min at 100 °C, slowly cooled down
Sorbitol/Tris buffer	1 M sorbitol

	50 mM Tris/HCl, pH 7.4 10 mM β-mercaptoethanol
SSC (20x)	3 M NaCl 0.3 M sodium citrate (dihydrate)
STE buffer	0.1 M NaCl 10 mM Tris/HCl, pH 8.0 1 mM EDTA, pH 8.0
Suc-buffer	15 mM HEPES-KOH, pH 7.5 10 mM KCl 5 mM $MgCl_2$ 0.05 mM EDTA 0.25 mM EGTA 1.2% (w/v) sucrose 1 mM DTT 0.1 mM PMSF
TAE	40 mM Tris acetate 1 mM EDTA, pH 8.0
TE, pH 7.4	10 mM Tris/HCl, 7.4 1 mM EDTA, pH 8.0
TFBI	30 mM K acetate 100 mM KCl 50 mM $MnCl_2$ 15% (v/v) glycerol pH 5.8
TFBII	10 mM MOPS/NaOH, pH 7.0 75 mM $CaCl_2$ 10 mM KCl 15% (v/v) glycerol
Tris/Glycine buffer (5x)	144 g/l glycine 30 g/l glycerol

2.1.1.5 Oligonucleotids and plasmids

2.1.1.5.1 Oligonucleotids

Oligonucleotids (Sigma) used for probe generation for indirect end labelling experiments:

Primer name	Primer sequence
SPCC613.10-F	TTCAAAGACTAAAGGAAGGGT
SPCC613.10-R	GTGGATTTGTTTAAAAGCTAAG
SPCC4G3.08-F	ACCTTGAGCCGATACCTGAG
SPCC4G3.08-R	TCTTCTTGAGACGCGCGTGT
SPBC1685.14c-F	GGACTGAGAATACTCCTAATGC
SPBC1685.14c-R	GATGAACAGTGCACAAAACAAAAGC

2.1.1.5.2 Strains

E. coli strain:

Strain	Selection marker	Source
DH5α	amp	Genentech, San Francisco

S. pombe strains:

Strain	Genotype	Source
Hu303	*h- 972*	Karl Ekwall
K240/Hu2261	*h- leu1-32*	Yamada et al. [136]
KYP176/Hu2262	h^- *leu1-32 snf21-36(ts)*	Yamada et al. [136]
Hu2314	h^+*snf21-36(ts)swr1D::ura4+ ura4D leu1-32*	Karl Ekwall, *snf21-36(ts)* allele from Yamada et al. [136]
Hu2239	h^- *hrp1::ura4 ade6-M210 leu1-32 ura4-D18*	Karl Ekwall
Hu0574/EJY322	h^+ *ade6-M216 leu1-32 ura4-D18 hrp3::leu2+*	Karl Ekwall, Jae et al. [167]
Hu0575/EJY321	h^- *ade6-M210 leu1-32 ura4-D18 hrp3::leu2+*	Karl Ekwall, Jae et al. [167]
Hu0807	h^- *hrp3:: leu2+ leu1-32*	Karl Ekwall, Walfridsson et al. [174]

Hu2303	*h^+ hrp1::ura4 hrp3::leu2+ ade6-M210/6 leu1-32 ura4-D18*	Karl Ekwall
Hu2304	*h^+ hrp1::ura4 hrp3::leu2+ ade6-M210/6 leu1-32 ura4-D18*	Karl Ekwall
Hu1294	*h^- mit1::KanMX6 leu1-32 ade6-210 ura4-DS/E*	H. Bhuiyan
Hu1582	*h^+ set2::KanMX leu1-32*	Karl Ekwall
Hu2127	*htz1::KanMX swr1::ura4 ade6-M210/6 leu1-32 ura4D18*	Karl Ekwall
Hu801	*h^- rpb7-G150D*	Karl Ekwall
Hu802	*h^- clr6-1*	Bjerling et al. [210]

2.2 Methods

2.2.1 General molecular biological methods

2.2.1.1 Generation of competent *E. coli* cells

Chemically competent *E. coli* cells

From an *E. coli* O/N culture, 100 ml LB-medium were inocculated and logarothmically grown until OD600 = 0.5 (Spectrophotometer, Pharmacia Biotech, Ultrospec 2000). Cells were centrifuged for 15 min at 6000 x g and 4°C (Heraeus Kendro, Cryofuge 6000i), resuspended in 30 ml icecold TFBI buffer followed by incubation for 30 min on ice. Cells were centrifuged for 5 min at 1000 x g and 4 °C (Eppendorf 5810R), resuspended in 4 ml icecold TFBII buffer and incubated for 10 min on ice. Aliquots of 100 µl- 200 µl were frozen in liquid nitrogen and stored at -80 °C.

Electrocompetent *E. coli* cells

Chemically competent *E. coli* DH5α were plated on LB-plates and grown over night (O/N) at 37 °C. The next day 50 ml LB-medium were inoculated with a single colony and grown O/N at 37 °C. Subsequently, 2 times 100 ml LB- medium were inoculated with 2 ml O/N culture each and grown until OD_{600}= 0.4-0.5. Cell cultures were centrifugated for 10 min at 4000 rpm and 4 °C (Cryofuge 6000i). Cell pellets were resuspended in 50 ml icecold ddH_2O and incubated on ice for 1 h. Cells were pelleted again, washed with 25 ml icecold ddH_2O followed by a wash with 10 ml icecold ddH_2O. Finally, pellets were resuspended in 200 µl icecold ddH_2O and directly used for transformation.

2.2.1.2 Transformation of *E. coli*

Transformation by heat shock

50-500 ng DNA were mixed with 100 µl chemically competent *E. coli* cells. The mixture was incubated for 20 min on ice. Next, cells were heat shocked for 45 sec at 42 °C followed by incubation for 2 min on ice. 1 ml pre-warmed LB-medium was added and cells were incubated for 45 min at 37°C while shaking. Subsequently, cells were plated on LB-agar plates containing appropriate antibiotics and grown O/N.

Transformation by electroporation

50-500 ng DNA were mixed with 100 µl freshly prepared electrocompetent *E. coli* cells. Subsequently, the mixture was transferred to a pre-cooled (4 °C) electroporation cuvette and the cuvette was inserted into the electroporation tray. A pulse was applied (2500 V, 25 µF, 200 Ω, Gene Pulser, Biorad), 1 ml pre-warmed LB-medium (37 °C) was added, the mixture was transferred to 15 ml falcon tubes and incubated for 1h at 37 °C shaking. Cells were plated in appropriate dilutions on LB-agar plates containing appropriate antibiotics.

2.2.1.3 Isolation of plasmids from *E. coli*

Plasmid DNA was isolated by use of QIAGEN Plasmid Mini, Midi and Maxi Kits according to manufactor's instructions.

2.2.1.4 Polymerase Chain Reaction (PCR)

PCRs were carried out in a total volume of 50 µl containing 1 x concentrated PCR reaction buffer, 200 µM dNTPs, 0.2 µM forward primer, 0.2 µM reverse primer, 50-200 ng template DNA and 1.25 U DNA Polymerase.

2.2.1.5 DNA purification by phenol/chloroform extraction

For phenol/chloroform extraction of samples $NaClO_4$ was added to a final concentration of 1M. One volume of phenol was added and samples were vortexed for 1-3 min on the highest setting. One volume of chloroform-isoamylalcohol (IAC, ratio 25:1) was added and samples were vortexed as before. Next, samples were centrifuged in a tabletop centrifuge for 5 min at maximum speed and RT. The supernatant was carefully transferred to a fresh tube, one volume of IAC was added and samples were centrifuged again. The supernatant was carefully transferred to a new tube.

2.2.1.6 DNA precipitation

DNA precipitation was carried out in the presence of salt (either $NaClO_4$ in a final concentration of 1M or NaCl in a final concentration of 0.2M) and 0.7 volumes of isopropanol or 2.5 volumes of ethanol. Samples were incubated for 10 min on ice or O/N at 4 °C and subsequently centrifuged for 20-45 min at maximum speed and 4°C (Eppendorf 5417 R or 5810R). Pellets were washed in 70% ethanol and centrifuged for 5 min at maximum speed and RT. Pellets were air-dried and resuspended in TE buffer or ddH_2O.

2.2.1.7 DNA quantification

DNA was quantified spectrophotometric measuring absorbance at a wavelength of 260 nm (Nanodrop ND 1000, Peqlab). Purity of DNA samples was determined by measuring absorbance at a wavelength of 280 nm (maximal absorbance of proteins and RNA) and calculation of the absorbance ratios at 260nm and 280nm (260/280). A clean DNA solution has a ratio of ~1.8.

2.2.1.8 Horizontal and vertical agarose gel electrophoresis

Horizontal gel electrophoresis

Depending on the size of DNA fragments, 1.0-1.7% agarose gels were prepared. Depending on the purpose, gels were prepared and run either in TAE buffer or Tris/glycine buffer. Ethidium bromide was added to the dissolved and cooled agarose to a final concentration of 0.5 µg/ml. DNA samples were mixed with 6x loading buffer containing Orange G. Gels were run at 80-150 V. DNA bands were visualized with UV light in a gel documentary system (Peqlab).

Vertical gel electrophoresis

For Southern blotting vertical gels were prepared. 6 g agarose were dissolved in 400 ml Loening buffer, 20 µl ethidium bromide was added and agarose was poored in vertical chambers. Loening buffer was used as running buffer and samples were mixed with 6 x loading buffer containing bromophenol blue. Gels were constantly cooled with tap water while runnig at 100V for ~3 h.

2.2.1.9 Southern blot, preparation of radioactively labelled probes and hybridization

DNA on agarose gels was denaturated for 20 min in denaturation buffer. Blot membranes were soaked first in ddH_2O followed by 20 x SSC buffer. Whatman papers were soaked in 20 x SSC as well. The gel was placed on two Whatman papers hanging over a glass plate into a tray filled with 20 x SSC and the blot membrane and three Whatman papers (two soaked in 20 x SSC, one dry) were placed on top. A thick stack of paper was placed on top followed by another glass plate and weight to allow even transfer of DNA onto the membrane. DNA transfer was conducted O/N. Subsequently, the membrane was baked for 2 h at 80 °C. The membrane was washed in 3 x SSC buffer for 30 min at 68 °C followed by 2 h at 68

°C in 3 x SSC/1 x Denhardt. Next, the membrane was prehybridized for 1 h at 68 °C (rotating oven) in 25 ml prehybridization buffer containing denaturated salmon sperm DNA to prevent unspecific binding of probe DNA.

For radioactively labelling of DNA fragments the Prime-It II Random Primer Labeling Kit was used. 12 µl DNA solution containing 50 ng probe DNA were mixed with 5 µl random primer mix, denatured at 95 °C for 5 min and cooled on ice. 5 µl dCTP buffer, 2.5 µl α^{32}p dCTP (3000 µCi/mmol) and 0.5 µl Klenow Polymerase were added and the mixture was incubated for 10 min at 37 °C. 100 µl STE buffer was added and the mixture was freed from unbound radioactive labelled dCTP by a Sephadex QuickSpin G-50 column.

The radioactively labelled probe was denatured for 5 min at 95 °C, cooled on ice and the membrane was incubated with 5 ml prehybridization buffer and 60 µl probe at 68 °C O/N in a rotating oven. The membrane was rinsed 3 times with 2 x SSC followed by 3 times in 2 x SSC/1 x Denhardt at 68 °C for 30 min each wash. Afterwards, the blot was wrapped in plastic wrap and exposed to an X-ray film.

2.2.1.10 DNA extraction from agarose gel

DNA bands were visualized on an UV table (Herolab UVT-20M) and desired bands were excised with a scalpel. DNA was either extracted with the QIAquick gel extraction kit (Qiagen) or the Freeze ‘N Squeeze Gel extraction kit (Biorad) according to the manufactor’s instructions.

2.2.2 General methods for working with *S. pombe*

2.2.2.1 Growth of *S. pombe* strains

With the exception of temperature sensitive strains, liquid cultures were grown in YES-medium at 30 °C. The *snf21-ts* mutant strain was grown for ~30 h at the permissive temperature (25 °C) followed by 6 h at the non-permissive temperature (34 °C). The *rpb7-ts* mutant strain was grown for ~30 h at the permissive temperature (25 °C) followed by 6 h at the non-permissive temperature (36 °C).

2.2.2.1.1 Nitrogen starvation

Wt cells (Hu303) were grown for ~24 h in minimal medium containing nitrogen (EMM) at 30 °C. Subsequently, cells were expanded in 1 l EMM and grown to 2 x 10^6 cells/ml O/N. Cells were counted employing a counting chamber (Bürker). Cells were harvested, washed three times in minimal medium lacking nitrogen (EMM-N), resuspended in EMM-N to a density of 2 x 10^7 cells/ml and grown for 48 h at 30 °C. Cells were counted. Viability of cells was checked by plating assay. For MNase-seq 2.5 x 10^9 cells were removed and processed immediately. To the remaining cells 4 x volume of EMM was added and cells were grown for 2 h at 30 °C. Cells were counted, check for viability was conducted and 2.5 x 10^9 cells were used for preparation of MNase-seq samples.

2.2.2.2 Viability assay

Viability was checked by a colony counting assay. K240 (wt) and KYP176 (*snf21-ts*) were grown for ~30 h at 25 °C followed by a shift to 34 °C. During the growth at 34 °C, cells were counted every 2 h and 200 cells were plated on YES-plates in duplicates and grown for four days at 25 °C. Colonies were counted and percentage survival was calculated with 200 cells set to 100 %. For the nitrogen starvation experiment, cells were plated likewise, but grown at 30 °C.

2.2.2.3 Spotting assay

YES-medium plates containing 5 mM, 7.5 mM and 10 mM hydoxyurea (HU) dissolved in ddH_2O, or 100 µg/ml, 200 µg/ml and 300 µg/ml 6-azauracil (6-AU) dissolved in 1M ammonium hydroxide were prepared. Logarithmically growing cells were counted and equal numbers were spotted in serial dilutions on freshly prepared plates.

2.2.2.4 Microscopy

K240 (wt) and KYP176 (*snf21-ts*) were grown for ~30 h at 25 °C followed by 6 h at 34 °C. 2 x 10^7 cells were harvested and fixed in ice-cold 70 % ethanol. After rehydration, cells were spotted on slides and embedded in DAPI-containing Vectashield mounting medium. Microscopy was carried out with an Axiovert 200 microscope (EC Plan-Neofluar 63x/1.4 NA oil Ph2 (differential interference contrast [DIC]II) objective (Carl Zeiss, Inc.)). Image processing was performed with AxioVision software (Carl Zeiss, Inc.).

2.2.2.5 Isolation of genomic DNA

2 x 120 ml of a logarithmical cell culture were grown to OD_{600} = 5.0. Cells were harvested by centrifugation for 10 min at 4000 rpm and RT (Eppendorf 5810R), washed in 50 ml ddH_2O and resuspended in genomic DNA buffer 1. Next, 12.5 mg zymolyase dissolved in 200 µl ddH_2O was added and incubated shaking in a water bath for 30 min at 30 °C. Spheroplasts were pelleted by centrifugation for 5 min at 4000 rpm, resuspended in genomic DNA buffer 2, and after addition of 150 µl 20% SDS incubated for 30 min at 65 °C. Next, 1 ml 5 M potassium acetate was added and the sample was incubated for 60 min on ice. Samples were centrifuged for 30 min at 15 000 rpm and 4 °C (Sorvall RC 6 plus, rotor SS34). The supernatant was transferred to a new falcon tube, DNA was precipitated with ethanol and NaCl and resuspended in 300 µl TE buffer, pH 7.5. After addition of 15 µl RNase A (10 mg/ml),

samples were incubated for 30 min at 37 °C. A phenol/chloroform extraction followed by DNA precipitation with isopropanol was conducted, samples were resuspended in 200 µl TE, pH 7.5 and stored at 4°C.

2.2.3 Nucleosome mapping by MNase-chip

2.2.3.1 Preparation of mononucleosomal DNA

The protocol published by Lantermann et al. [211] was used with slight adaptations. Cells were grown to a density of 5 x 10^6 cells/ml (OD_{600} ~0.5) and crosslinked with 0.5% formaldehyde for 20 min at RT. The crosslinking reaction was stopped by addition of glycine to a final concentration of 125 mM for 10 min at RT. Cells were harvested by centrifugation for 10 min at 4000 rpm and 4 °C (Heraeus Cryofuge 6000i) and washed with 50 ml ddH_2O. Cell pellet was resuspended in 20 ml preincubation solution and incubated at 30 °C in a waterbath with shaking for 10 min. Cells were pelleted, resuspended in 10 ml Sorbitol/Tris buffer, 10 mg zymolase dissolved in 300 µl ddH_2O was added and samples were incubated at 30 °C in a waterbath with shaking for 30 min. Spheroplasts were pelleted, washed with 40 ml Sorbitol/Tris buffer and resuspended in NP-buffer in an endvolume of 7.5 ml. To achieve a normal digestion degree MNase was added to an endconcentration of 667 U/ml and to achieve a lower degree of digestion MNase was added to an endconcentration of 133 U/ml. Samples were incubated in a waterbath at 37 °C for 20 min. MNase digest was stopped with 1 ml 5% SDS/ 100 mM EDTA. 400 µl RNase A (10 mg/ml) was added and samples were incubated at 37 °C for 45 min. Subsequently, 450 µl Proteinase K was added and for Proteinase K digest and reverse crosslinking samples were incubated in a waterbath at 65 °C for 16 h. Samples were pre-cooled on ice, 2.5 ml 3 M potassium acetate pH 5.5 (Qiagen Maxi Prep Kit, Buffer P3) was added, samples were incubated for 10 min on ice, centrifuged for 10 min at 4000 rpm and 4 °C (Eppendorf 5810R) and the supernatant was transferred to a new tube. The supernatant was phenol/chloroform extracted, DNA was precipitated with isopropanol in the presence of 5 µl glycogen (20 mg/ml) and the pellet was resuspended in 200 µl ddH_2O. Samples were supplied with 6 x loading buffer containing Orange G and gelelectrophorised in 1.7% agarose gels prepared with Tris/Glycine buffer for 2-3 h at 150 V. DNA bands corresponding to mononucleosomal DNA were cut out and DNA was extracted by usage of the Freeze N' Squeeze kit. DNA was precipitated with isopropanol and NaCl and the pellet was resuspended in 100 µl ddH_2O.

2.2.3.2 Sample fragmentation and hybridization to Affymetrix tiling arrays

In order to achieve proper hybridization to the Affymetrix tiling arrays, DNA needs to be fragmented to an average fragment length of ~50 bases. 10 µg mononucleosomal

DNA was transferred to a new tube, lypholyzed to a volume of 20.25 µl and Tris buffer pH 7.4 was added to a final concentration of 10 mM. Fragmentation was carried out with the AffymetrixGeneChip Human Mapping 10 K Xba assay Kit according to manufactor's instructions. 22.5 µl containing 10 µg mononucleosomal DNA were mixed with 2.5 µl 10 x Fragmentation buffer and 2.5 µl Fragmentation Reagent dilution mix (containing DNase I) and incubated for 1 h at 37 °C. DNase I was inactivated by heat (15 min at 95 °C). Fragment size was checked on the Bioanalyzer (Agilent Technologies) with RNA 6000 Nano chips (programme: Eukaryote Total RNA Nano). Biotin-labelling of fragmented samples was carried out by employing the AffymetrixGeneChip Human Mapping 10 K Xba assay Kit according to manufactor's instruction. In short, 25.5 µl fragmented mononucleosomal DNA sample was mixed with biotinylated deoxynucleotidanalogon (Biotin-11-dXTP), terminal deoxynucleotide transferase (TdT) and TdT buffer followed by incubation for 2 h at 37 °C. TdT was heat-inactivated for 15 min at 95 °C. Samples were stored at -20 °C. For hybridization to Affymetrix GeneChip S. pombe Tiling 1.ORF Arrays the Affymetrix GeneChip Hybridization, Wash and Stain Kit was used according to manufactor's instructions. 28 µl of fragmented and biotin-labelled DNA samples were mixed with 14 µl DMSO, 100 µl 2 x Hybridization Mix, 3.3 µl Control Oligo B2 and 54.7 µl ddH$_2$O. The hybridization cocktail was incubated for 5 min at 99 °C followed by 5 min at 45 °C and centrifugated in a tabletop centrifuge for 1 min at maximum speed to spin down possible debris. 130 µl of hybridization cocktail were injected into a microarray and the microarray was incubated in a heating oven with a turning wheel for 16 h at 45 °C and 60 rpm. Washing and staining with streptavidin-phycoerythrin was conducted according to manufactor's instructions in a Fluidics 450 wash station. The arrays were scanned in a 3000 7G scanner and signal quantification was carried out with the GeneChip Command Console Software.

2.2.3.3 Data processing

Processing of microarray data and spectral analysis data were conducted as described in Lantermann et al. [8].

2.2.4 Nucleosome mapping by MNase-ChIP-seq

Cells were grown and treated as described for nucleosome mapping by MNase-chip until the MNase digestion step. MNase digest was stopped with 1 ml 100 mM EDTA. Buffer was exchanged against NP-S w/o Mg^{2+} Ca^{2+} buffer containing 10 mM EDTA and neither MgCl$_2$ nor CaCl$_2$ by centrifugation in Amicon Centrifugal Units, MWCO 50K (Millipore). In total 30 ml of NP-S w/o Mg^{2+} Ca^{2+} buffer were centrifuged through the column and finally, the chromatin sample was concentrated to 1 ml. 1 x Complete Protease Inhibitor and PMSF to an endconcentration of 0.2 mM were added. Samples were stored on ice in a 4 °C coldroom and shipped to USA at 4 °C. Anti-H3

ChIP and library preparation were conducted in the Pugh laboratory as described in Wal et al. [212] and raw data were analysed as described in Zhang et al. [2].

2.2.5 Nucleosome mapping by indirect end labelling

Loci examined by indirect end labelling:

Locus	Enzyme for secondary cleavage
SPCC613.10	NdeI
SPCC4G3.08	PmlI
SPBC1685.14c	SpeI

2.2.5.1 Preparation of chromatin, MNase digest and DNA purification

Cells were grown and treated as described for nucleosome mapping by MNase-chip until the washing step in 40 ml Sorbitol/Tris but crosslinking was omitted. Pellets were resuspended in 1.5 ml NP-buffer and divided into six aliquots of 300 µl. MNase was added to yield final concentrations of 0, 25, 50, 100, 225 and 450 U/ml and incubated for 10 min at 37 °C. MNase digest was stopped with 75 µl 5% SDS/50 mM EDTA. 20 µl proteinase K (20 mg/ml) was added and the samples were incubated for 1 h at 37 °C. DNA was purified by phenol/chloroform extraction in presence of $NaClO_4$ followed by DNA precipitation with ethanol. Pellets were resuspended in 250 µl TE buffer, 20 µl RNase A (10 mg/ml) was added and samples were incubated for 1 h at 37 °C. DNA was precipitated with ethanol and pellets were resuspended in 50 µl TE buffer. 5 µl of each sample were gelelectrophoresed in a 1% TAE gel and three samples digested to appropriate degrees were chosen. For indirect end-labelling samples are digested to much lower degree as for MNase-chip. For an appropriate digestion degree only a smear but no clear laddering should be observable.

2.2.5.2 MNase digest of free DNA

To control for sequence preferences of MNase free DNA was digested with MNase. DNA was prepared as described for the chromatin samples, but the MNase digestion step was omitted. Subsequently, to 20 µl purified DNA 80 µl NP-buffer was added and digested with final concentrations of 2 U/ml and 4 U/ml MNase for 10 min at 37 °C. Digest was stopped with 10 µl 0.2 M EDTA, DNA was purified by precipitation with ethanol and NaCl and resuspended in 20 µl TE buffer.

2.2.5.3 Secondary cleavage

20 µl of MNase digested chromatin samples (including mock digest) and MNase digested free DNA sample were digested in a volume of 150 µl with 40 U of an

appropriate restriction enzyme for 2 h. DNA was purified by precipitation with ethanol and NaCl and resuspended in 20 µl TE buffer.

2.2.5.4 Generation of markers

For each marker band 9 µl of DNA (from the preparation of free DNA samples but without MNase digest) were digested with the respective restriction enzyme and with the restriction enzyme used for secondary cleavage. DNA was purified by precipitation with ethanol and NaCl and resuspended in 20 µl TE buffer. For southern blotting 6.5 µl were used per lane.

2.2.5.5 Generation of probe DNA

For southern blot probe generation, DNA segments of ~300 bp length lying 300- 500 bp downstream of the secondary cleavage site were amplified by employing PCR. Amplified fragments were purified by gelextraction and precipitation with ethanol and NaCl.

2.2.6 Generation of *in vitro* chromatin

2.2.6.1 Expansion of libraries

For generation of in vitro chromatin, the *S. pombe* genomic plasmid libraries pDB248 (Ekwall laboratory), pSPL10.1 (kind gift from Mari Davidson), and pURSP1 (kind gift from Jürgen Stolz) were used. The libraries pSPL10.1 and pURSP1 were expanded in electrocompetent *E. coli* DH5α cells, cells were plated on LB-agar plates containing the appropriate antibiotics and colonies were counted to assess transformation efficiency. All colonies were pooled, glycerine cultures were prepared and stored at -80 °C. Two times 1l LB-medium were inocculated with 100 µl glycerine culture of the respective library and plasmid DNA was isolated applying the Qiagen Maxi Prep kit.

2.2.6.2 Purification of histone octamers from *D. melanogaster* embryos

Histone octamers from *D. melanogaster* embryos were purified as described in Krietenstein et al. [213]. 0-12 h old fly embryos were collected for 4-5 days and stored at 4 °C. Embryos were dechorionated in 3% sodium hypochlorid and 50 g dechorionated embryos were resuspended in 40 ml lysis buffer. Embryos were homogenized (Yamato LSC LH-21, 1000 rpm, 6 strokes), filtered through a Miracloth and centrifuged for 15 min at 8000 rpm and 4 °C (Sorvall RC 6 plus, GSA rotor). The supernatant was discarded and the upper layer of the two-phased pellet was resuspended in 50 ml suc-buffer. The pellet was washed in 50 ml suc-buffer, resuspended in 30 ml suc-buffer and homogenized with a glass dounce homogenizer (Wheaton/Fisher Scientific, pestle B, 20 dounces). 90 µl 1 M $CaCl_2$ was added and the sample was digested with 125 µl of 0.59 U/µl MNase for 5 min at 26 °C. Digest was stopped by addition of 600 µl 0.5 M EDTA. Chromatin was pelleted for 15 min at 8000 rpm and 4 °C (Sorvall GSA rotor) and pellet was resuspended in 6 ml TE pH 7.6 containing 1mM DTT and 0.2 mM PMSF. Lysed nuclei were centrifugated for 30 min at 14 000 rpm and 4 °C (Sorvall RC 6 plus, SS-34 rotor), supernatant was kept, adjusted to 0.63 M KCl and centrifugated again for 15 min at 14 000 rpm and 4 °C (Sorvall RC 6 plus, SS-34 rotor). Supernatant was filtered (with a 0.45- µm and a 0.22 µM filter) and applied to an equilibrated hydroxylapatite column. The column was washed with 0.63 M KCl/0.1 M potassium acetate, pH 7.2 for at least two column volumes and eluted with 2 M KCl/0.1M potassium phosphate, pH 7.2 and 3-ml fractions were collected. Peak fractions were tested on 18 % SDS-PAGE gels. Appropriate fractions were pooled, concentrated by ultrafiltration and stored in equal volume of 87% glycerol plus 1x complete protease inhibitors and 5mM DTT at -20 °C.

2.2.6.3 Chromatin assembly via salt gradient dialysis

Salt gradient dialysis was performed as described in Krietenstein et al. [213]. In 100 µl endvolume, 10 µg of plasmid library DNA, 10 µg of histone octamers, 20 µg bovine serum albumin, 50 µl 2x high salt buffer w/o Igepal and 5 µl 1% Igepal were mixed and transferred to a dialysis chamber. The mixture was dialysed by slowly diluting 300 ml high-salt buffer with 3 l low-salt buffer with a peristaltic pump. Subsequently, dialysis chambers were transferred to 1 l low-salt buffer and dialysed for another 1-2 h. Chromatin samples were stored at 4 °C.

2.2.6.4 MNase-ChIP-seq of *in vitro* chromatin

Mononucleosomes were generated according to Krietenstein et al. [213]. In an endvolume of 100 µl, 10 µl of chromatin assembled by salt gradient dialysis were mixed with 25 µl 4x Shifting mix lacking ATP and $MgCl_2$, 4 µl 0.25 M ammonium sulfate and 50 ng/µl creatine kinase. The mixture was incubated for 2 h at 30 °C. Subsequently, chromatin was crosslinked with a final concentration of 0.05% formaldehyde for 15 min at 30 °C. The crosslinking reaction was quenched with a final concentration of 125 mM glycine for 5 min at 30 °C. Samples were incubated with 4 µl of 50 U/ml apyrase for 30 min at 30 °C. Apyrase depletes ATP, which is only important for reconstitution experiments with cell extract, but apyrase is routinely also added to salt gradient dialysis samples to keep conditions similar. $CaCl_2$ was added to a final concentration of 1.5 mM and samples were digested with 0.0059 U/µl MNase for 5 min at 30 °C. Digest was stopped with EDTA in a final concentration of 10 mM. Samples were supplied with protease inhibitors and shipped to USA at 4°C. Anti-H3 ChIP and library preparation were conducted in the Pugh laboratory as described in Wal et al. [212] and raw data were analysed as described in Zhang et al. [2].

3 Results

3.1 Improvement of methodology

In order to map nucleosome occupancy genome-wide in *S. pombe*, chromatin was isolated and digested with MNase. Mononucleosomal DNA was gelpurified, further fragmented with DNase I to an average fragment length of 50 bp, labelled and hybridized to Affymetrix tiling arrays [211]. Fragmentation of mononucleosomal DNA turned out to be very critical to ensure proper binding of DNA to the oligonucleotides on the tiling array. We observed that fragmentation efficiency was quite variable when using the original protocol published by Lantermann et al. [211] resulting in TSS-aligned nucleosome occupancy plots of low quality (Fig. 4A, B). To ensure consistent length of DNA fragments, we improved the conditions for DNase I digest by omitting EDTA from the DNA purification step and all subsequent steps. DNase I requires Ca^{2+} and Mg^{2+} for its enzymatic activity [214]. EDTA chelates these bivalent cationes and thus, varying traces of EDTA in the preparations influence the fragmentation reaction. Applying this slightly changed protocol, we obtained not only consistency of the fragmentation reaction but also composite nucleosome occupancy maps of all genes aligned at the TSS with higher peak-trough ratio compared to occupancy maps generated with the old protocol (Fig. 4C). Apart from that, all previous observed characteristic of stereotypic nucleosome occupancy pattern around TSSs remained unchanged: A nucleosome depleted region (NDR) lies just upstream of the TSS and is followed by a downstream nucleosomal array (Fig. 4C). Upstream of the NDR no nucleosomal array forms which is contrary to nucleosome patterns observed at *S. cerevisiae* promoters [8]. Furthermore, applying the autocorrelation function for these samples revealed clear periodic patterns (data not shown). To include some degree of experimental variability, we decided to use a combination of wildtype replicates prepared with the old protocol (two replicates that showed the highest degree of periodicity compared to the other samples prepared with the old protocol) and with the new protocol (three replicates) as our standard wildtype nucleosome occupancy pattern (Fig. 4D).

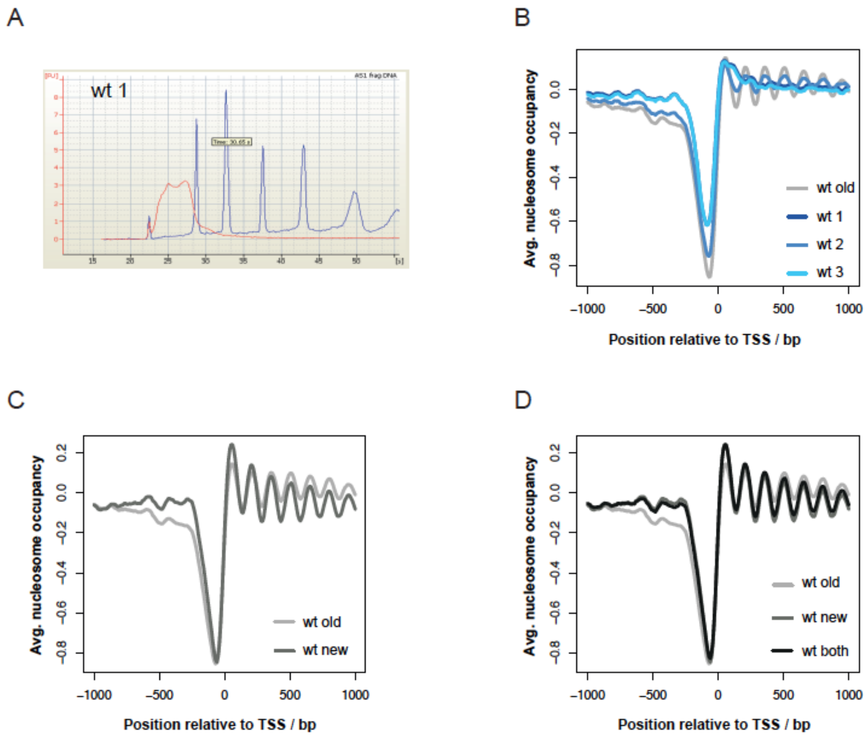

Figure 4 Slight changes of the DNase I fragmentation protocol result in nucleosome occupancy data with higher peak-trough ratio. (A) Fragment size analysis with the bioanalyzer (Agilent) exemplarily for sample wt 1 prepared with the old protocol (red line). Marker (blue line) indicates 25, 200, 500, 1000, 2000 and 6000 nt. (B) Overlay of nucleosome occupancy profiles for 4013 genes for wt (Hu303) prepared with the old protocol. Wt old (4 replicates) was generated by Alexandra Lantermann, wt 1-3 (1 sample each) showed varying fragment size after DNase I digest. (C) Overlay of nucleosome occupancy profiles for 4013 genes for wt generated with the old (Hu303, 4 replicates) and the new protocol (Hu303, 3 replicates) (D) For all further plots a combination of data sets (wt both) is used (Hu303, 2 replicates old protocol + 3 replicates new protocol).

3.2 Comparison of nucleosome occupancy maps generated by microarray hybridization (MNase-chip) and Illumina sequencing (MNase-ChIP-seq)

As the *S. pombe* Affymetrix tiling arrays we used have only a resolution of 20 bp, we wondered if a nucleosome occupancy map with higher resolution would look similar or reveal new chromatin features. Therefore, we performed Illumina sequencing on mononucleosomal DNA of wildtype cells (HU303) in collaboration with the Frank Pugh laboratory. Chromatin was isolated and digested with MNase as described for microarray experiments. Subsequently, chromatin samples were shipped to USA for anti-H3 chromatin immunoprecipitation (anti-H3 ChIP), library preparation and Illumina sequencing. We included an anti-H3 ChIP step for the following reason: Crosslinking of chromatin with formaldehyde is never complete, and when scoring all nucleosome-sized DNA fragments, crosslinked nucleosomes cannot be distinguished from not-crosslinked nucleosomes. Nucleosomes could potentially assemble at NDRs during preparation (Frank Pugh, personal communication) and such nucleosomes would be scored, too. An additional anti-H3 IP step selects for crosslinked nucleosomes and hence only true *in vivo* nucleosome positions are monitored. High-resolution nucleosome occupancy maps revealed in general nucleosome occupancy features similar to the ones seen when applying MNase-chip, i.e. a NDR followed by a downstream nucleosomal array (Fig. 5). However, the amplitude of downstream nucleosomal arrays was clearly higher in the MNase-ChIP-seq data compared to the MNase-chip data, and in addition, a weak upstream nucleosomal array could be detected.

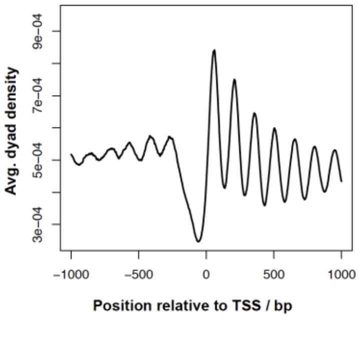

Figure 5 Weak upstream nucleosomal arrays appear in high-resolution nucleosome occupancy maps. Overlay of TSS-aligned nucleosome occupancy profiles for 4013 genes for wt (Hu303, 1 sample). Nucleosome occupancy was mapped by MNase-ChIP-seq.

3.3 Effect of MNase digestion degree on nucleosome occupancy patterns

As nucleosomes might be differently susceptible to MNase digestion, the degree to which a chromatin sample is digested might influence nucleosome occupancy maps. Yuan et al. [76] generated nucleosome occupancy maps of chromatin digested to ~80% or ~40% mononucleosomal DNA by hybridization to microarrays with a resolution of ~20 bp. They did not find significant differences between the two nucleosome occupancy maps when looking at about 6000 bp of chromosome III. However, applying high-throughput sequencing, Weiner et al. [208] showed for *S. cerevisiae* that the degree of chromatin digestion with MNase influences the nucleosome occupancy pattern around TSSs. Chromatin digestion to a lower degree resulted in higher occupancy of the -1 and the +1 nucleosome and increased occupancy at NDRs in composite nucleosome occupancy maps aligned at the TSS. Weiner et al. concluded from their results that easily digestible nucleosomes are present in the NDR that are lost during too harsh MNase digestion, while nucleosomes in the mid-coding region are rather stable. The presence of instable nucleosomes at promoter NDRs was also reported by others. In *D. melanogaster*, H3.3-containing nucleosomes were found at promoters in chromatin prepared under low to moderate salt conditions [215]. Furthermore, the presence of nucleosomes containing two histone variants, H3.3 and H2A.Z, at NDRs was demonstrated in low salt sequential-ChIP experiments in human cells [216]. However, these two studies are in dispute as in both studies crosslinking was omitted, and thus, movement of nucleosomes during preparation cannot be excluded.

We wondered if the effect monitored for less digested chromatin in *S. cerevisiae* could also be seen in *S. pombe*. Composite nucleosome occupancy maps of wildtype chromatin digested to normal degree (Fig. 6A, left panel and B) were compared to occupancy maps of chromatin digested to lower degree (1/5th of MNase) (Fig. 6A, right panel and B). Indeed, a similar and even stronger effect could be observed in *S. pombe*. Occupancy of the -1 and the +1 nucleosome was much higher and the NDR depth dramatically diminished compared to samples digested to normal degree. In addition, occupancy of nucleosomes in the gene body was decreased in the samples digested to lower degree. As these nucleosomes at NDRs could potentially be nucleosomes assembled during the preparation process, we wanted to check if we see the same effects of digestion degree when selecting for crosslinked nucleosomes with anti-H3 ChIP followed by Illumina Sequencing (Fig. 6C). In line with our microarray data we could observe higher occupancy of the -1 and +1 nucleosome and a slightly diminished NDR in chromatin samples digested to lower degree when applying anti- H3 ChIP and Illumina Sequencing. However, the occupancy changes were less pronounced in the MNase-ChIP-seq data set compared to the MNase-chip data set (Fig. 6A, C).

Instead of explaining these results from a biological point of view, i.e. unstable nucleosomes in NDRs [208], they could be explained similarly well from a purely technical point of view. MNase cuts with higher probability at longer linkers compared to shorter linkers and NDRs can be viewed as the longest linkers. Thus, when digesting chromatin with limiting amounts of MNase NDRs are preferentially digested, and hence the nucleosomes flanking the NDR, i.e. the -1 and + 1 nucleosomes are overrepresented while nucleosomes with short linkers, i.e. nucleosomes in genic regions, are underrepresented. This is exactly what can be seen in TSS-aligned nucleosome occupancy plots for chromatin digested to low degree: High occupancy of the -1 and +1 nucleosome and decreasing occupancy in genic regions in 3' direction.

As the digestion degree has such a big impact on nucleosome occupancy patterns, MNase has to be titrated carefully and digestion degree has to be kept constant between wildtype and mutant samples in order to distinguish effects ascribed to the respective mutation from effects ascribed to digestion degree.

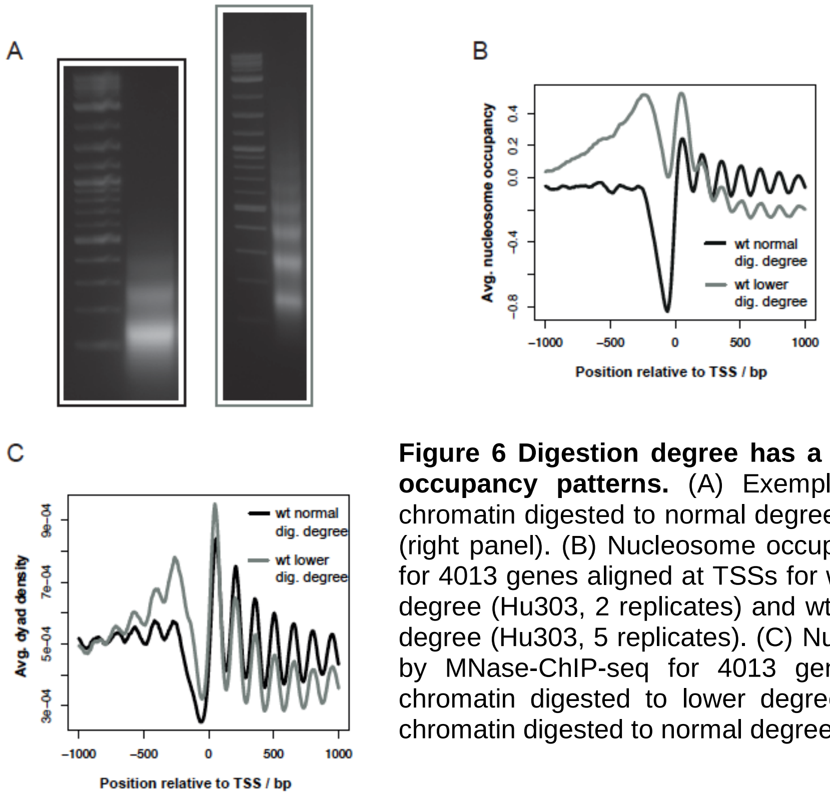

Figure 6 Digestion degree has a large effect on nucleosome occupancy patterns. (A) Exemplary agarose gel pictures of chromatin digested to normal degree (left panel) and lower degree (right panel). (B) Nucleosome occupancy mapped by MNase-chip for 4013 genes aligned at TSSs for wt chromatin digested to lower degree (Hu303, 2 replicates) and wt chromatin digested to normal degree (Hu303, 5 replicates). (C) Nucleosome occupancy mapped by MNase-ChIP-seq for 4013 genes aligned at TSSs for wt chromatin digested to lower degree (Hu303, 1 sample) and wt chromatin digested to normal degree (Hu303, 1 sample).

3.4 Annotation of bidirectional and tandem promoters

Comparison of nucleosome occupancy around TSSs between *S. pombe* and *S. cerevisiae* revealed both similarities and differences [8]. While in *S. cerevisiae* nucleosomal arrays are present both up- and downstream of the TSS in TSS-aligned composite nucleosome occupancy plots, a nucleosomal array solely downstream of the TSS is present in *S. pombe*. When plotting nucleosome occupancy for a large number of genes aligned at TSSs, upstream nucleosomal arrays are only visible when they are in register with the alignment point, i.e. the TSS. This means that even if upstream nucleosomal arrays are not present in composite nucleosome occupancy plots, they can still be present at individual loci, but just not in register with the TSS. Thus, from *S. pombe* composite nucleosome occupancy plots one cannot judge if upstream nucleosomal arrays are really not present at individual loci or if they are just not in register with the TSS.

Detailed transcriptome mapping of *S. cerevisiae* wildtype and exosome mutant (*rrp6Δ*) strains uncovered that transcription is quite pervasive in the *S. cerevisiae* genome [217]. For example, 36% of all annotated elements were found to start within a shared 5' NDR. Therefore, we wondered if appearance of upstream nucleosomal arrays in *S. cerevisiae* can be explained by upstream transcription. Thus, we took the annotation of transcriptional elements either initiating at the same NDR as downstream elements initiate (i.e. bidirectional/divergent genes) or ceasing at the same NDR as downstream elements initiate (tandem genes) of Xu et al. [217] and plotted *in vivo* (Fig. 7A) and *in vitro* reconstituted (Fig. 7B) *S. cerevisiae* nucleosome occupancy data [2] separately for genes of these two categories and for genes which do not fall in any of these two categories. Genes with bidirectional and tandem partners showed indeed very clear nucleosomal arrays, while upstream nucleosomal arrays of genes without such a partner were rather faint.

We next asked if the absence of upstream nucleosomal arrays in *S. pombe* can be explained accordingly. For this analysis we employed a list of TSSs annotated for open reading frames (ORFs) in wildtype [8], a list of TSSs annotated for non-coding transcripts in wildtype [218] and a list of cryptic unstable transcripts (CUTs) in a *rrp6Δ* mutant for a large part of chromosome II [219]. Rrp6 is a ribonuclease subunit of the exosome [220]. The exosome is responsible for RNA degradation connected to all kinds of cellular processes like RNA maturation, RNA quality control or degradation of unstable RNAs. Destruction of functional exosomes by depletion of one of its subunits allows mapping of transcripts, which are usually rapidly degraded by the exosome, so called CUTs. We first computationally defined transcripts either initiating within a common 500 bp window (potential bidirectional/divergent genes) or initiating and ceasing within a common 500 bp window (potential tandem genes). Subsequently, for the coding and non-coding genes (not for CUTs as TSSs were not assigned), we used our nucleosome occupancy data to check by eye if those transcripts share a NDR, and thus are really bidirectional or tandem genes. From this analysis we obtained a list of 564 bidirectional genes (both bidirectional partners counted separately) or 282 bidirectional promoters (shared promoters counted) and 386 tandem genes. Furthermore, for 128 ORFs, CUTs lying within a 500 bp window from the ORF's TSS could be mapped. Thus, only about 15% of annotated elements seem to share a 5' NDR in *S. pombe*.

However, for the analysis a list of CUTs annotated for only a large part of chromosome II and not the whole genome was used. Furthermore, also the list of non-coding transcripts is very likely not complete. To make reliable statements on the pervasiveness of transcription in the *S. pombe* genome, more complete transcriptome data are needed.

As with the *S. cerevisiae* data, we plotted nucleosome occupancy separately for bidirectional elements, tandem elements and remaining elements (Fig. 7C). For nucleosome occupancy data generated by MNase-chip upstream nucleosomal arrays of genes with bidirectional or tandem partners were only slightly pronounced compared to genes without such partners. We wondered if TSS-TSS distances for bidirectional promoters and TTS-TSS distances for tandem genes are too heterogeneous in *S. pombe*, and thus generating nucleosomal arrays of different registers, which would cancel each other. Therefore, we binned bidirectional or tandem transcripts according to their TSS-TSS or TTS-TSS distances, respectively, and plotted nucleosome occupancy for genes in the respective bins. Indeed, such binning uncovered upstream nucleosomal arrays for both, bidirectional and tandem genes (Figure 7E, F). As the employed Affymetrix tiling arrays have only a resolution of 20 bp and as we could detect faint upstream nucleosomal arrays in composite plots of all genes aligned at TSSs when using nucleosome occupancy maps generated by Illumina sequencing, we plotted our high-resolution nucleosome occupancy data for the three transcript classes as well (Fig. 7D). And in fact, upstream nucleosomal arrays were more pronounced for elements with bidirectional partners, however not so much for elements with tandem partners.

Another reason for the worse correlation of two TSSs in bidirectional NDRs and TTS and TSS in tandem NDRs observed in *S. pombe* in comparison to *S. cerevisiae*, could also be ascribed to improper TSSs annotations of *S. pombe* transcriptional elements.

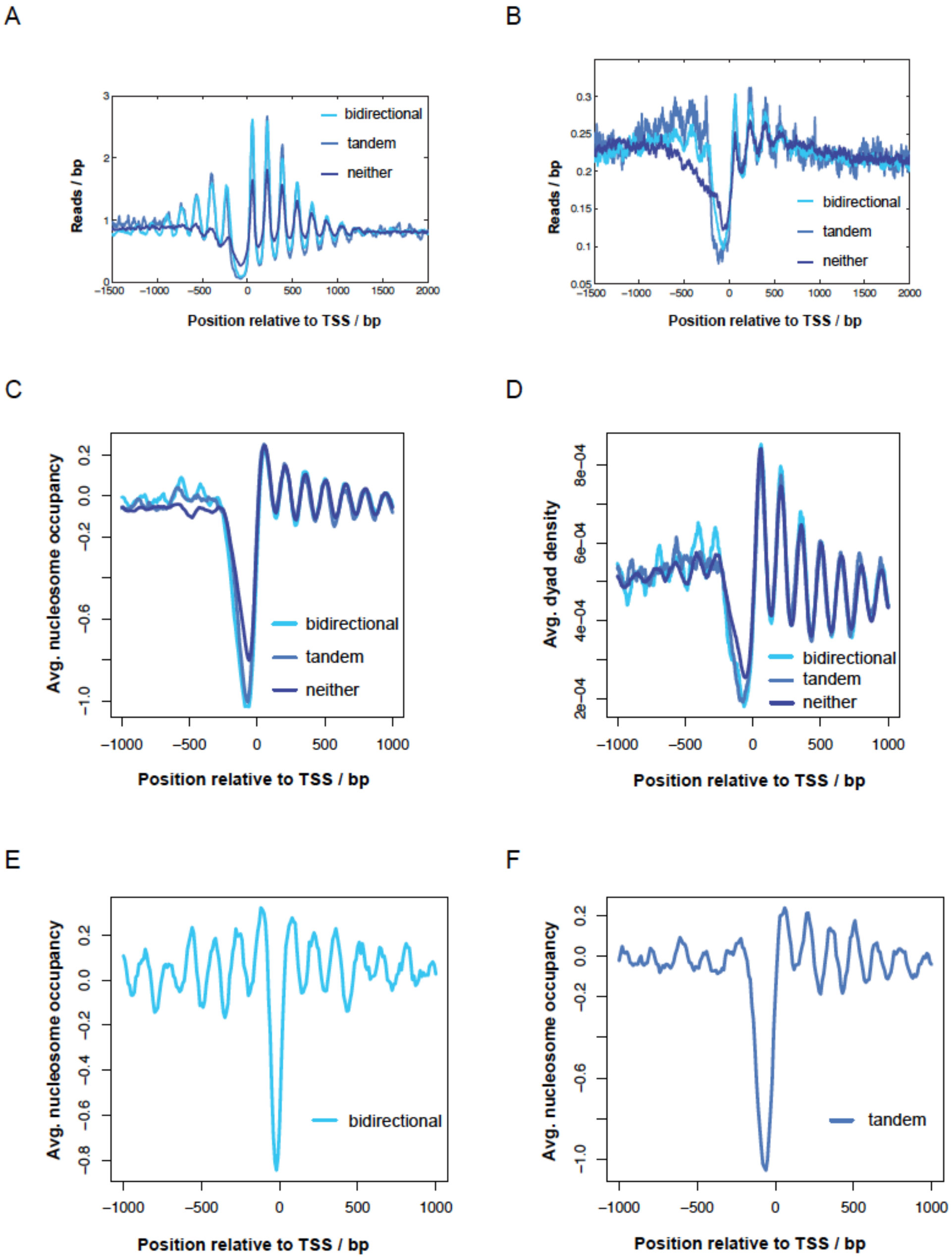

Figure 7 Upstream nucleosomal arrays can be mainly ascribed to upstream transcriptional elements sharing the 5’ NDR of the downstream transcriptional element. (A,B) Nucleosome occupancy profiles divided into 2535 bidirectional genes, 551 tandem genes and 4160 genes which are neither bidirectional nor tandem for (A) *S. cerevisiae* wt *in vivo* and for (B) *S. cerevisiae* in vitro chromatin reconstituted with cell extract and ATP [2]. (C,D) Nucleosome occupancy profiles divided into 274 bidirectional promoters, 276 tandem genes and 3465 genes which are neither for (C) *S. pombe* wt (Hu303, 5 replicates) mapped by MNase-chip and (D) *S. pombe* wt (Hu303) mapped by MNase-ChIP-seq. (E,F) Nucleosome occupancy profiles for (E) 39 bidirectional genes with TSS-TSS distance of 1-100 bp and (F) 81 tandem genes with TTS-TSS distance of 101-200 bp for *S. pombe* wt (Hu303, 5 replicates) mapped by MNase-chip. Nucleosome occupancy plots for genes in remaining bins are not shown.

3.5 Comparison of TSS annotations by RNA-chip, RNA-seq and RNA-CAGE-seq

Motivated by the observed differences between *S. cerevisiae* and *S. pombe* nucleosome occupancy periodicities upstream of the TSS, we decided to have a closer look at TSS annotations in *S. pombe* and compared three different annotations. The annotations used for comparison were an RNA-chip [221] based annotation published by Lantermann et al. [8], an RNA-seq based annotation published by Rhind et al. [9] and another RNA-seq based annotation generated by the Baehler laboratory (unpublished). The RNA-chip transcriptome data [221] were generated by directly hybridizing RNA to 50 bp resolution microarrays and binding was detected with an antibody specifically recognizing RNA-DNA hybrids. TSSs were mapped by eye for every single gene by Alexandra Lantermann. Rhind et al. and the Baehler laboratory produced cDNA from RNA and sequenced cDNA ends with high-throughput methods. TSSs were not annotated by hand but computationally. For comparison of the three data sets we plotted nucleosome occupancy for all genes aligned at their respective TSSs (Fig. 8A). Surprisingly, nucleosome occupancy patterns of genes aligned at TSSs annotated by Rhind et al. or the Baehler laboratory were not only different from nucleosome occupancy patterns aligned at TSSs annotated by Lantermann, but also worse in the following sense: The amplitude of downstream nucleosomal arrays was clearly diminished when aligning at Rhind et al. or Baehler laboratory TSSs. Furthermore, the NDR depth was slightly diminished when applying the Rhind et al. TSS annotation and remarkably diminished when applying the Baehler TSS annotation. The same was true when plotting nucleosome occupancy only for genes with TSSs annotated by all three approaches (Fig. 8B).

These differences were quite unexpected as higher resolution transcriptome mapping should result in higher resolution annotation of TSSs, which then should provide the more accurate alignment points for nucleosome occupancy maps. We think that it is very unlikely that the nominally less precise TSS annotation due to low resolution of the microarray could lead by chance to generation of “better” nucleosomal arrays. The high-throughput approaches differ in two other ways from the Lantermann TSS annotation. First, reverse transcription of RNA into cDNA not solely generates full-length but also shortened transcripts due to premature transcription termination. Accurate recognition of such aborted transcripts can be difficult and complicates reliable mapping of 5’ ends. Lantermann et al. used transcriptome data generated by directly hybridizing RNA to microarrays, and thus omitting the possibly error-prone cDNA synthesis step. Second, Rhind et al. and the Baehler laboratory mapped TSSs computationally. Such algorithms may be confounded by unclear or ambiguous signals in the data. In contrast, Lantermann et al. mapped TSSs by eye and considered only transcripts with relatively constant transcript levels over the whole gene body.

Given these discrepancies, a method combining high-resolution and confident mapping of 5’ ends is necessary. These two criteria are met by the cap analysis gene expression approach (CAGE). Here, true 5’ ends are extracted from the cDNA pool by applying a specific antibody recognizing the 5’ cap structure. Subsequently, DNA fragments are sequenced employing high-throughput technologies. We decided to annotate TSSs by this method in collaboration with the Baehler laboratory. In a first attempt, only a small fraction of the transcriptome could be confidently sequenced and used for TSS annotation. Alignment of nucleosome occupancy data to those TSSs resulted in nucleosome patterns similar to those using the Lantermann TSSs (Fig. 8C). Thus, as CAGE allows reliable mapping of 5’ ends, we conclude that the nucleosome occupancy pattern observed when aligning at Lantermann TSSs is the biologically true one.

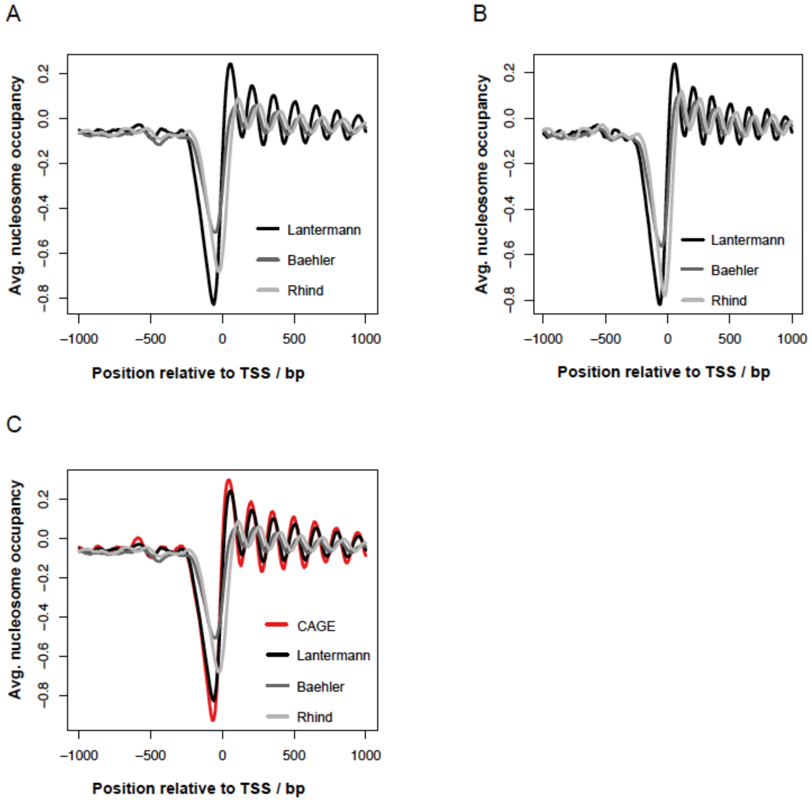

Figure 8 TSS annotation critically influences nucleosome occupancy patterns. (A) Nucleosome occupancy profiles for 4013 genes aligned at TSSs annotated by Lantermann et al. [8], for 5803 genes annotated by the Baehler laboratory, and for 5148 genes annotated by Rhind et al. [9] for wt (Hu303, 5 replicates). (B) Nucleosome occupancy profiles for 2128 genes that are all annotated by Lantermann et al., the Baehler laboratory and Rhind et al. (C) Same as (A) but additionally 999 genes aligned at TSSs annotated by CAGE.

3.6 Nucleosome occupancy patterns of strains carrying mutations in genes coding for chromatin-related factors

In order to identify factors involved in generation of nucleosome occupancy patterns around TSSs, we systematically screened strains depleted for potential nucleosome positioning determinants. We mapped nucleosome occupancy for those mutants. Furthermore, as only subgroups of genes might be affected by the respective mutation and as those effects might be masked in an overlay plot of all genes, we distinguished binding targets of the respective factor from non-binding targets for wildtype and/or transcriptional responders from non-responders for strains depleted for the respective factor. All transcriptome analyses were conducted in collaboration with the Ekwall laboratory.

3.6.1 The histone variant H2A.Z and the remodeler ATPase Swr1 do not play a major role in nucleosome positioning around TSSs

H2A.Z is highly conserved in eukaryotes [42]. Strikingly, H2A.Z was found enriched in the very well positioned +1 nucleosomes or both, +1 and -1 nucleosomes in many organisms (see introduction chapter 1.3.3). In *S. pombe*, H2A.Z (encoded by the gene pht1) is enriched at the +1 nucleosome of lowly expressed genes [49]. Its location and implication in transcriptional regulation make the histone variant H2A.Z a very attractive candidate for a possible factor involved in nucleosome positioning around TSSs. However, in *S. cerevisiae* H2A.Z does not play a direct role in nucleosome positioning at promoters [107]. An artificial NDR was generated *in vivo* by insertion of a Reb1 binding site next to a poly(dT) tract into the body of a transcriptionally quiescent gene. Here, H2A.Z deposition was not necessary for NDR formation, but followed NDR formation.

The chromatin remodeling complex SWR1 loads H2A.Z onto chromatin in two steps. First, an H2A-H2B dimer is removed and second, an H2A.Z-H2B dimer is incorporated [48]. Deletion of H2A.Z alone leads to quite strong phenotypes as H2A-H2B dimers are removed from chromatin also in the absence of H2A.Z [222]. To prevent such indirect effects, we used a *pht1Δ swr1Δ* double mutant.

Mononucleosomal DNA was prepared from a *pht1Δ swr1Δ* strain and hybridized to an Affymetrix tiling array. When comparing TSS-aligned nucleosome occupancy overlay plots of all genes for the *pht1Δ swr1Δ* mutant and wildtype, the nucleosome occupancy patterns were highly similar (Fig. 9A). Only nucleosome occupancy of the +1 nucleosome was very mildly affected, i.e. reduced, in the mutant strain. We then looked at loci bound versus unbound by H2A.Z (ChIP-chip Buchanan et al. [49]) (Fig. 9B). As already described in Lantermann et al. [8], the H2A.Z bound loci showed a very distinct nucleosome occupancy pattern, i.e. a much more shallow and more narrow NDR due to a shoulder just downstream of the -1 nucleosome and distinct peaks for the -1 to -3 nucleosome. Strikingly, this distinct nucleosome occupancy pattern was also present in the *pht1Δ swr1Δ* mutant, and thus, it cannot be caused by H2A.Z. When looking at high-resolution nucleosome occupancy data (MNase-ChIP-seq) in wildtype, a clear nucleosome peak within the NDR, i.e. just downstream of the -1 nucleosome, became visible instead of the shoulder (Fig. 9F). Next, we distinguished transcriptional responders, i.e. up- and downregulated annotated elements, from non-responders in the *pht1Δ swr1Δ* mutant compared to wildtype in collaboration with the Ekwall laboratory. When setting a threshold of 1.5 fold change, 1182 annotated elements were upregulated and 761 were downregulated, while 2949 annotated elements were unchanged (Table 2). Not all of these elements appear in the nucleosome occupancy plot as some lack a TSS annotation. Also for these subgroups of genes, no changes in nucleosome occupancy patterns between the *pht1Δ swr1Δ* mutant and wildtype could be detected (Fig. 9C, D). Interestingly, there was only very little overlap between the three subgroups (H2A.Z binding targets, upregulated transcripts and downregulated transcripts) (Fig. 9E).

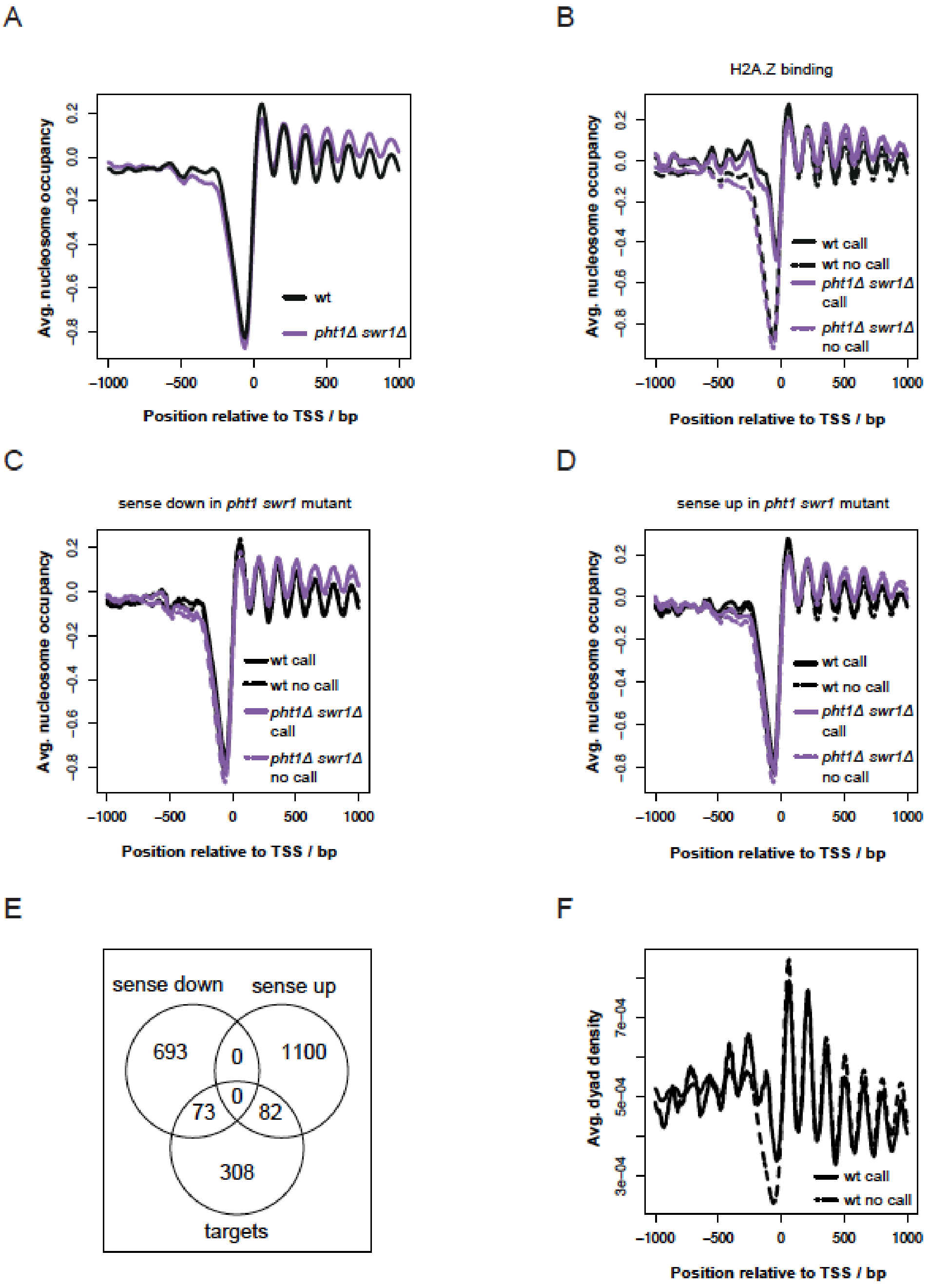

Figure 9 The histone variant H2A.Z and the remodeler ATPase Swr1 do not play a major role in nucleosome positioning around TSSs. (A) TSS-aligned nucleosome occupancy profile for 4013 genes in wt (Hu303, 5 replicates) and *pht1Δ swr1Δ* (Hu2127, 2 replicates). (B) Nucleosome occupancy data as in (A) but divided into H2A.Z bound (384 calls) and unbound (3629) loci, (C) divided into downregulated sense genes (591 calls) and genes with unchanged transcription (1463 calls) and (D) divided into upregulates sense genes (589 calls) and genes with unchanged transcription (1463 calls). (E) Venn diagram of loci calls in (B)-(C). (F) TSS-aligned nucleosome occupancy profile generated by MNase-ChIP-seq in wt (Hu303) divided into H2A.Z bound (384 calls) and unbound (3629) loci.

3.6.2 The RSC remodeling complex seems not to be involved in nucleosome positioning around TSSs

In *S. cerevisiae*, the RSC remodeling complex promoted NDR formation in an artificial system *in vivo* and was necessary for NDR maintenance at many promoters [107]. As the gene for the ATPase subunit of the RSC complex is the only essential gene encoding a remodeler ATPase in both *S. cerevisiae* and *S. pombe*, we wondered if the role of the RSC complex in *S. cerevisiae* was also conserved in *S. pombe*. We obtained an *S. pombe* mutant strain carrying a temperature-sensitive (ts) allele of the gene coding for the RSC remodeler ATPase Snf21 (*snf21-ts*) [136]. To ensure that we map nucleosome occupancy at the right time-point, i.e. mutant phenotype induction of still viable cells, after shifting from the permissive (25 °C) to the non-permissive (34 °C) temperature, we investigated the phenotype of the *snf21-ts* mutant at 34 °C. We measured in a time course experiment viability of the cells after shift to 34 °C via replating them at 25 °C and counting the colonies. We followed cell growth over time at 34 °C by counting the cells, and monitored cell shape by microscopy (Fig. 10A, B). After 6 h at 34 °C cell growth slowed down, viability decreased and the cells exhibited an elongated shape and defects in chromosome segregation as judged by DAPI staining.

The *snf21-ts* mutant and an isogenic wildtype strain (K240) were grown for 6 h at 34 °C, mononucleosomal DNA fragments were generated, hybridized to Affymetrix tiling arrays and nucleosome occupancy was calculated. Displaying all genes aligned at their TSSs in a nucleosome occupancy overlay plot, revealed very similar nucleosome occupancy patterns for both (Fig. 10C). In collaboration with the Ekwall laboratory, we performed transcriptome analysis for the *snf21-ts* mutant grown at 25 °C and for 6 h at 34 °C, respectively, to search for genes with changed transcript levels upon Snf21 degradation. After growth at the non-permissive temperature for 6 h, 395 transcripts were more than 1.5 fold upregulated and 413 transcripts were more than 1.5 fold downregulated (Table 2). When plotting nucleosome occupancy for those transcriptionally responding genes separately, still no change in nucleosome occupancy patterns could be observed (Fig. 10D, E). Also comparison to the corresponding wildtype patterns did not reveal any differences.

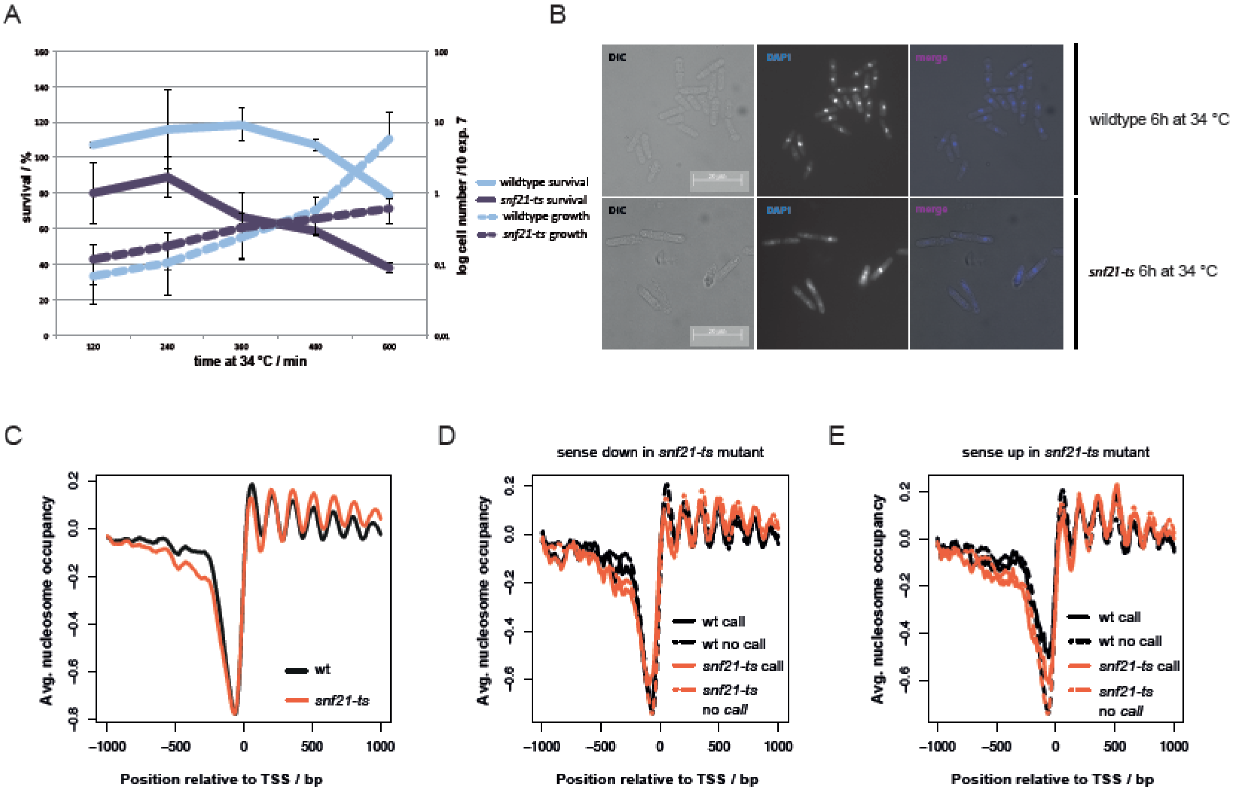

Figure 10 The remodeler ATPase Snf21 seems not to have a role in nucleosome positioning around TSSs. (A,B) *snf21-ts* phenotype characterization at 34 °C. (A) Growth kinetics after shift to 34 °C by cell counting and survival kinetics by colony counting after replating at 25 °C, for wt (K240/Hu2261) and *snf21-ts* (KYP176/Hu2262) cells after shift to 34 °C. (B) Differential interference contrast (DIC) and fluorescence (DAPI stain) microscopy of wt and *snf21-ts* (as in (A)) under the indicated conditions. TSS-aligned nucleosome occupancy profile for (C) 4013 genes in wt (K240, 2 replicates) and *snf21-ts* 2 replicates) after 6 h at 34 °C. (D) Nucleosome occupancy data as in (C) but divided into 1.5 fold downregulated genes (228 calls) and genes with unchanged transcription (1256 calls) and (E) divided into 1.5 fold upregulates genes (138 calls) and genes with unchanged transcription (1256 calls).

As RSC remodels promoter nucleosomes in *S. cerevisiae* [107] and as SWR1 exchanges canonical H2A against H2A.Z preferentially at +1 nucleosomes [49], we wondered if these two chromatin remodelers might act in concert in shaping promoter chromatin structure. In collaboration with Karl Ekwall, we combined the *snf21-ts* allele with a *swr1* deletion and measured nucleosome occupancy for this *snf21-ts swr1Δ* strain after growth for 6 h at 34 °C (Fig. 11A). However, even in the double mutant nucleosome occupancy was not changed in comparison to wildtype. Transcriptome analysis was performed for the *snf21-ts swr1Δ* mutant (Table 2), but again nucleosome patterns of transcriptionally responding genes in the *snf21-ts swr1Δ* mutant grown for 6 h at 34 °C compared to the *snf21-ts* mutant grown at 25 °C did not alter (Fig. 11B, C).

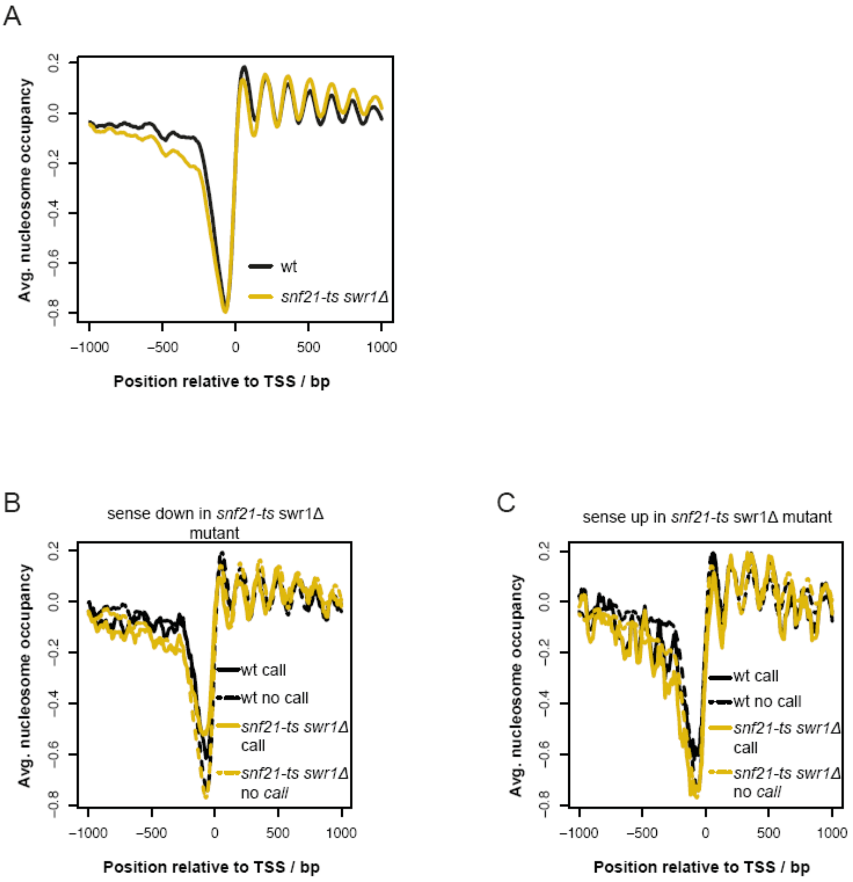

Figure 11 Also the combined ablation of Snf21 and Swr1 does not significantly change nucleosome occupancy profiles around TSSs. TSS-aligned nucleosome occupancy profile for (A) 4013 genes in wt (K240, 2 replicates) and *snf21-ts swr1Δ* (Hu2314, 2 replicates) after 6h at 34°C. (B) Nucleosome occupancy data as in (A) but divided into 1.5 fold downregulated genes (175 calls) and genes with unchanged transcription (1425 calls), and (D) divided into 1.5 fold upregulates genes (55 calls) and genes with unchanged transcription (1425 calls).

3.6.3 The Mi-2 remodeler ATPase Mit1 does not substantially participate in nucleosome positioning around TSSs

The remodeler ATPase Mit1 belongs to the Mi-2 subfamily [11]. The SHREC complex contains two catalytic subunits, the HDAC Clr3 and the ATPase Mit1, and was described to be important for nucleosome positioning and transcriptional gene silencing at heterochromatic loci [137]. Lantermann et al. [8] published a global role for Mit1 in nucleosome positioning at coding sequences (CDSs). In a *mit1Δ* mutant the amplitudes of nucleosome peaks over CDSs were diminished, which is indicative for compromised regularity of nucleosome positioning. Furthermore, regularity of nucleosome patterns as analysed by spectral analysis was completely abolished in the *mit1Δ* mutant.

We wondered if those effects could be reproduced with our improved nucleosome mapping protocol (see chapter 3.1). We measured nucleosome occupancy for the *mit1Δ* mutant as described above, but we were not able to reproduce the published effects. In a TSS-aligned overlay plot of all genes, the nucleosome patterns of the *mit1Δ* mutant were highly similar to the wildtype patterns and spectral analysis revealed the same regularity of nucleosomes as seen in wildtype, namely 6.5 nucleosomes per 1000 bp (Fig. 12A, B). We also plotted nucleosome occupancy for genes up- and downregulated in a *mit1Δ* mutant compared to wildtype (transcription data Lantermann et al. [8]) (Fig. 12C, D). However, no clear changes in nucleosome occupancy for those two subgroups of genes could be detected when comparing them either within the *mit1Δ* mutant or to wildtype.

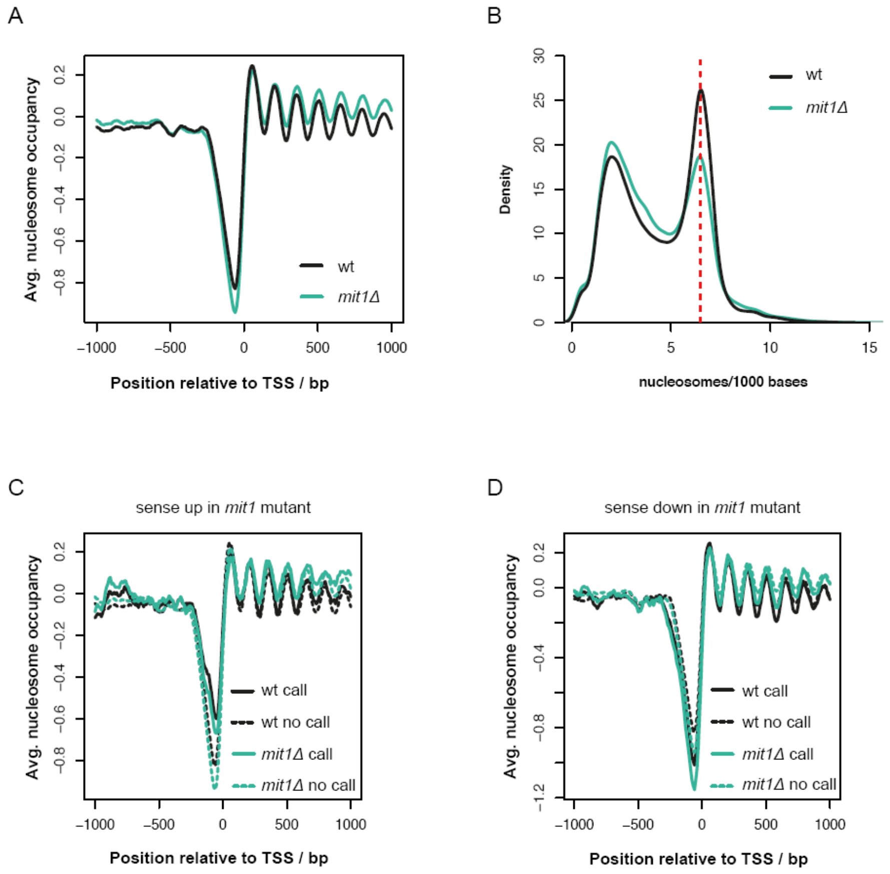

Figure 12 The remodeler ATPase Mit1 is not significantly involved in nucleosome positioning around TSSs. (A) TSS-aligned nucleosome occupancy profile for 4013 genes in wt (Hu303, 5 replicates) and *mit1Δ* (Hu1294, 2 replicates). (B) Spectral analysis for the data in (A). (C,D) Nucleosome occupancy data as in (A) but divided into loci > 1.5 fold (C) upregulated (187 calls) or not (3826), and (D) downregulated (309 calls) or not (3704).

3.6.4 The CHD1 remodeler ATPases Hrp1 and Hrp3 are crucial for regular nucleosomal array formation downstream of the +1 nucleosome

So far, we could show that neither the INO80 subfamily remodeler ATPase Swr1 nor the SWI/SNF subfamily remodeler ATPase Snf21 nor the Mi-2 subfamily remodeler ATPase Mit1 were involved in nucleosome positioning around TSSs. As *S. pombe* does not harbour any chromatin remodelers of the ISWI subfamily, we decided to screen the CHD1 subfamily for a possible role in nucleosome positioning at promoter regions and 5` ends of gene bodies. There are two CHD1 remodelers in *S. pombe*, Hrp1 and Hrp3 [11]. Hrp1 and Hrp3 were shown to physically interact with each other and with the histone chaperone Nap1 *in vivo* [174]. Furthermore, the two CHD1 remodelers and the histone chaperone Nap1 were found at intergenic regions (IGRs) and ORFs. Interestingly, especially at IGRs the overlap of binding targets of Hrp1, Hrp3 and Nap1 was quite high and significant.

3.6.4.1 Nucleosome occupancy of all genes aligned at TSSs and spectral analysis

We mapped nucleosome occupancy for the *hrp1Δ,* the *hrp3Δ* and the *hrp1Δ hrp3Δ* mutants. In a TSS-aligned overlay of nucleosome occupancy for all genes, the *hrp1Δ* mutant showed a slightly changed nucleosome pattern in comparison to wildtype (Fig. 13A). The peak-trough ratios of the downstream array were visibly diminished in the *hrp1Δ* mutant compared to wildtype. This effect became even more distinct in the *hrp3Δ* mutant and furthermore, nucleosome peaks faded out from the +5 nucleosome onwards (Fig. 13B). In TSS-aligned nucleosome occupancy overlay plots of the *hrp1Δ hrp3Δ* double mutant, positions of only the +1 and +2 nucleosomes were preserved, while regular positioning of all further nucleosomes got completely abolished (Fig. 13C). We also calculated regularity of nucleosomal distances for all three mutants by applying spectral analysis (Fig. 13D-F). In the *hrp1Δ* mutant, nucleosomes were ordered in a regular way, however, nucleosomes seem to have genome-wide a larger spacing as only 6.2 nucleosomes were calculated per 1000 bp instead of 6.5 nucleosomes per 1000 bp in wildtype (Fig. 13D). In the *hrp3Δ* mutant regularity was severely diminished as no distinct peak but only a broad shoulder could be detected in spectral analysis (Fig. 13E). This effect was even stronger in the *hrp1Δ hrp3Δ* double mutant (Fig. 13F). We concluded that regularity of nucleosome positioning relative to the TSS is lost upon depletion of Hrp1 and Hrp3.

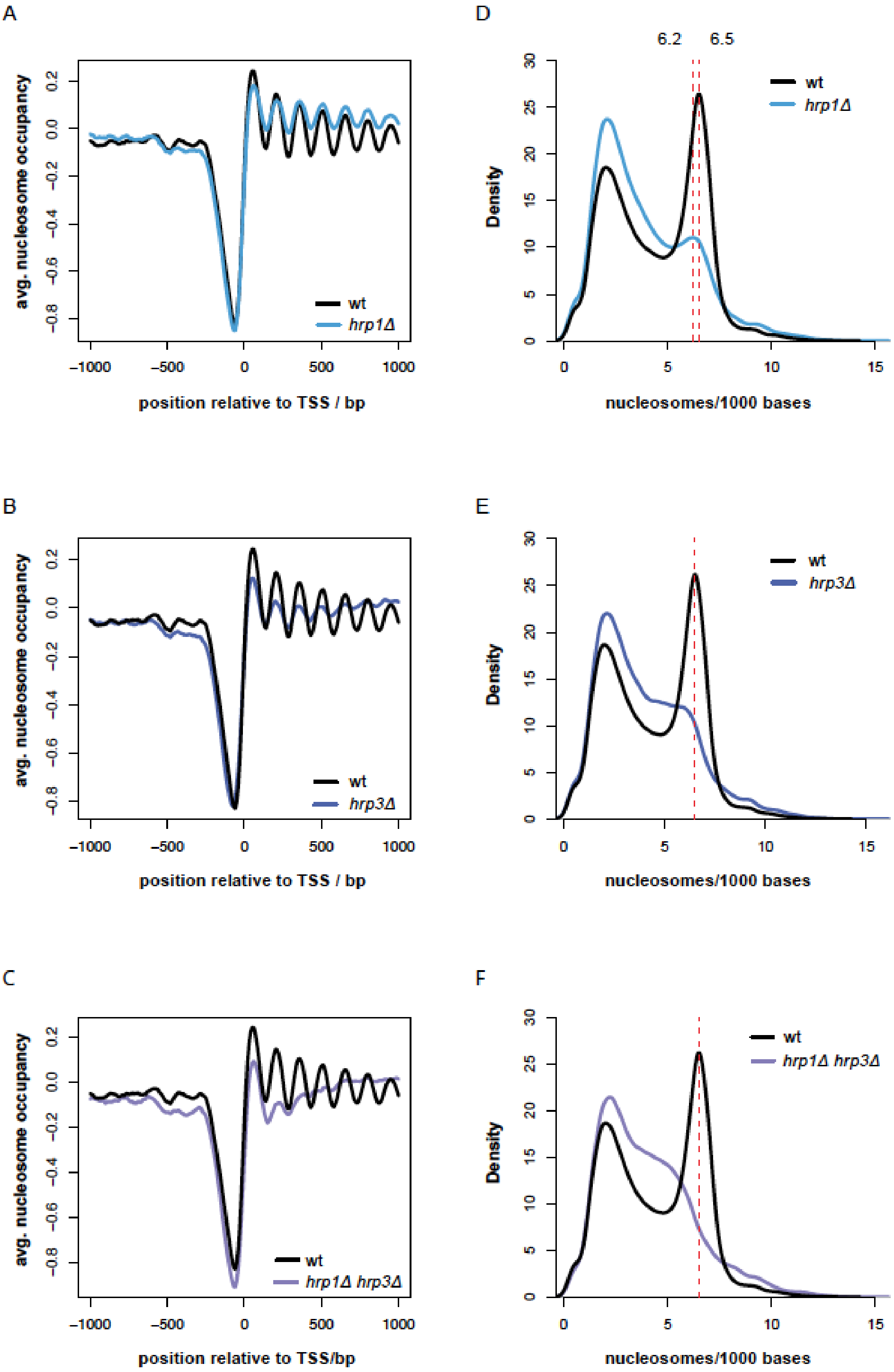

Figure 13 The CHD1-type remodeler ATPases Hrp1 and Hrp3 play an important role in generation of 5' nucleosomal arrays. TSS-aligned nucleosome occupancy profile for 4013 genes in wt (Hu303, 5 replicates) and (A) *hrp1Δ* (Hu2239, 2 replicates), (B) *hrp3Δ* (Hu0575, 2 replicates) and (C) *hrp1Δ hrp3Δ* (Hu2303, 2 replicates). (D-F) Spectral analysis for data in (A-C), respectively.

3.6.4.2 Hrp1 and Hrp3 binding-targets

We next asked if changed overall nucleosome patterns around TSSs in those three mutants could be explained by chromatin changes at only a subgroup of genes, which could possibly dominate the overlay nucleosome occupancy patterns. Therefore, we distinguished Hrp1 or/and Hrp3 binding targets from non-binding targets (ChIP-chip data, Walfridsson et al. [174]). When plotting nucleosome occupancy of Hrp1 binding-targets (IGRs and ORFs) for the *hrp1Δ* mutant and wildtype, the effect of Hrp1 depletion on this subgroup of genes was similar to the effect seen for all genes, i.e. a diminished amplitude of nucleosomal peaks (Fig. 14A). Interestingly, promoters bound by Hrp1 had a broadened NDR, which still existed in the *hrp1Δ* mutant and therefore does not depend on Hrp1 presence. Nucleosome occupancy data of Hrp3 IGR and ORF binding-targets for the *hrp3Δ* mutant and wildtype revealed even more pronounced mutant effects compared to the overlay of nucleosome occupancy data for all genes (Fig. 14B). At Hrp3 binding-targets in the *hrp3Δ* mutant nucleosomal peaks started to fade-out already at the +2 nucleosome while clear nucleosomal peaks were visible until the +5 nucleosome in the all genes overlay. However, also targets not bound by Hrp3 showed compromised nucleosomal arrays in the *hrp3Δ* mutant. As observed for the Hrp1 binding-targets, Hrp3 binding targets showed a similarly broadened NDR in both wildtype and *hrp3Δ* mutant. Thus, these specific chromatin structures are not generated by Hrp remodelers, but might possibly be mandatory for them in order to fulfil their tasks. Subsequently, we looked at nucleosome occupancy data of Hrp1 and Hrp3 binding targets for the *hrp1Δ hrp3Δ* double mutant (Fig 14C, D). Nucleosomal array patterns of Hrp1 binding targets were not further compromised. However, Hrp3 binding targets exhibited an even worsened pattern compared to the overlay of all genes as only a positioned +1 nucleosome remained.

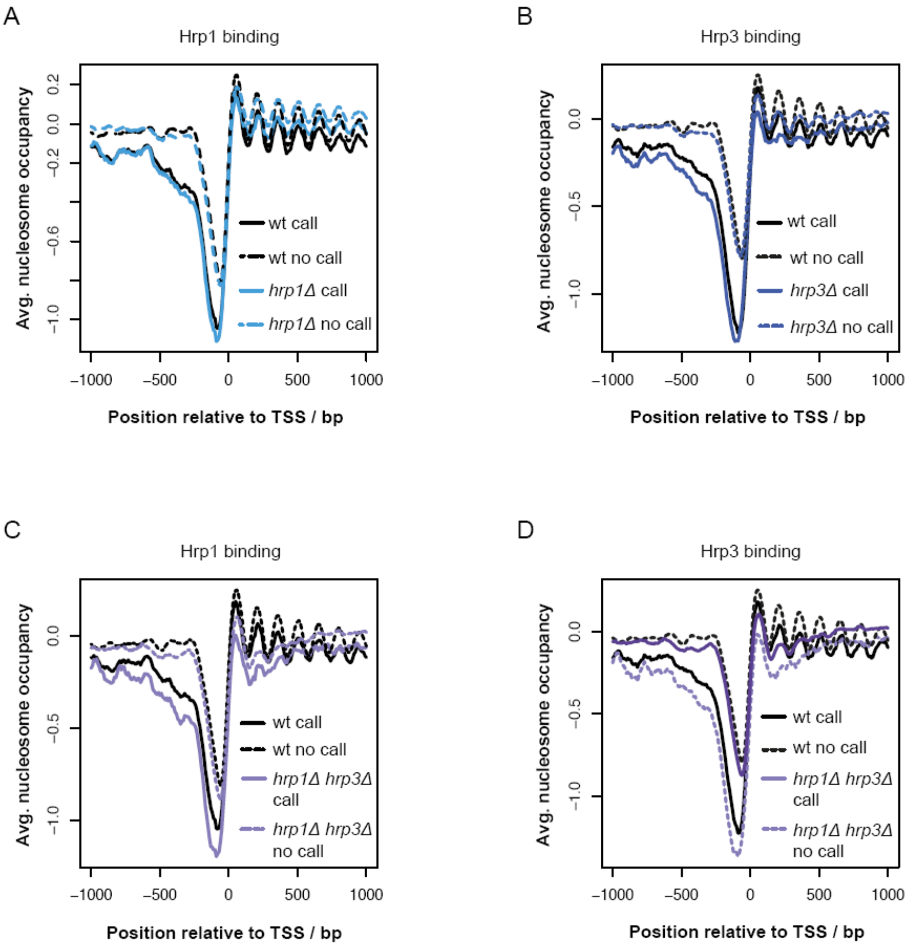

Figure 14 Genes bound by Hrp3 showed increased chromatin perturbation in the *hrp3Δ* and *hrp1Δ hrp3Δ* mutants. (A) TSS-aligned nucleosome occupancy profiles in wt (Hu303, 5 replicates) and *hrp1Δ* (Hu2239, 2 replicates) for genes bound by Hrp1 (428 calls) or not (3585). (B) TSS-aligned nucleosome occupancy profiles in wt (Hu303, 5 replicates) and *hrp3Δ* (Hu0575, 2 replicates) for genes bound by Hrp3 (369 calls) or not (3644). (C) Same as in (A) but in wt (Hu303, 5 replicates) and *hrp1Δ hrp3Δ* (Hu2303, 2 replicates). (D) Same as in (B) but in wt (Hu303, 5 replicates) and *hrp1Δ hrp3Δ* (Hu2303, 2 replicates).

3.6.4.3 Transcriptional responders of Hrp1 and/or Hrp3 depletions

Next, we wanted to look specifically at chromatin patterns of genes transcriptionally responding to single or double deletions of Hrp remodelers. In collaboration with the Karl Ekwall laboratory, transcriptome data for the *hrp1Δ*, *hrp3Δ* and *hrp1Δ hrp3Δ* mutants were generated. In order to reliably map antisense transcription, too, reverse transcription of RNA into cDNA was conducted in presence of actinomycin D. Perocchi et al. [223] reported that actinomycin D impedes spurious second-strand synthesis during reverse transcription by preventing DNA-dependent DNA synthesis. We found 743 sense transcripts in the *hrp1Δ* mutant that were upregulated relative to wildtype, 466 downregulated sense transcripts and 711 upregulated cryptic antisense transcripts (Table 2). The nucleosome occupancy patterns of these three groups were not different from those of transcripts without any changes (Fig. 15A-C). For the *hrp3Δ* mutant, the number of transcripts with transcriptional changes relative to wildtype was slightly higher. 955 upregulated sense transcripts, 749 downregulated sense transcripts and 875 upregulated cryptic antisense transcripts could be detected (Table 2). But again, nucleosome occupancy patterns for these subgroups were unchanged in the *hrp3Δ* mutant (Fig. 15D-F). In the *hrp1Δ hrp3Δ* double mutant 783 sense transcripts were upregulated, 665 sense transcripts were downregulated and 1027 cryptic antisense transcripts were upregulated (Table 2). Regarding nucleosome occupancy of elements with changed transcription, we again did not see any changes compared to elements without any transcriptional changes (Fig. 15G-H). At this point, it should be emphasised that for all three Hrp mutants nucleosome occupancy patterns were also changed at elements without any transcriptional changes (Fig. 15A-J). This means that changes in chromatin structure, even quite severe changes as seen for the *hrp1Δ hrp3Δ* double mutant, do not necessarily lead to transcriptional changes. It is interesting to note that changes in cryptic antisense transcription did not influence expression of the respective sense transcripts (Fig. 16A-C).

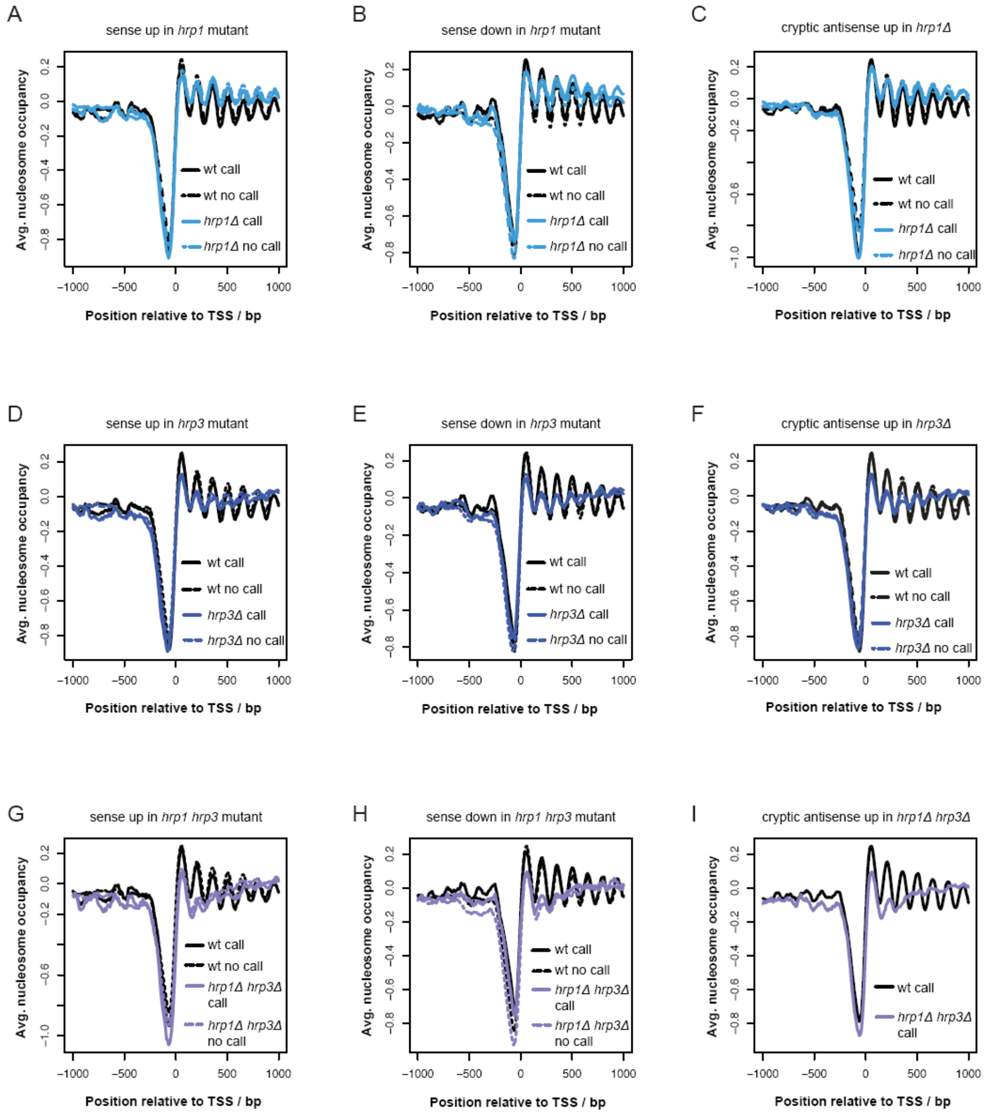

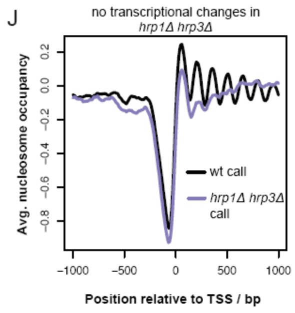

Figure 15 Transcriptional responders in the Hrp mutants do not show enhanced chromatin perturbation. (A-C) TSS-aligned nucleosome occupancy profiles in wt (Hu303, 5 replicates) and *hrp1Δ* (Hu2239, 2 replicates) for transcriptional elements (A) upregulated in *hrp1Δ* in comparison to wt (374 calls) or not (2835), (B) downregulated (374 calls) or not (2835), and (C) with upregulated cryptic antisense transcripts (560 calls) or not (2835). (D-F) TSS-aligned nucleosome occupancy profiles in wt (Hu303, 5 replicates) and *hrp3Δ* (Hu0575, 2 replicates) for transcriptional elements (D) upregulated in *hrp3Δ* in comparison to wt (515 calls) or not (2481), (E) downregulated (507 calls) or not (2481), and (F) with upregulated cryptic antisense transcripts (697 calls) or not (2481). (G-J) TSS-aligned nucleosome occupancy profiles in wt (Hu303, 5 replicates) and *hrp1Δ hrp3Δ* (Hu2303, 2 replicates) for transcriptional elements (G) upregulated in *hrp1Δ hrp3Δ* in comparison to wt (341 calls) or not (2570), (H) downregulated (450 calls) or not (2570), (I) with upregulated cryptic antisense transcripts (828 calls) or not (2570), and (J) for elements without transcriptional changes (2570 calls).

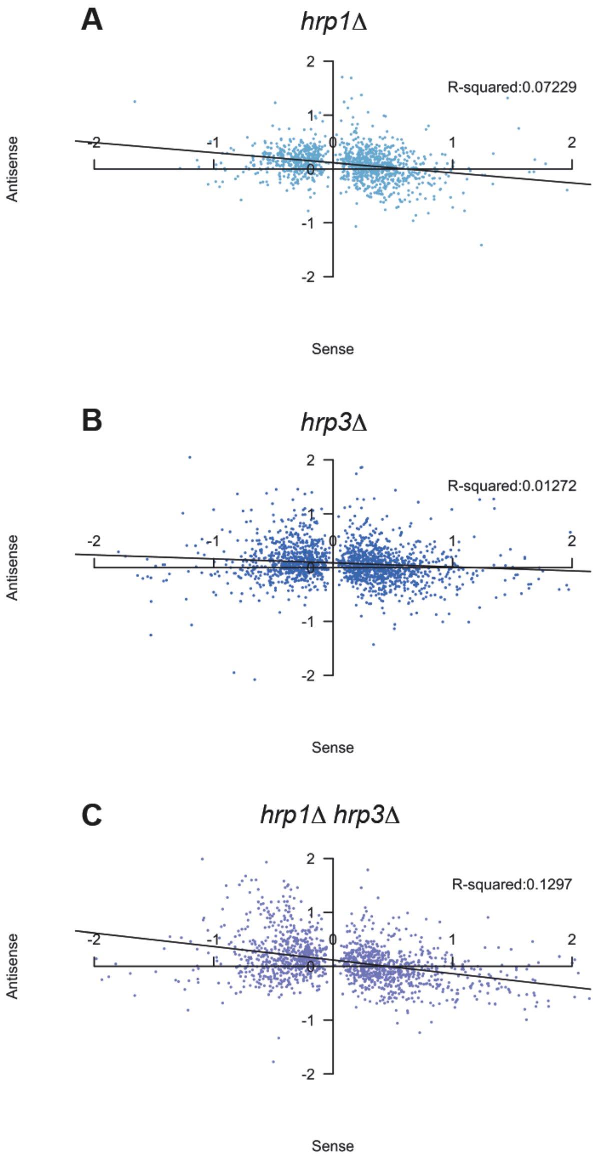

Figure 16 Changes of sense transcription and changes of cryptic antisense transcription are mostly not correlated. Scatter plots of sense and cryptic antisense transcriptional changes in mutant versus wt for (A) *hrp1Δ*, (B) *hrp3Δ*, and (C) *hrp1Δ hrp3Δ*.

3.6.4.4 Bulk MNase ladders were not much disturbed in Hrp mutants

Next, we wondered if the diminished or lost nucleosomal arrays in the *hrp3Δ* and *hrp1Δ hrp3Δ* mutants were also mirrored in bulk nucleosomal ladders. Chromatin of wildtype, *hrp3Δ* or *hrp1Δ hrp3Δ* mutant cells was digested with a range of MNase concentrations, DNA was purified and visualised by ethidium bromide in an agarose gel. For wildtype and the *hrp3Δ* mutant, clear MNase ladders were visible. For the *hrp1Δ hrp3Δ* mutant, MNase ladders were slightly more smeary and signal strength was weaker (note that twofold more material was loaded for the *hrp1Δ hrp3Δ* mutant), but overall still very well visible.

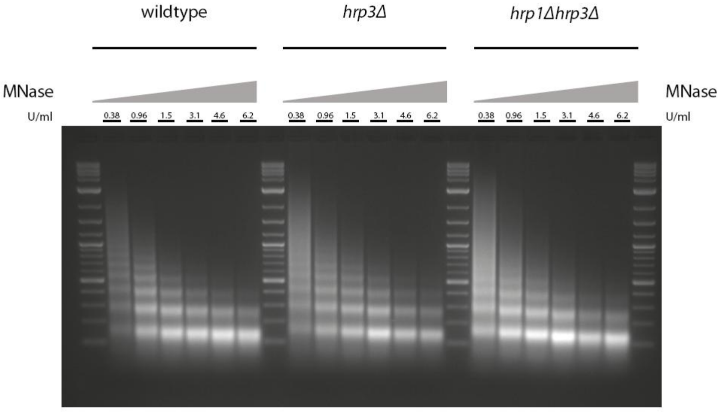

Figure 17 Bulk MNase ladders are not much affected in Hrp mutants. MNase ladders for wt (Hu303), *hrp3Δ* (Hu0575/EJY321) and *hrp1Δ hrp3Δ* (Hu2303) strains. One of two biological replicates is shown. Twice the amount of material was loaded for Hu2303. Wedges on top of the lanes indicate increasing MNase concentrations of 0.38; 0.96; 1.5; 3.1; 4.6; 6.2 U/ml.

3.6.4.5 Confirmation of chromatin changes at single loci by indirect end-labelling

To verify the clear genome-wide changes in nucleosome occupancy for the *hrp3Δ* and *hrp1Δ hrp3Δ* mutant, we analysed nucleosome occupancy patterns for wildtype, the *hrp1Δ*, the *hrp3Δ* and the *hrp1Δ hrp3Δ* mutant at three exemplary loci by indirect end labelling as described in Lantermann et al. [211]. At all three loci, the nucleosome patterns of the *hrp1Δ* mutant and wildtype were very similar (Fig. 18A-C). However, there were differences between wt and the *hrp3Δ* mutant and the *hrp1Δ hrp3Δ* mutant, respectively (Fig. 18A-C). Thus, nucleosome pattern changes around TSSs and in gene bodies in the *hrp3Δ* and the *hrp1Δ hrp3Δ* mutant relative to wildtype can also be revealed at single loci.

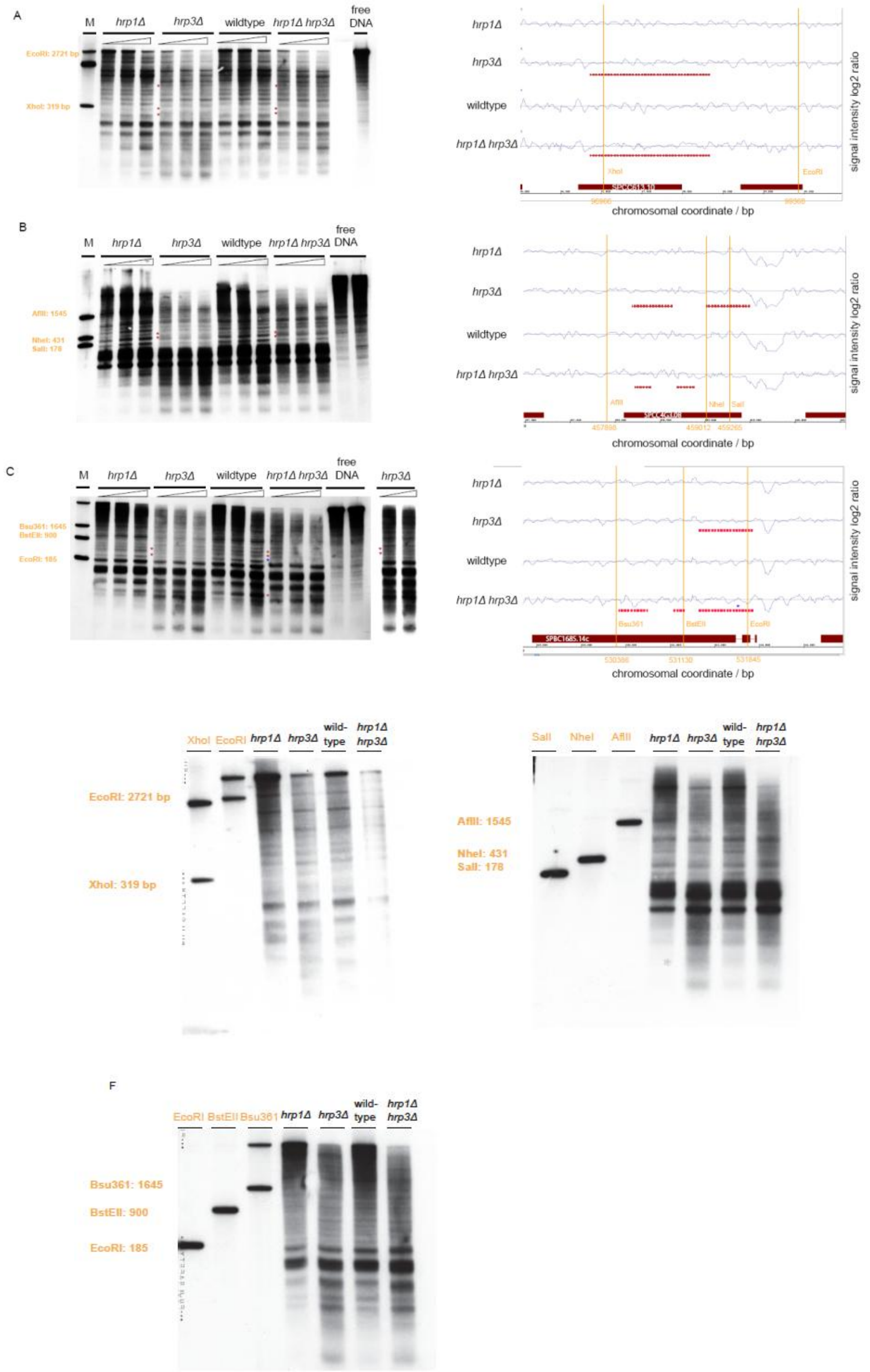

Figure 18 Chromatin changes upon depletion of Hrp remodelers can also be revealed at single loci. (A-C) Indirect end labelling of MNase digested chromatin of wt (Hu303), *hrp1Δ* (Hu2239), *hrp3Δ* (Hu0575) and *hrp1Δ hrp3Δ* (Hu2303) strains and corresponding nucleosome occupancy data by microarray hybridization as well as (D-F) mock MNase control for indirect end labelling are shown for the loci (A, D) SPCC613.10, (B, E) SPCC4G3.08 and (C, F) SPBC1685.14c). (A-C) Wedges above the lanes denote increasing MNase concentrations. All samples per locus were electrophoresed in the same gel, but an additional longer exposure is shown for *hrp3Δ* in panel C, two rightmost lanes. Red asterisks indicate chromatin pattern changes relative to wt. Blue asterisks indicate changed pattern detected by both techniques at the same position. Red dashed horizontal lines in microarray data panels show changed nucleosome patterns relative to wt. (D-F) Mock controls were treated in the same way as samples but MNase digest was omitted. (A-F) Sizes of marker fragments are indicated relative to the transcriptional start site.

3.6.4.6 The *hrp1Δ hrp3Δ* mutant shows increased sensitivity to 6-azauracil

To check globally if the nucleosome positioning defects detected for the Hrp mutants, especially the *hrp1Δ hrp3Δ* mutant, influence DNA repair, DNA replication or transcription elongation, we compared all three Hrp mutants with wildtype in drug sensitivity assays. When spotting the respective strains on plates containing methylmethanesulfonate (MMS), an indicator for DNA repair defects, no differences in growth behaviour could be seen for all three Hrp mutants in comparison to wildtype (in collaboration with Karl Ekwall) (Fig.19A). The same was true when performing the spotting assay on plates containing hydroxyurea (HU), which causes replication fork arrest as a consequence of dNTP pool depletion (Fig. 19B). 6-azauracil (6AU) impedes purine and pyrimidine biosynthesis causing problems in transcriptional elongation. Strikingly, when spotting cells on plates containing 6AU, the *hrp1Δ hrp3Δ* mutant showed growth defects in presence of high concentrations of the drug, i.e. 300 µg/ml, while the Hrp single mutants and wildtype grew fine (Fig. 19C). This result is in line with the observed nucleosome positioning defects in gene bodies of *hrp1Δ hrp3Δ* mutant cells.

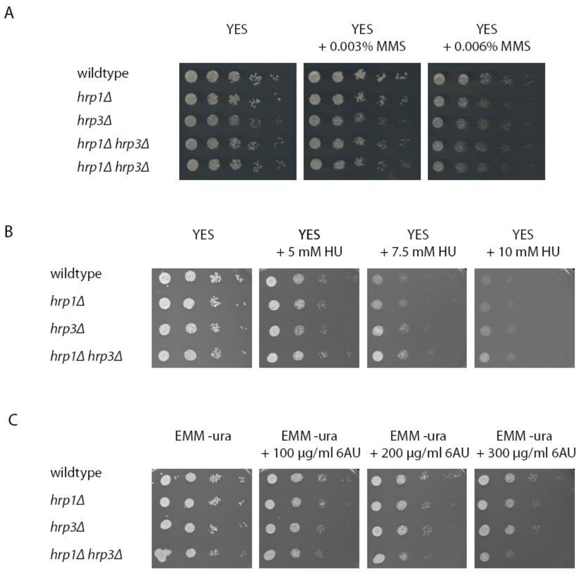
A
YES
YES + 0.003% MMS
YES + 0.006% MMS
wildtype
hrp1Δ
hrp3Δ
hrp1Δ hrp3Δ
hrp1Δ hrp3Δ
B
YES
YES + 5 mM HU
YES + 7.5 mM HU
YES + 10 mM HU
wildtype
hrp1Δ
hrp3Δ
hrp1Δ hrp3Δ
C
EMM -ura
EMM -ura + 100 µg/ml 6AU
EMM -ura + 200 µg/ml 6AU
EMM -ura + 300 µg/ml 6AU
wildtype
hrp1Δ
hrp3Δ
hrp1Δ hrp3Δ

Figure 19 The *hrp1Δ hrp3Δ* mutant is sensitive to 6-azauracil. The sensitivity for (A) methylmethanesulfonate (MMS, 0.003% or 0.006%), (B) hydroxyurea (HU, 5 mM, 7.5 mM or 10 mM), and (C) 6-azauracil (6AU, 100 µg/ml, 200 µg/ml or 300 µg/ml) was determined by spotting assay for wt (Hu303), *hrp1Δ* (Hu2239), *hrp3Δ* (Hu0807) and *hrp1Δ hrp3Δ* (Hu2303). (A-C) One of two replicates is shown.

3.6.5 The histone deacetylase Clr6 and the histone lysine methyltransferase Set2 are not substantially involved in nucleosome positioning around TSSs

The histone deacetylase Clr6 is a member of two distinct complexes. While complex I primarily targets gene promoters, complex II is found at transcribed chromosomal regions and centromere cores [224]. The methyltransferase Set2 methylates specifically H3K36 at gene bodies of Pol II-transcribed genes [225]. In *S. cerevisiae*, there exist two histone deacetylase complexes, Rpd3L and Rpd3S [226], which resemble *S. pombe* complex I and complex II, respectively. Rpd3S is recruited to gene bodies via phosphorylated Pol II CTD [227] and its activity is stimulated by H3K36 methylation, the mark set by Set2 [226]. Recently in *S. cerevisiae*, a very interesting connection between H3K36 methylation, the action of the remodeler ATPases Isw1b and Chd1 and prevention of histone turnover at gene bodies was described [228-230]. As decribed above, we could show that the two CHD1 remodeler ATPases Hrp1 and Hrp3 play a major role in nucleosome positioning in gene bodies in *S. pombe*. For *S. pombe*, it is so far not known if H3K36 methylation prevents histone turnover and is functionally connected to CHD1 remodelers. With view of a possible conservation of mechanisms preventing histone turnover, we tested if mutation of Set2 or Clr6 were linked to defects in nucleosome positioning around TSSs and at gene bodies.

Nucleosome occupancy maps for the *set2Δ* deletion and the *clr6* mutation strains did not reveal differences in nucleosome positioning compared to wildtype, only slightly lower occupancy of the +1 nucleosome in the *set2Δ* (Fig. 20A) and the *clr6* mutant (Fig. 20B) in comparison to wildtype. As elevated histone turnover in an *S. cerevisiae set2Δ* mutant took mainly place at long genes [230], we specifically compared nucleosome occupancy patterns of genes ≥ 2000 bp for the *set2Δ* (Fig. 20C) and the *clr6* mutant strains (Fig. 20D) to wildtype. Yet, there were no striking changes. Furthermore, we compared targets containing histones methylated at lysine 36 (ChIP-chip data Sinha et al. [231]) for the *set2Δ* mutant and wildtype (Fig. 20E) and for the *clr6* mutant and wildtype (Fig. 20F). Also for this subclass of genes no changes in nucleosome occupancy patterns could be seen. Collectively, neither Clr6 nor Set2 seem to be required for proper nucleosome positioning in gene bodies.

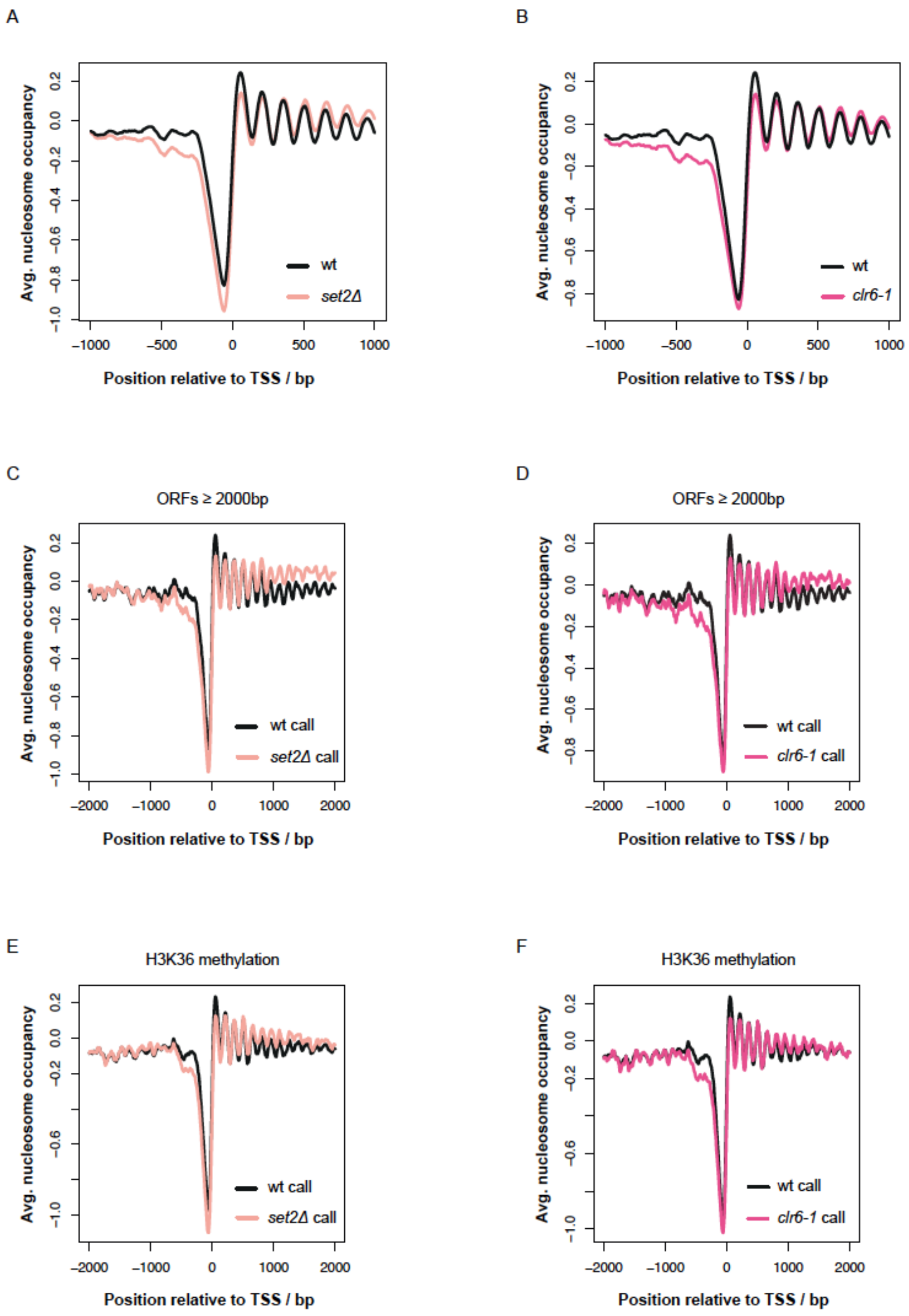

Figure 20 Set2 and Clr6 are not required for proper nucleosome positioning in gene bodies. TSS-aligned nucleosome occupancy profiles in wt (Hu303, 5 replicates) and (A,C,E) *set2Δ* (Hu1582, 2 replicates), or (B,D,F) *clr6* (Hu802, 2 replicates) for (A,B) 4013 genes, for (C,D) genes with ORFs ≥ 2000 bp (526 calls), and for (E,F) dived into genes carrying a H3K36 methylation mark (469 calls) or not (3544).

3.7 The role of transcription in nucleosome positioning

There are several hints that RNA-polymerase II, associated factors, or the transcription process itself might be directly or indirectly involved in nucleosome positioning at promoters and gene bodies. Lantermann et al. [8] showed in *S. pombe* that nucleosomal arrays extended from the TSS mainly into the downstream direction and hence were co-directional with transcription. Furthermore, the array length correlated well with transcript length and silent genes did not show regular arrays. In *S. cerevisiae*, ablation of the largest RNA polymerase II subunit Rpb1 via a temperature-sensitive allele (*rpb1-ts*) caused slight downstream shifting of NDRs and downstream nucleosomal arrays [208].

3.7.1 Relation between RNA synthesis rate and promoter nucleosome occupancy

At highly transcribed genes, nucleosomes are depleted from promoter regions [232], while promoter nucleosome occupancy is comparatively high at silent genes [8]. This correlation seems to hold true for the whole continuum of transcriptional activity when binning genes according to total mRNA levels [8]. However, on a gene-by-gene basis total mRNA levels and promoter nucleosome occupancy did not correlate well with each other. We wondered if this correlation improved, when RNA synthesis rates instead of total mRNA levels were used as it is much more important how often a gene is transcribed than what happens to the transcript after transcription. We binned genes according to their RNA synthesis rate [1] and plotted average nucleosome occupancy for every bin. Similar to plotting average bin total mRNA levels clear differences in nucleosome occupancy could be seen between different bins (Fig. 21A). NDR nucleosome occupancy decreased with increasing RNA synthesis rate. Moreover, nucleosomal arrays were progressively perturbed with increasing RNA synthesis rate. Subsequently, we checked if a gene-by gene correlation between mRNA synthesis rate and promoter nucleosome occupancy existed (Fig. 21B). However, this was not the case.

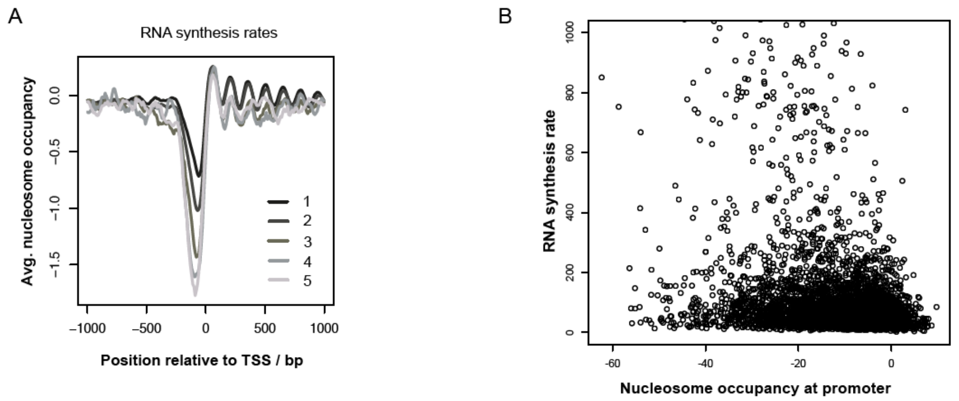

Figure 21 RNA synthesis rate and promoter nucleosome occupancy are correlated when comparing gene groups but not on a gene-by-gene basis. (A) TSS-aligned nucleosome occupancy profiles in wt (Hu303, 5 replicates) for genes binned according to their synthesis rates [1] from slow (1) to high (5), bin 1: 2738 calls, bin 2: 878 calls, bin 3: 80 calls, bin 4: 70 calls, bin 5: 77 calls. (B) Scatterplot of RNA synthesis rate versus nucleosome occupancy at promoters.

3.7.2 Nucleosome positioning patterns around TSSs do not significantly change in a *rpb7-ts* mutant under restrictive conditions

In order to investigate if inactivation of RNA-polymerase II by depletion of one of its subunits changes nucleosome positioning patterns at promoters or in gene bodies, we obtained an *rpb7-ts* mutant, at this time point the only available mutant directly affecting RNA-polymerase II activity. The *rpb7-ts* mutant strain was grown for 6 h at the non-permissive temperature (36 °C) as transcription of a large group of genes was substantially downregulated under these conditions (in collaboration with Karl Ekwall). Subsequently, mononucleosomal DNA was isolated and nucleosome occupancy was calculated after microarray hybridization. Nucleosome occupancy data for both biological replicates of the *rpb7-ts* mutant were plotted separately in a TSS-aligned overlay of all genes and compared to wildtype (Fig. 22A). The two *rpb7-ts* mutant replicates differed slightly from each other as nucleosome occupancy of the -1 nucleosome, the +1 nucleosome and the NDR were higher in replicate 2 compared to replicate 1. However, these differences can be traced back to differences in MNase digestion degree (see chapter 3.3). For unknown reasons it turned out to be technically very challenging to achieve the desired MNase digestion degree for the *rpb7-ts* mutant samples. This could be indicative of global changes in chromatin structure and might be worth further investigation. Apart from the differences between the two *rpb7-ts* mutant replicates attributed to digestion degree variations, nucleosome occupancy patterns around TSSs of the *rpb7-ts* mutant replicate 1 and wildtype were very similar. Only a very subtle downstream shift of nucleosomal arrays could be revealed for the *rpb7-ts* mutant compared to wildtype.

To look only at genes directly affected by degradation of Rpb7, we distinguished genes downregulated in the *rpb7-ts* mutant in comparison to wildtype from transcriptionally unaffected genes in collaboration with Karl Ekwall. Still, even for this class of genes we did not see substantial nucleosome occupancy changes in the *rpb7-ts* mutant compared to wildtype (Fig. 22B).

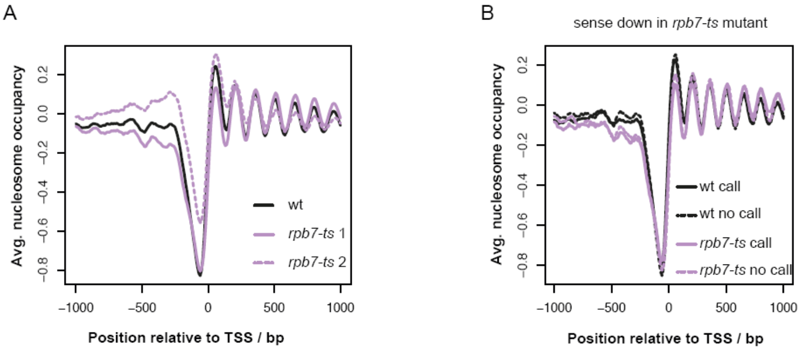

Figure 22 Nucleosome positioning patterns do not substantially change in a *rpb7-ts* mutant at restrictive conditions. TSS-aligned nucleosome occupancy profiles in wt (Hu303, 5 replicates) grown at 30 °C and *rpb7-ts* (Hu801) grown for 6 h at 36 °C for (A) 4013 genes, replicate 1 and 2 for *rpb7-ts* plotted separately, and (B) divided into genes downregulated in the *rpb7-ts* mutant (1499 calls) or not (2514), average of replicate 1 and 2 for *rpb7-ts* plotted.

3.7.3 The impact of changes in the transcriptional program on chromatin structure

To monitor the chromatin state before and after transcriptional changes more adequately than achieved with a conditional polymerase mutant, we decided to search for a biological condition, which is accompanied by widespread changes in transcriptional program. When arresting cells in G0 by nitrogen-starvation for 48 h and releasing them afterwards from G0 through add-back of a nitrogen source for 2 h, extensive transcriptional changes occur [3]. In collaboration with the Karl Ekwall laboratory we conducted transcriptome analysis of such nitrogen-depleted cells and planned to map nucleosome occupancy under these conditions according to our established protocol. However, this turned out to be unfeasible. G0-arrested cells build up very thick cell walls, and therefore we were not able to sufficiently open them with zymolyase. Also other methods, like for example bead-beating, were not suitable as they had the undesirable side effect of chromatin sheering. Eventually, we stuck to zymolyase to destroy at least the cells walls of a small percentage of cells. We had to adjust MNase concentrations as much less chromatin was accessible. With this approach we were able to isolate only very little amounts of mononucleosomal DNA and therefore we had to switch to Illumina sequencing instead of microarray hybridisation for nucleosome occupancy mapping. It should be mentioned that nucleosome occupancy maps look slightly different when applying MNase-seq instead of MNase-chip. The NDR broadens in upstream direction and the +1 nucleosome does not necessarily have the highest nucleosome occupancy (Fig. 23A). We saw these effects already for a few wildtype and various mutant samples, but we cannot explain how these differences arise (data not shown). As it is not yet conclusively answered if technical problems caused those differences, the following data are only preliminary. However, as we did not wish to derive absolute nucleosome occupancy information but rather compare relative nucleosome occupancy patterns between the nitrogen-starved and the nitrogen-replenished sample, we considered these data as adequate. Comparison of TSS-aligned all gene overlay nucleosome occupancy plots revealed quite similar nucleosome patterns for nitrogen starved and nitrogen replenished cells (Fig. 23A). Next, we plotted separately nucleosome occupancy data for genes, which were up- or downregulated in the replenished state in comparison to the starved state (Fig. 23B-E). As the overlap between the transcription data published by Shimanuki et al. [3] and the transcription data generated in the Ekwall laboratory was not sufficiently large, both data sets were used in parallel. On the one hand, only small differences in the experimental procedure can influence transcriptome mapping and lead to different results. On the other hand, analysis of transcriptome data can be done in various ways and thus, lead to different results, too. Nucleosome occupancy patterns of genes upregulated upon nitrogen-replenishment did not change (Fig. 23B, D). This was true for both sets of transcriptome data. Average nucleosome occupancy of a subset of genes downregulated upon nitrogen-replenishment, revealed very interesting changes in the promoter regions: Downregulation was accompanied by nucleosome movement into the NDR (Fig. 23C, E). Again, this was true for both sets of transcriptome data. Thus, even if the transcriptome data did not overlap very well, they must both contain genes for which downregulation is accompanied by nucleosome movement into the NDR and which might dominate the average nucleosome occupancy patterns. The observed nucleosome occupancy changes in the NDR might accompany, assist or even induce downregulation of this subset of genes. Zawadzki et al. [233] investigated chromatin changes at promoters of genes up- or downregulated upon glucose addition in *S. cerevisiae*. They found chromatin changes at only 10% of promoters, even though transcriptional changes were detected at 50% of genes. In most cases only a single nucleosome showed changed occupancy. Similar to what we observed in *S. pombe*, repressed genes mainly gained a nucleosome. Activated genes on the other hand mainly lost a nucleosome. Thus, the authors concluded that transcriptional regulation is not extensively regulated by nucleosome repositioning. Importantly, transcriptional downregulation upon nitrogen-replenishment did not lead to changes in formation of regular nucleosomal arrays downstream of the TSS (Fig. 23C, E). From these observations two possible scenarios can be imagined. First, transcription might just not be involved in setting up nucleosomal arrays in gene bodies. Second, once established nucleosomal arrays are rather stable and transcription might not be necessary to maintain nucleosomal arrays that were set up before. However, to test *in vivo* a role for transcription in setting up nucleosomal arrays genome-wide or at least for a large subset of genes is rather difficult as one would need to find a condition in which transcription of a sufficiently large subgroup of genes is prevented over several cell cycles.

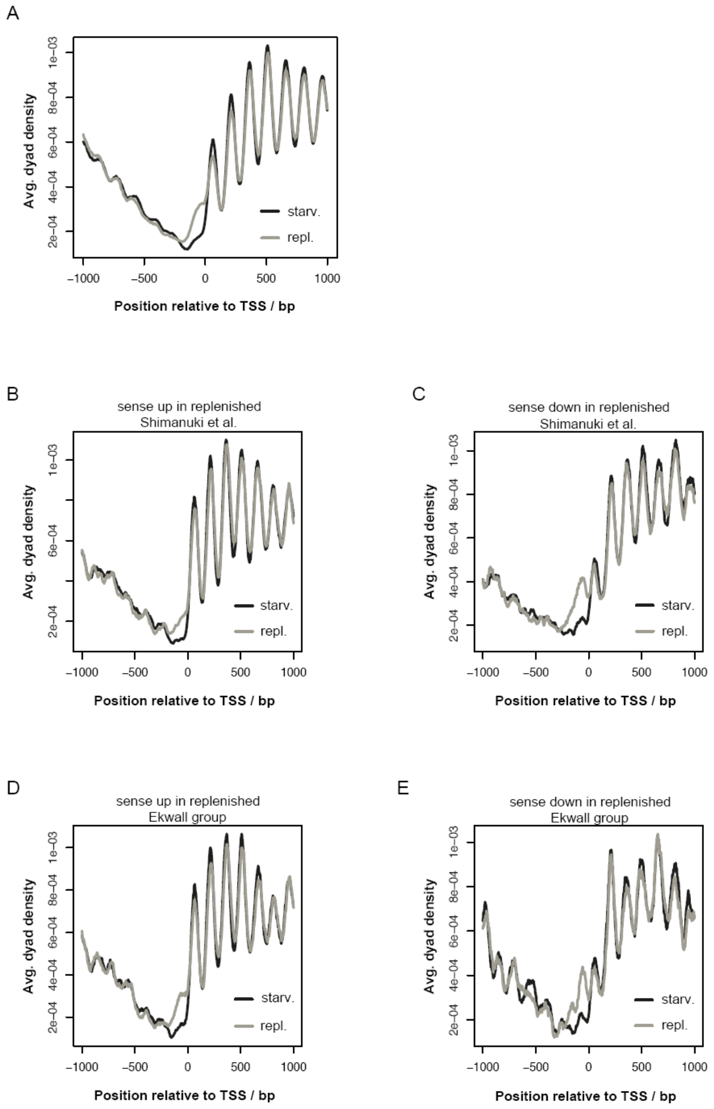

Figure 23 Transcriptional changes upon switch of nitrogen availability seem to be accompanied by only minor chromatin changes (preliminary data). TSS-aligned nucleosome occupancy profiles in wt (Hu303) after 48 h nitrogen starvation (starv.) or 48 h nitrogen starvation followed by 2 h growth in nitrogen-containing medium (repl.) for (A) 4013 genes, (B,C) genes (B) upregulated (494 calls) or (C) downregulated (345 calls) after nitrogen replenishment according to Shimunaki et al. [3], and (D,E) genes (D) upregulated (437 calls) or (E) downregulated (172 calls) after nitrogen replenishment according to the Ekwall laboratory.

3.8 Chromatin assembled by salt gradient dialysis *in vitro* has a nucleosome occupancy pattern around TSSs that is very different from the *in vivo* pattern

During the last years, the role of DNA sequence as an intrinsic determinant of nucleosome positioning was fiercely debated [4, 96, 234]. One way to investigate the isolated dependence of nucleosome positioning on DNA sequence is by assembling purified histones onto DNA *in vitro* via salt gradient dialysis followed by nucleosome occupancy measurements. Zhang et al. [2] employed this technique genome-wide in the following way. Histones purified from fly embryos and a plasmid library of *S. cerevisiae* genomic DNA were mixed together in a 1:1 mass ratio under high-salt conditions. Dialysis against low-salt buffer allowed for increasing interactions between histones and DNA and ultimately, formation of nucleosomes. Mononucleosomal DNA was purified and mapped to the genome via high throughput sequencing. This nucleosome occupancy was very different from *in vivo* nucleosome occupancy. At a large fraction of promoters NDRs could be recapitulated. Thus, homopolymeric (dA:dT) tracts seem to have an *in vivo*-relevant impact on nucleosome occupancy, especially on generating NDRs [235, 236]. However, these NDRs were not as nucleosome depleted as they were *in vivo*. Furthermore, some nucleosome positions and some nucleosome occupancies were similar in *in vivo* and *in vitro* chromatin. Incubation of chromatin generated by salt gradient dialysis (SGD) with cell extracts and energy in form of ATP, resulted in *in vivo* like nucleosome occupancy patterns. NDRs became very similar to *in vivo* NDRs and much more nucleosome positions and nucleosome occupancies were similar to the *in vivo* situation compared to the SGD chromatin sample.

Strikingly, homopolymeric (dA:dT) tracts are not enriched in *S. pombe* promoters [8]. On this background, we wondered if chromatin assembled on *S. pombe* DNA libraries *in vitro* showed *in vivo*-like promoter NDRs. We isolated histones from fly embryos, obtained recombinant *S. pombe* histones from Punit Prasad in the Ekwall group and three different *S. pombe* plasmid libraries. SGD chromatin was prepared using fly embryo histones and all three libraries (pDB248, pSPL10.1 and pURSP1) as well as recombinant *S. pombe* histones and the library pURSP1. *In vitro* nucleosome occupancy maps of all four experimental settings looked very similar (Fig. 24A). Strikingly, in *in vitro* nucleosome occupancy maps a nucleosome covers the region just upstream of the TSS, which is nucleosome depleted in *in vivo* samples. Besides this rather well-positioned nucleosome, no further nucleosomal arrays can be detected in the *in vitro* SGD nucleosome occupancy maps in relation to the TSS. Kaplan et al. [4] developed a computational model predicting nucleosome occupancy based on their *S. cerevisiae in vitro* nucleosome occupancy data. Application of this on *S. cerevisiae* SGD data trained algorithm on the *S.*

pombe genome did not work well. The algorithm predicted a nucleosome in the NDR, which is not present in TSS-aligned *in vivo* nucleosome occupancy plots (Fig. 24B). Strikingly, as mentioned above a nucleosome occupying the NDR was also present in *in vitro* SGD chromatin samples. Hence, the algorithm trained on *S. cerevisiae in vitro* data is able to predict *S. pombe in vitro* nucleosome occupancy to some extent, however, *in vivo* nucleosome occupancy differs largely from *in vitro* nucleosome occupancy and cannot be predicted by the algorithm. Furthermore, in the style of the experiments done in *S. cerevisiae*, we tried to reconstitute *in vivo* nucleosome patterns by addition of *S. pombe* cell extract and ATP to SGD chromatin. However, nucleosome occupancy pattern did not change at all (data not shown). It needs to be thoroughly investigated if biological or technical reasons account for the inability of the extract to change nucleosome occupancy patterns.

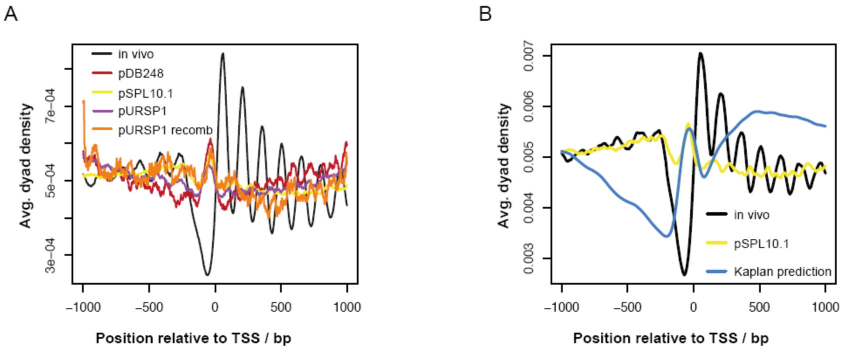

Figure 24 Nucleosome occupancy patterns of *in vitro* assembled chromatin are substantially different from nucleosome occupancy patterns observed in *vivo*. (A) TSS-aligned nucleosome occupancy profiles of chromatin prepared *in vitro* by assembly of purified fly embryo histones or recombinant *S. pombe* histones on plasmid libraries (pDB248, pSPL10.1 or pURSP1) and *in vivo* chromatin of wt (Hu303). (B) TSS-aligned nucleosome occupancy profiles of chromatin assembled *in vitro* (pSPL10.1) and *in vivo* chromatin as in (A) and nucleosome occupancy predicted by the Kaplan et al. algorithm [4].

Table 2. Numbers of transcripts with changed expression levels.

	> 2fold up	> 1.5fold up	total up	> 2fold down	> 1.5fold down	total down
strain comparison	**sense transcripts**[a]					
hrp1Δ vs. wt	21 [10] (0.3%)	130 [59] (1.9%)	743 [233] (11%)	7 [2] (0.1%)	47 [9] (0.7%)	466 [46] (6.9%)
hrp3Δ vs. wt	62 [37] (0.9%)	231 [119] (3.4%)	955 [282] (14.1%)	38 [15] (0.6%)	131 [43] (1.9%)	749 [130] (11.1%)
hrp1Δ hrp3Δ vs. wt	96 [67] (1.4%)	251 [154] (3.7%)	783 [284] (11.6%)	28 [11] (0.4%)	142 [42] (2.1%)	665 [104] (9.9%)
snf21-ts 34 °C vs. 25 °C	111 [74] (1.6%)	395 [193] (5.9%)	2209 [470] (32.8%)	108 [30] (1.6%)	413 [98] (6.1%)	1964 [295] (29.1%)
snf21-ts swr1Δ 34 °C vs. *snf21-ts* 25 °C	48 [36] (0.7%)	187 [102] (2.8%)	1977 [381] (29.3%)	54 [17] (0.8%)	306 [77] (4.5%)	1961 [361] (29.1%)
pht1Δ swr1Δ vs. wt	435 [144] (6.5%)	1182 [375] (17.5%)	2120 [550] (31.4%)	252 [23] (3.7%)	761 [45] (11.3%)	1673 [110] (24.8%)
	cryptic antisense transcripts[b]					
hrp1Δ vs. wt	24 [2] (0.36%)	150 [40] (2.2%)	711 [379] (10.5%)	0 [3] (0%)	5 [14] (0.1%)	41 [132] (0.6%)
hrp3Δ vs. wt	60 [21] (0.9%)	278 [74] (4.1%)	875 [401] (13.0%)	12 [6] (0.2%)	35 [29] (0.5%)	112 [214] (1.7%)
hrp1Δ hrp3Δ vs. wt	125 [10] (1.9%)	457 [41] (6.8%)	1027 [355] (15.2%)	4 [30] (0.1%)	27 [95] (0.4%)	93 [202] (1.4%)

[a] Sense transcripts correspond to all 6742 annotated elements (2008 version) including ncRNAs that may be antisense to a coding RNA. The number of ncRNAs is given in square brackets. The percentage of all annotated elements is given in round brackets. Note that not all loci have proper TSS annotations, which is why numbers in this table are not the same as numbers for genes in TSS-aligned nucleosome occupancy composite plots.

[b] Cryptic antisense transcripts correspond to transcripts that are antisense to an annotated element, unless the antisense transcript overlaps with and shows a similar (□ 20%) change as an annotated element already scored as a sense transcript. The number of antisense transcripts filtered out according to the latter criterion is given in square brackets.

4 Discussion

4.1 The role of H2A.Z in nucleosome positioning

The histone variant H2A.Z was found enriched at nucleosomes flanking the NDR in various organisms [49, 78, 87, 110, 189]. Its localisation made it a potential candidate for a factor involved in nucleosome positioning around TSSs. In *S. pombe*, H2A.Z was mainly enriched at the +1 nucleosome [49] and promoters binding H2A.Z showed a distinct chromatin structure with a regular upstream nucleosomal array and a clearly diminished NDR ([8], Fig. 9B, F). The group of H2A.Z-bound genes is generally enriched for genes lowly expressed in G2 (the predominant phase of an unsynchronized *S. pombe* culture) [49] and specifically for meiotic and stress response genes [237]. Hence, the shallow promoter NDR matches the expression status in an unsynchronized culture. Strikingly, double deletion of the genes encoding H2A.Z and Swr1, the remodeler responsible for H2A.Z incorporation, did neither change chromatin structure in general nor chromatin structure of H2A.Z-bound genes or genes transcriptionally responding to deletion of H2A.Z and Swr1 (Fig. 9A-D). This is similar to the findings in *S. cerevisiae* [107]. Thus, H2A.Z seems not to shape chromatin structure at promoters and gene bodies in *S. pombe* and *S. cerevisiae*. Remarkably, transcriptional changes were relatively pronounced in the *pht1Δ swr1Δ* mutant (Table 2). So one can speculate that H2A.Z might not shape chromatin structure but act further downstream, e.g. regulate transcription initiation or elongation.

There exist several studies, mainly in *S. cerevisiae* and mammals, proposing a role for H2A.Z in transcriptional regulation. Early studies in *Tetrahymena thermophile* demonstrated that H2A.Z is associated with the transcriptionally active macronucleus while the inactive micronucleus was devoid of H2A.Z [238]. In *S. cerevisiae*, H2A.Z is incorporated at non-induced *GAL1-10* and *PHO5* genes and lost upon transcriptional induction of those genes [239]. Similar observations were made for genes activated or repressed after heat-shock [240]. While activated genes lost H2A.Z, repressed genes gained H2A.Z. In another genome-wide *S. cerevisiae* study, H2A.Z could be mapped to the +1 and -1 nucleosomes of both, active and inactive genes and no correlation between H2A.Z amount and transcription rate could be found [110]. This missing correlation between H2A.Z presence and transcription rate does not exclude that H2A.Z is involved in transcriptional regulation as regulation might happen on the level of post-translational modifications of H2A.Z. And indeed, it could be shown that acetylated H2A.Z is mainly enriched at active promoters while unacetylated H2A.Z is predominantly found at repressed promoters [241, 242]. *In vivo*, H2A.Z is mainly acetylated at lysine 14 by Gcn5 and Esa1, the catalytic subunits of the SAGA complex and the NuA4 complex, respectively, after assembly into chromatin [243]. Also loading of H2A.Z seems to be linked to histone acetylation in *S. cerevisiae*. A significant fraction of the SWR1 complex contains the subunit Bdf1, which harbours two acetyl-lysine-binding bromodomains [240]. Thus, SWR1 might be recruited to promoters via interaction of Bdf1 with acetylated histone tails. H2A.Z occupancy correlates with certain histone acetylation modifications, e.g. H3K14 acetylation, and a strain depleted for the histone acetyltransferase subunit Gcn5 of the SAGA complex showed reduced levels of H2A.Z occupancy at distinct promoters [240]. Another study found that not SAGA-directed histone H3 acetlylation but NuA4-directed histone H4 acteylation is involved in recruitment of Bdf1 [244]. Strikingly, the HAT complex NuA4 shares four subunits with the SWR1 complex and Esa1 genetically interacts with Bdf1 [245]. Deletion of Eaf1, the subunit necessary for assembly of the NuA4 complex, led to decreased levels of H2A.Z at the *PHO5* promoter [246]. Remarkably, Bdf1 can also be part of the TFIID complex [245] and depletion of Esa1 resulted in reduced occupancy of Bdf1, TFIID, SWR1 complex and H2A.Z at many promoters [244]. Thus, it is tempting to speculate that pre-initiation complex (PIC) assembly and H2A.Z loading might be linked via NuA4 dependent histone acetylation.

In mammals, the link between H2A.Z and transcriptional regulation seems to be even stronger. In human CD4$^+$ T-cells H2A.Z is also enriched up- and downstream of the TSS [87]. Interestingly, in human cells binding levels of H2A.Z and gene activity positively correlated with each other. Furthermore, reduced levels of H2A.Z were found in -1 nucleosomes at genes activated upon T-cell receptor signalling possibly linked to RNA-polymerase II loading onto promoters [79]. Investigating H2A.Z occupancy at promoters revealed cycles of H2A.Z binding dependent on the transcription cycle [247]: Promoters poised for activation incorporated H2A.Z, H2A.Z assisted the recruitment of RNA-polymerase II, binding of Pol II to promoters led to eviction of H2A.Z- containing nucleosomes, both at promoters and in coding regions, followed by reloading of H2A.Z-containing nucleosomes after Pol II passage. In mouse liver and brain cells a connection between H2A.Z and RNA-polymerase II occupancy was found, too [248]. At a majority of genes a single H2A.Z-containing nucleosome was detected in the promoter region upstream of the TSS. Strikingly, the distance between the H2A.Z-containing nucleosomes and the TSS were inversely correlated with steady-state expression level and Pol II occupancy. These data fit quite well with the observed RNA-polymerase II recruitment activity of H2A.Z.

In short, it is quite likely that H2A.Z and Pol II recruitment are somehow linked. Regulation of this relationship seems to be achieved via amount of H2A.Z in mammals and acetylation state of H2A.Z in *S. cerevisiae*. In *S. pombe*, promoter H2A.Z binding and mRNA levels were negatively correlated [49]. Interestingly, the overlap between H2A.Z bound targets and targets transcriptionally responding to H2A.Z and Swr1 deletion, was very little (Fig. 9F). Thus, similar to *S. cerevisiae*, also in *S. pombe* the acetylation state of H2A.Z might be crucial for transcriptional regulation. However, the little overlap could also be explained differently. ChIP of H2A.Z might be incomplete or transcriptional changes upon H2A.Z and Swr1 depletion might be secondary effects possibly attributing to the boundary functions of H2A.Z [187].

4.2 The role of RSC in nucleosome positioning

In *S. cerevisiae*, a role for the RSC complex in nucleosome positioning could be demonstrated in various *in vivo* and *in vitro* experiments [68, 107, 129, 249]. *S. cerevisiae* and *S. pombe* RSC have several common features [115]: the ATPase subunits of both complexes are homologous and essential, both complexes are implicated in mitosis and contain several homologous subunits. This made us expect that *S. pombe* RSC should function in NDR formation similar to *S. cerevisiae* RSC. Strikingly, we did not observe any chromatin changes around TSSs in a *snf21-ts* mutant at the non-permissive temperature (Fig. 10C-E). However, as we checked only for induction of a phenotype, i.e. growth defects and change of cell shape, but not directly for reduction of Snf21 protein levels, we cannot ensure that we really mapped nucleosome positions in a strain sufficiently depleted for Snf21. A rather prominent difference between *S. cerevisiae* and *S. pombe* RSC is that *S. cerevisiae* RSC contains a subunit specifically binding DNA, Rsc3 [68]. Binding sequences for Rsc3 are enriched at NDRs and depletion of Rsc3 resulted in filled-up NDRs as also observed after depletion of the ATPase subunit Sth1 [107]. There is no homologous Rsc3 subunit in *S. pombe* and it has not been shown so far if *S. pombe* RSC contains a subunit with DNA-binding properties. *S. pombe* RSC contains two subunits of which homologs are lacking in S. cerevisiae RSC, i.e. Actin-related protein (Arp) 42 and Ssr4. Arps can interact with histones [243, 250], and Ssr4 belongs to a so far uncharacterized protein family [115]. If *S. pombe* RSC really lacks a subunit harbouring DNA-binding properties similar to Rsc3, then this might explain the functional differences of the two complexes.

4.3 The role of CHD1 remodelers in nucleosome positioning

What is the role of the CHD1 remodeler ATPases Hrp1 and Hrp3 for nucleosome positioning around TSSs in *S. pombe*? Nucleosomal arrays from the +3 nucleosome onwards were completely abolished in a strain lacking Hrp1 and Hrp3 (Fig. 13C).

How can such a loss of nucleosomal arrays arise? Several explanations are possible.

First, deletion of the genes encoding the two CHD1 remodeler ATPases could lead to histone depletion, which would result in decreased amount of nucleosomes and less nucleosomes occupying gene bodies and thus, loss of the nucleosomal array. However, Hennig et al. [251] could show by Western blot that histones levels were not reduced in the CHD1 mutant background compared to wildtype and hence, nucleosomes were not depleted. Furthermore, anti-H3 ChIP experiments revealed rather an increase of histone H3 at IGRs and ORFs in the absence of Hrp1 or Hrp3 [174, 252]. However, the corresponding experiment with the *hrp1Δ hrp3Δ* double mutant was not conducted.

Another explanation could be that Hrp1 and Hrp3 are involved in stabilization and assembly of canonical histones over gene bodies. Mapping nucleosomal DNA via MNase-protection selects for canonical nucleosomes as only canonical nucleosomes resist MNase digestion. Not properly assembled nucleosomes are rather sensitive to MNase. Supporting this hypothesis, Punit Prasad in the laboratory of Karl Ekwall showed *in vitro* that Hrp1 and Hrp3 have nucleosome spacing and nucleosome assembly activity [66]. Furthermore, nucleosome occupancy was somewhat (about two-fold) reduced in the *hrp1Δ hrp3Δ* double mutant in our TSS-aligned nucleosome occupancy map (Fig. 13C). However, bulk MNase ladders of the *hrp1Δ hrp3Δ* double mutant were hardly affected and still showed nucleosomal arrays, albeit with less signal compared to wildtype, i.e. about two-fold less occupancy (Fig. 17). This degree of decreased occupancy is less than the degree of loss of arrays in the TSS-aligned composite plots. So it cannot explain the loss of arrays on its own.

A third scenario would be that Hrp1 and Hrp3 are responsible for regularly spacing nucleosomes over gene bodies and loss of nucleosomal arrays in the *hrp1Δ hrp3Δ* mutant arises from irregular movement of nucleosomes in *cis* upon depletion of Hrp1 and Hrp3. As just mentioned Hrp1 and Hrp3 space nucleosomes *in vitro*. But if Hrp1 and Hrp3 really are involved in nucleosome spacing over gene bodies, how can nucleosome spacing be affected in TSS-aligned nucleosome occupancy maps (Fig. 13C) and spectral analysis (Fig. 13F) but not when monitoring bulk MNase ladders (Fig. 17)? Both, TSS-aligned nucleosome occupancy maps and spectral analysis monitor nucleosomal arrays relative to genomic coordinates. Thus, not only regularity of nucleosomes but also a fixed distance to a reference point is mirrored. For TSS-aligned nucleosome occupancy maps, such a reference point is the TSS or the +1 nucleosome position as the TSS- +1 nucleosome distance is relatively constant. In contrast, bulk MNase ladders are completely independent from genomic coordinates and solely image regularity of nucleosomes. As about 95% of the genome is genic in *S. pombe* [66], bulk MNase ladders are dominated by genic arrays. So, the observed chromatin changes in the *hrp1Δ hrp3Δ* mutant cannot be due to compromised nucleosomal arrays as such.

However, a randomized and no longer fixed distance between the TSS and the nucleosomal array could explain the chromatin features observed in the *hrp1Δ hrp3Δ* mutant. Thus, the function of Hrp1 and Hrp3 could be to link nucleosomal arrays to a reference point, most likely the TSS or the +1 nucleosome (Fig. 25).

Very strikingly, in *S. cerevisiae* double deletion of the genes coding for the CHD1 family remodeler Chd1 and the ISWI family remodeler Isw1 very much resembled the double deletion of the genes encoding the two CHD1 remodelers in *S. pombe* regarding TSS-aligned nucleosome occupancy maps and bulk MNase ladders ([66, 160], Fig. 13C and Fig. 17). On the one hand, an evolutionary shift in remodeler usage from a combination of ISWI and CHD1 remodelers to CHD1 remodelers only must have happened. On the other hand, the outcome of the remodeling reactions seems to be highly conserved.

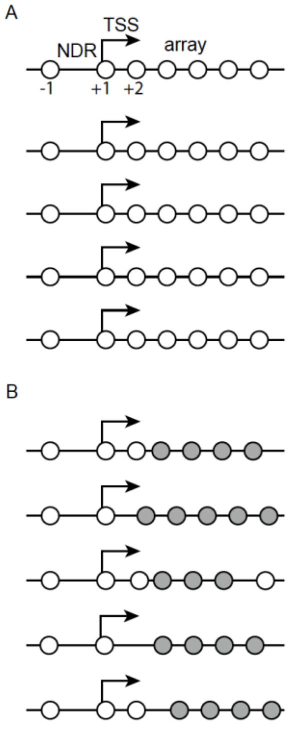

Figure 25 Hrp1 and Hrp3 link nucleosomal arrays to TSSs. (A) Wildtype situation: TSS-aligned regular nucleosomal arrays are attributed to a similar register between the TSS and the array and regular nucleosome spacing of many different genes in a population of cells. (B) *hrp1Δ hrp3Δ* mutant situation: Linkage of nucleosomal arrays to TSSs is lost leading to loss of nucleosomal arrays in TSS-aligned composite plots. However, most nucleosomes are still regularly spaced (grey circles) giving rise to bulk MNase ladders that are comparable to wildtype.

4.4 What positions the +1 nucleosome?

Remarkably, the position of the +1 nucleosome, the best-positioned nucleosome, was not affected in the *hrp1Δ hrp3Δ* mutant (Fig. 13C) and the respective *S. cerevisiae* mutants [160]. A simple explanation would be that positioning of the +1 nucleosome just does not belong to the tasks of CHD1 and/or ISWI remodelers in both yeasts. However, in *S. cerevisiae* ISW2 and ISW1a interact with the +1 nucleosome indicating involvement of these remodelers in positioning of the +1 nucleosome [130]. Thus, correct positioning of the +1 nucleosome might be achieved by redundant mechanisms. This would also fit the observation that so far no viable mutant with severely altered +1 nucleosome positions was found. However, minor shifts of the +1 nucleosome were detected in several mutants, for example Isw2 [157], Isw1 or Ino80 mutants [253]. Interestingly, mapping nucleosome positions of an *S. cerevisiae* strain carrying only about half of the amount of histone H3 (inducible H3 shutoff strain) revealed that positions of the +1 and +2 nucleosome were preserved – even though nucleosome occupancy was reduced- while positioning of subsequent nucleosomes was more affected [254]. *In vitro* reconstitution of *S. cerevisiae* chromatin in the presence of cell extract and ATP with a histone:DNA mass ratio of only 0.5:1 resulted likewise in positioned +1 and +2 nucleosomes and fuzzy subsequent nucleosomes [2]. However, van Bakel et al. [253] investigated nucleosome positions in an *S. cerevisiae* strain with reduced amounts of histone H4 and underscored slight changes in positioning of the +1 nucleosome upon histone depletion. Their analysis of the *in vitro* data of Zhang et al. [2] revealed shifts of the +1 nucleosome in a similar range. Remarkably, at the highly transcribed ribosomal genes only the +1 nucleosome is well-positioned while the other nucleosomes show strongly increased fuzziness compared to genes with stereotypical positioning patterns [190]. Thus, correct positioning of the +1 nucleosome and to some extent also of the +2 nucleosome seems to be very important for the cell. What is mechanistically so special about the +1 nucleosome? In *S. cerevisiae* and *S. pombe*, the +1 nucleosome covers the TSS [8, 75], while it lies just downstream of the TSS in fly and human [78, 79]. Thus, the +1 nucleosome is the gateway for RNA-polymerase to active transcription. In higher eukaryotes polymerase pausing just upstream of the +1 nucleosome is frequently observed [255]. At such genes the +1 nucleosome is shifted downstream in comparison to active genes [78, 79]. Hence, the +1 nucleosome could be involved in regulation of polymerase pausing. Positioning of the PIC and the +1 nucleosome seem to be linked. The Pugh laboratory performed ChIP-exo mapping of several PIC components in *S. cerevisiae* [256]. Their experiments revealed interaction of TFIID with the +1 nucleosome and TATA elements. They proposed that binding of TFIID to both encloses and thereby positions Pol II. On the contrary, the Rando and Struhl laboratories hypothesized the converse relationship between positioning of the PIC and the +1 nucleosome, namely that the PIC fine-tunes the position of the +1 nucleosome [209]. They compared nucleosome positioning and transcription of endogenous *K. lactis* or *D. hanseii* loci and the respective loci on YACs in *S. cerevisiae*. Their hypothesis was based on the finding that shifts of the +1 positions were accompanied by shifts of the TSSs in the same direction on genes contained on YACs in comparison to the corresponding endogenous genes. However, their results could be explained evenly well with the direction of causality favoured by the Pugh laboratory. In conclusion, there is some evidence that positioning of the +1 nucleosome and the PIC depend on each other. Such a relationship would indeed make the +1 nucleosome special and explain why the cell might need redundant mechanisms to ensure its proper positioning.

4.5 Why are nucleosomes so well-positioned at gene bodies?

Why at all does the cell put effort into establishing such regularly aligned arrays over gene bodies? In the *hrp1Δ hrp3Δ* mutant, this chromatin structure is disturbed starting from the +2 nucleosome (Fig 13C). Interestingly, the CHD1 remodeler single and double mutants do not show a strong phenotype regarding sense transcript levels and generation time and are relatively healthy. So, from a global point of view maintenance of genic nucleosomal arrays seems to be of minor importance for the cell. However, we and others found cryptic antisense transcription over gene bodies upregulated in the *hrp1Δ hrp3Δ* mutant as was also seen for the corresponding *S. cerevisiae* CHD1 and ISWI remodeler mutants [229, 257, 258]. Now there exist three independent studies, including ours [66, 251, 252], on the effects of CHD1 remodelers on nucleosome positioning and transcription in *S. pombe*. While we found in the *hrp1Δ hrp3Δ* mutant for 15.2% of annotated elements upregulated cryptic antisense transcripts, Hennig et al. [251] reported upregulation of cryptic antisense transcripts for 44% of analysed elements. Shim et al. [252] did not examine a *hrp1Δ hrp3Δ* double mutant but only a *hrp3Δ* single mutant. They found significant upregulation of cryptic antisense transcripts in the *hrp3Δ* mutant, but did not state any numbers. The large difference in detected cryptic transcription between the Hennig et al. and our study might be attributed to differences in the experimental setup. While we performed reverse transcription in presence of actinomycin D to avoid spurious second-strand synthesis [223], Hennig et al. omitted actinomycin D. In collaboration with Ulrika Norman-Axelsson from the Karl Ekwall laboratory, we analysed the influence of actinomycin D on transcriptome data. In the absence of actinomycin D, sense and antisense transcription correlated with each other (wildtype, R=0.5), while this correlation was lost when performing reverse transcription in the presence of actinomycin D (wildtype, R=0.12). Interestingly, the corresponding analysis of transcriptome data generated without a reverse transcription step by directly hybridizing RNA on a microarray [221] revealed an intermediate correlation coefficient (wildtype, R=0.39). Thus, the correlation between sense and antisense transcription seems to be at least in parts biologically real and cannot solely be attributed to spurious second-strand synthesis during the reverse transcription step. In addition, the antisense transcription data generated without actinomycin D correlated slightly better with the data generated by direct hybridization of RNA compared to the data generated with actinomycin D (data not shown). In conclusion, actinomycin D seems to prevent generation of false positive transcripts, but due to lower sensitivity several transcripts are missed. Thus, the real number of cryptic antisense transcripts upregulated upon depletion of Hrp1 and Hrp3 might lie between the numbers found by Hennig et al. and us.

Apparently, when nucleosomes are not properly positioned over gene bodies DNA segments are more exposed than in wildtype and can function as cryptic promoters.

4.6 Factors involved in prevention of cryptic transcription

Upregulation of cryptic transcription was also reported for other mutants. There seem to be three independent but each essential ways to protect coding regions from cryptic transcription: regular TSS-aligned spacing (see above), high nucleosome occupancy, and low histone turnover. Impairment of one of these pathways presumably leads to exposure of DNA segments harbouring the properties of promoters and hence serving as initiation points for cryptic transcription.

First of all transcription initiation from a cryptic promoter accompanied by reduced histone H4 levels was shown for a *S. cerevisiae* strain depleted for the histone chaperone and transcription elongation factor Spt6 [259]. Both, *S. cerevisiae* [258, 260] and *S. pombe* [251] strains depleted for subunits of the FACT chaperone complex showed an increase of cryptic transcription and a decrease of histone levels, too. FACT is a histone chaperone that travels with elongating polymerase and is thought to disassemble nucleosomes -most probably by removal of an H2A-H2B dimer- in front of polymerase and reassemble nucleosomes after polymerase passage [261]. Interestingly, nucleosome positioning was only mildly affected in the *S. pombe* FACT mutant (*pob3Δ*) [251] and in a *S. cerevisae* strain depleted for the non- essential components of the FACT complex Nhp6a and -b [260]. FACT mutants exhibit reduced histone levels and hence more DNA that is not assembled into nucleosomes (Fig. 26).

S. pombe and *S. cerevisiae* strains depleted for the HDAC Clr6 complex II (Rpd3S complex in *S. cerevisiae*) or the histone methyltransferase Set2 show increased cryptic transcription, too [229, 230, 251]. The histone methyltransferase Set2 specifically methylates histone H3 at lysine residue 36 (H3K36me) [262] in the middle and at 3’ ends of long (> 1kb) and less transcribed genes [230]. The HDAC Rpd3S is recruited to gene bodies via interaction with phosphorylated CTD of Polymerase II and its deacetylation activity is stimulated by the H3K36me3 methyl mark [227]. In *S. pombe*, neither nucleosome positions around TSSs (Fig. 20) nor histone levels [251] were changed in Clr6 complex or Set2 mutants.

For the *alp13Δ* (Clr6 complex II) mutant changed H3 acetylation levels with increased acetylation in gene bodies could be shown [251]. However, in the *set2Δ* mutant acetylation patterns were only mildly altered and in the *hrp1Δ hrp3Δ* mutant H3 acetylation patterns were unchanged. This suggests that the H3K36me3 mark is not the way of recruitment for the Clr6 complex, but might stimulate Clr6 activity as was already seen for the homologous *S. cerevisiae* complexes [227]. Elevated acetylation levels in the *alp13Δ* mutant might be responsible for the observed cryptic transcription initiation in this strain as acetylated nucleosomes are potential targets for bromodomain-containing chromatin remodelers which might expose cryptic promoters through nucleosome disassembly [251] and as acetylation might weaken histone-DNA interactions (Fig. 26).

H3K36 methylation by Set2 might keep histone turnover low through recruitment of CHD1 and/or ISWI remodelers. The remodeler ATPases Isw1 and Chd1 associated with nucleosomes methylated at H3K36 *in vitro* and the remodeler complex ISW1b was recruited by H3K36me3 *in vivo* [229]. Furthermore, increased histone turnover at gene bodies was shown for *S. cerevisiae* Isw1 and Chd1 mutants, too [228, 229]. Corresponding histone exchange experiments in *S. pombe* are still missing, but it is very likely that this connection to regulation of histone turnover can be drawn for *S. pombe* as well. In *S. cerevisiae*, upregulation of cryptic transcripts and elevated H4 acetylation levels are similar in a *set2Δ* single mutant and *set2Δ isw1Δ* or *set2Δ chd1Δ* double mutants. Interestingly, also in *S. pombe* cryptic antisense transcription profiles of Hrp, Set2 and Clr6 complex mutants were very similar [251, 252]. However, as nucleosome positioning patterns were unchanged in Set2 and Clr6 complex II mutants but affected in CHD1 and/or ISWI remodeler mutants, CHD1 and/or ISWI remodelers mediated stabilization of H3K36 methylated nucleosomes and linkage of nucleosomal arrays to TSSs must be two independent mechanisms. The observed higher histone turnover in *S. cerevisiae* Isw1 and Chd1 mutants might also be directly linked to the perturbed nucleosomal arrays. RNA-polymerase II might need a fixed distance of the TSS and the nucleosomal array and evenly spaced nucleosomes to be able to transcribe through chromatin. Changed nucleosome positions in the absence of CHD and/or ISWI remodelers might lead to increased nucleosome eviction during polymerase passage and thus higher histone turnover. The observed increase in sensitivity to 6AU of the *hrp1Δ hrp3Δ* mutant compared to wildtype supports a preference of Pol II for regular nucleosomal arrays (Fig. 19 C). Thus, in the absence of CHD1 and/or ISWI remodelers cryptic promoters might either be exposed by nucleosome movement in *cis* or by increased histone turnover either through missing stabilization of H3K36 methylated histones and/or through Pol II mediated histone eviction (Fig. 26).

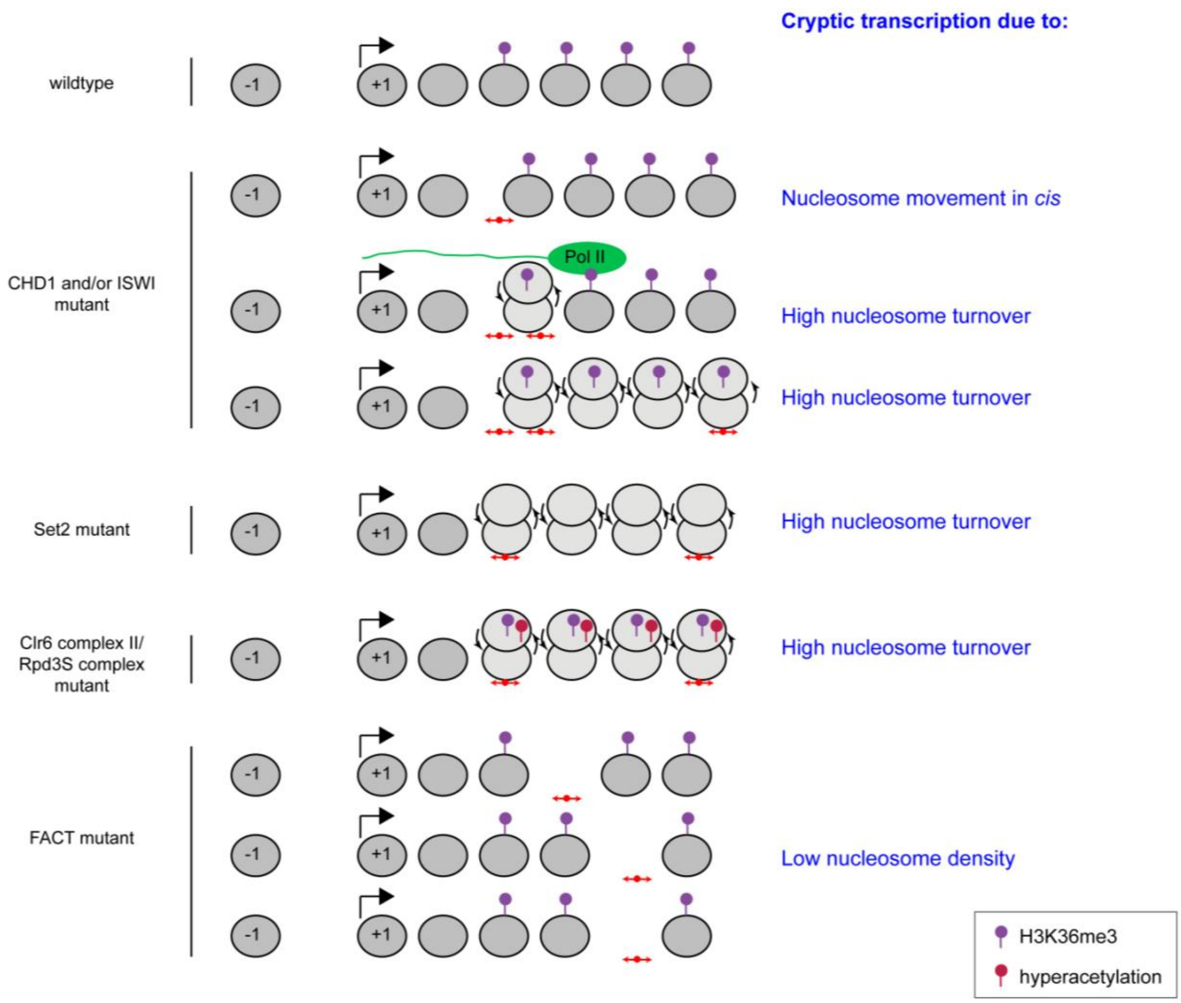
Cryptic transcription due to:
wildtype
-1
+1
CHD1 and/or ISWI mutant
Nucleosome movement in *cis*
Pol II
High nucleosome turnover
High nucleosome turnover
Set2 mutant
High nucleosome turnover
Clr6 complex II/ Rpd3S complex mutant
High nucleosome turnover
FACT mutant
Low nucleosome density
H3K36me3
hyperacetylation

Figure 26 Factors involved in prevention of cryptic transcription in *S. pombe* and *S. cerevisiae*. CHD1 and/or ISWI remodelers, Set2, Clr6 complex II/ Rpd3S complex and FACT prevent initiation of cryptic transcription via generation of nucleosomal arrays in register to TSSs, via ensuring low nucleosomal turnover in gene bodies, or via ensuring high nucleosome density at gene bodies. In CHD1 and/or ISWI remodeler mutants cryptic promoters are accessible due to nucleosome movement in *cis* and high nucleosome turnover possibly generated by Pol II transcribing through perturbed nucleosomal arrays and/or generated through missing stabilization of H3K36 methylated nucleosomes. In Set2 mutants cryptic promoters are accessible due to high nucleosome turnover attributed to missing H3K36 methylation and along with this missing stabilization of nucleosomes. In Clr6 complex II/Rpd3S mutants cryptic promoters are accessible due to high nucleosome turnover as a consequence of histone hyperacetylation. In FACT mutants cryptic promoters are accessible due to reduced histone levels and consequentially lower nucleosome density. Nucleosomes are depicted in dark grey, nucleosomes with increased turnover in light grey, red circles depict cryptic promoters with transcription possibly initiating in both directions (red arrows), black arrows depict TSSs and direction of sense transcription. Purple pins depict H3K36 trimethylation, pink pins depict hyperacetylation.

Remarkably, in the *S. pombe hrp1Δ hrp3Δ* mutant cryptic transcription happens with only at ~7 to ~15 % of annotated elements (Table 2) not very frequently while the effect on chromatin is rather widespread. Several reasons might contribute to this. As already discussed, the actual number of cryptic antisense transcripts might be higher as we might have missed some cryptic antisense transcription due to performing reverse transcription in the presence of actinomycin D (see chapter 4.5). In addition, due to bioinformatic reasons we could call only antisense but not sense cryptic transcripts and hence most probably have missed some cryptic transcription in the sense direction. Moreover, in most cases cryptic transcripts are degraded by RNases of the exosome immediately after their generation. To detect these transcripts the transcriptome of exosome mutants (*rrp6Δ*) should be analysed. However, a *hrp1Δ hrp3Δ rrp6Δ* triple mutant was not viable (Tamas Fischer, personal communication). Furthermore, transcription cannot initiate from any DNA sequence, but the sequence must fulfil certain requirements to serve as a promoter and such sequences might just not be widespread in the *S. pombe* genome.

Cells seem to put quite a lot of effort into preventing cryptic transcription. However, yeast strains showing increased cryptic transcription upon depletion of the before discussed factors are rather healthy. So, why does the cell spend so much energy on cryptic transcription prevention if in the end it does not care so much about cryptic transcription? For organisms of higher complexity prevention or regulation of cryptic intragenic transcription does indeed play a role. It was shown in mouse embryonic stem cells (ESCs) that the H3K4me3 demethylase KDM5B is involved in ensuring effective transcriptional elongation of genes important for self-renewal of ESCs by preventing intragenic transcriptional initiation. Interestingly, similar to yeast the Set2-Clr6/Rpd3S pathway comes into play in this context as KDM5B is targeted to sites carrying the H3K36me3 mark via association with an Rpd3S-like complex [263]. We could not find a correlation between changes in cryptic antisense transcription and the respective sense transcripts in *S. pombe* (Fig. 16). Possibly, in comparatively simply organised unicellular organisms cryptic transcription does not extensively perturb nuclear processes at steady state growth in rich media, but prevention of cryptic transcription might be important during changes of biological states, e.g. stress response. However, one can easily imagine that multicellular organisms need a higher degree of nuclear regulation to ensure cell type specificity and thus, are overall more sensible to transcriptional changes.

4.7 Models of nucleosome positioning at promoters and gene bodies

We and others could show that chromatin remodelers are involved in nucleosome positioning around TSSs. Furthermore, GRFs play a direct or indirect role in nucleosome positioning [68, 107], and DNA sequence features define rotational positioning and -at least in *S. cerevisiae*- determine NDRs to some extent [4, 94, 97, 264]. But how do all these activities come together in order to generate this specific chromatin structure around TSSs? Does a master regulator or driving force exist? So far three different concepts of nucleosome positioning were proposed.

4.7.1 Statistical positioning

Already in 1988, Kornberg and Stryer proposed the model of statistical positioning to explain the periodicity of nucleosomes observed in DNA gels after MNase digestion [265]. They assumed that barriers exist which cannot be crossed by nucleosomes and that nucleosomes passively align at those barriers. With the help of these and some other assumptions, they were able to mathematically model nucleosome periodicity similar to the experimentally observed periodicity. In this model periodicity exists only until a certain distance from the barrier due to a dampening effect. *In vivo* such barriers could be sequence specific DNA-binding proteins, nucleosome excluding sequences like homopolymeric (dA:dT) tracts or a nucleosome positioned by any of the discussed positioning mechanisms. Indeed, when nucleosome occupancy of a subset of the *S. cerevisiae* genome was mapped in high resolution, the observed nucleosome occupancy around TSSs did generally match the concept of statistical positioning [76]. Mavrich et al. [190] employed genome-wide nucleosome positioning data to investigate the mechanisms of statistical positioning in more detail. They found evidence that the +1 nucleosome, and to some extent also the -1 nucleosome, are possibly positioned through nucleosome exclusion sequences in NDRs, AA positioning sequences, AT and TA dinucleotide periodicities near nucleosome borders and GRF binding sites. They proposed that the +1 and -1 nucleosomes function as barriers and that the subsequent nucleosomes are positioned statistically. However, they did not exclude that chromatin remodelers facilitate nucleosome movement. Further support for the existence of a statistical positioning mechanism provided nucleosome occupancy studies of *S. cerevisiae* strains depleted for chromatin-related factors [208]. Depletion of the RNA-polymerase II subunit Rpb1, the remodeler ATPase Isw2 or Sth1, the remodeler ATPase of the RSC complex, resulted in movement of the whole nucleosomal array and not of single nucleosomes. The same was true for genes with paused polymerase in *D. melanogaster* [78]. Such a movement is consistent with the concept of statistical positioning as it implies that movement of the barrier, possibly the +1 nucleosome, entails movement of the whole nucleosomal array.

Another feature of the theoretical concept of statistical positioning is that the distance between nucleosomes must increase with decreasing nucleosome density. This aspect was tested recently in *S. cerevisiae* in three *in vivo* [253, 254, 260] studies and one *in vitro* [2] study. All four studies could show that decreased histone amounts did not change nucleosome spacing and thus argue against a statistical positioning mechanism. According to the model of statistical positioning chromatin remodelers only facilitate movement of nucleosomes and thus their activity should not be specific. However, the chromatin remodeling activity of RSC was highly specific and could not be replaced by other remodelers [249] arguing against statistical positioning, too.

4.7.2 Barrier/organising centre packing model

After disproving the relevance of statistical positioning as originally proposed *in vitro*, Zhang et al. suggested an active nucleosome packing model [2]. Here, nucleosomes are actively packed against a barrier or organising centre at the 5`end. Such a model can explain all the observed features of *in vivo* chromatin and also of *in vitro* reconstituted chromatin. Different remodeler usage in different species or cell types could explain the observed differences in linker length. Furthermore, in 3’ direction increasing fuzziness of the nucleosomal array, which was explained by dampening in the statistical positioning model, could result from local high remodeler concentrations at the 5`end, which decreases towards the 3’ end. Yen et al. refined this model on the basis of mapping chromatin remodelers to nucleosome positions [130]. They proposed that NDRs function as organising centres and that nucleosomes can be moved towards or away from organising centres and thus, organising centres have the property to impose directionality on the nucleosome positioning process. The hypothesis that CHD1 and/or ISWI remodelers link nucleosomal arrays to fixed points like the TSS or the +1 nucleosome is in line with the organising centre packing model as it also includes movement of nucleosomes in relation to reference points.

Möbius et al. [266] developed a physical model, the so called active soft-core nucleosome gas model, to describe nucleosome positioning patterns observed with reduced histone levels [2, 260]. Here, a strongly positioned +1 nucleosome and the activity of a nucleosome spacing factor were sufficient to describe the observed patterns while directionality of packing was not necessary.

4.7.3 Transcription

What is the role of transcription elongation in formation of nucleosomal arrays? Several aspects are suggestive of involvement of transcription elongation in array formation. In *S. pombe* nucleosomal arrays are co-directional with transcription [8]. At first glance, in *S. cerevisiae*, nucleosomal arrays up- and downstream of the TSS are relatively symmetrical [75]. However, when selecting for genes that do not share a NDR with another gene, i.e. genes, which have neither a bidirectional nor a tandem partner upstream arrays are clearly diminished *in vivo* (Fig. 7A). Thus, when selecting for genes without any related transcription (in terms of shared NDRs) in the upstream direction, nucleosomal arrays are no longer symmetrical, but co-directional with transcription, too. Furthermore, in *S. pombe* and on foreign YACs in *S. cerevisia*e array length correlated well with transcript length [8, 209]. In addition, nucleosomal arrays reconstituted in transcription-free *in vitro* experiments resembled *in vivo* nucleosomal arrays only to some extent as the positions of reconstituted nucleosomes were slightly shifted downstream compared to *in vivo* positions and as nucleosomal arrays were shorter in case of reconstituted chromatin in comparison to *in vivo* chromatin [2]. However, there are also arguments against a role of transcription elongation in formation of nucleosomal arrays. Co-directionality of transcription and nucleosomal arrays was preserved in chromatin reconstituted by the transcription-free *in vitro* system (Fig. 7B). Thus, co-directionality cannot be generated by transcription. Furthermore, the correlation between array length and transcript length could arise through perturbation of nucleosomal arrays by transcription termination just as well. Most importantly, even if not perfect in sense of similarity to the *in vivo* situation, nucleosomal arrays could be generated in a transcription-free system [2]. Thus, transcription cannot have a major role in nucleosome positioning in *S. cerevisiae*. However still, positioning in the transcription-free reconstitution system has its limitations and generates only *in vivo*-like but not *in vivo* patterns and transcription might be the factor responsible for the gap between *in vivo*-like and *in vivo* positions.

4.7.4 Combined nucleosome positioning model

Neither the organising centre packing nor the transcription model seems to fully explain nucleosome positioning patterns. However, a combination of both models could explain most of the data quite well: According to the organising centre packing model, chromatin remodelers are responsible for regularly spacing nucleosomes at gene bodies and for directly or indirectly determining directionality via linkage of nucleosomal arrays to the TSS. Chromatin remodelers can be recruited to promoters and gene bodies either via transcription-independent factors (which are of course still transcription-related) like sequence specific DNA-binding proteins [68, 107] and histone modification marks (ISW1b-H3K36me: [229]) and/or via transcription-dependent factors like elongating polymerase itself and elongation associated factors (Chd1 interacts with PAF, DSIF,FACT [173]). In the reconstitution system chromatin remodeler recruitment can be conducted solely via transcription-independent factors and also directionality of nucleosomal array assembly or packing is achieved by factors constituting the organising centre. Assuming that the concentration of transcription-independent remodeler-recruiting factors like for example transcription factors is much higher at promoters and 5`ends of genes in comparison to the middle of genes, *in vivo*-like nucleosome positions can be generated at promoters and 5’ ends but not so much in the middle of genes. *In vivo*, elongating Pol II and elongation-associated factors might additionally recruit remodelers throughout elongation possibly leading to correlation of nucleosomal array length and transcript length. It has been observed in *S. pombe* and mammals that silent genes do not show any nucleosome positioning patterns [8, 79], while silenced meiotic genes in *S. cerevisiae* do so [190]. Thus, in *S. pombe* and higher eukaryotes transcription might still play a larger role in generating nucleosomal arrays than in *S. cerevisiae*.

4.8 Relationship of transcriptional changes and chromatin changes

Chromatin is not a rigid structure but highly dynamic and also transcription is a highly dynamic process. This raises the question of how strongly chromatin and transcription influence each other and if changes of one automatically lead to changes of the other. There is clear evidence that chromatin can regulate transcription, i.e. that chromatin changes can result in transcriptional changes. The *PHO5* promoter of *S. cerevisiae* is a good example for regulation of transcription through chromatin [267]. Promoter chromatin remodeling also precedes activation of heat shock genes [120]. Furthermore, the Segal group constructed a multitude of HIS3 promoter versions varying in length and quality of nucleosome disfavouring poly(dA:dT) tracts and could show that promoter variation affected nucleosome organisation and transcriptional output [264]. However, investigation of the chromatin-transcription relationship at genomic level resulted in opposing findings. For example, Zawadski et al. [233] reported a weak correlation between changes in transcript level and chromatin structure for glucose-induced transcriptional reprogramming. On the contrary, Zaugg et al. [268] found that chromatin regulates the difference between on and off transcriptional states, but not the expression levels. In the *hrp1Δ hrp3Δ* mutant, we could observe that a subgroup of genes exhibited chromatin changes independently of any transcriptional changes (Fig. 15J). Thus, chromatin changes can but do not have to lead to transcriptional changes. The weak correlation between transcriptional changes and chromatin structure changes in the glucose-induction experiment also indicates that transcriptional changes not necessarily give rise to changes in chromatin structure. Nevertheless, there exist some hints that transcriptional changes can cause chromatin changes. For example, activation of the *S. cerevisiae GAL10* locus is accompanied by histone eviction through Pol II [117]. Though, one has to add that histone eviction could also immediately precede Pol II elongation. And again in *S. cerevisiae*, deletion of the Pol II subunit Rpb1 resulted in shifts of the nucleosomal array [208]. However, those arguments are rather weak and we could show in several *S. pombe* mutants, that changes in sense transcription never caused changes in chromatin structure (Fig.

9C,D; 10D,E; 11B,C; 12C,D; 15). Alike could be shown in our nitrogen starvation experiment as genes up- or downregulated upon nitrogen replenishment exhibited no chromatin changes over gene bodies (Fig. 23). Additionally, chromatin seems to be not only quite robust against transcriptional changes in sense but also against upregulation of cryptic antisense transcripts as depletion of Set2 led to upregulation of cryptic transcripts [251] without changes in chromatin structure (Fig. 20A).

4.9 Outlook

4.9.1 Involvement of remodelers and transcription in nucleosome positioning around TSSs

In this work, it could be demonstrated that the CHD1 remodelers Hrp1 and Hrp3 play a crucial role in positioning nucleosomes over gene bodies. Very strikingly, the effects of Hrp1 and Hrp3 depletion mirrored combined depletion of the CHD1 remodeler Chd1 and the ISWI remodelers Isw1 and Isw2 in *S. cerevisiae* [160]. Thus, the outcome of the remodeling reactions seem to be evolutionary conserved while the repertoire of remodelers changed during evolution. It came to us as a surprise, that the role of RSC in NDR formation in *S. cerevisiae* [129] seemed not to be conserved in *S. pombe*. Due to lack of an antibody against Snf21, we could not check for protein levels but only for induction of a phenotype after temperature shift. To confirm the results obtained with a strain harbouring a temperature-sensitive *snf21* allele, the Snf21 protein depletion should be achieved via a different approach as well and nucleosome occupancy should be mapped. For this purpose, the auxin-inducible degron (AID) system will be utilized [269, 270]. This system employs the auxin-dependent protein degradation pathway from plants to achieve inducible and temperature-independent degradation of proteins. Auxin family hormones bind to the F-box transport inhibitor response 1 (TIR1) protein that is present in a complex with the E3 ubiquitin ligase SCF leading to interaction with auxin/IAA transcript repressors (AUX/IAA). Subsequently, an E2 ubiquitin conjugating enzyme is recruited, AUX/IAA is polyubiquitylated and degraded. Fusion of a plant-specific AUX/IAA protein (AID-tag) to the protein of interest and expression of the also plant-specific TIR1 protein was shown to lead to degradation of the protein of interest upon addition of auxin in budding and fission yeast [269, 270]. The AID-tag will be fused to the C-terminus of Snf21 via homologous recombination in a strain expressing TIR1. Snf21 degradation upon addition of auxin will be controlled by Western blot with an antibody specific to the AID-tag. Mononucleosomal DNA will be prepared from cells harbouring the Snf21-AID allele after induction of protein degradation with auxin and nucleosome occupancy will be mapped by microarray hybridization.

The INO80 remodeler is implicated in transcriptional regulation [48, 183, 184]. Furthermore, INO80 could be mapped to nucleosomes at the 5' and the 3' end of genes [130] and it is connected to H2A.Z removal in gene bodies [73]. Thus, INO80 is yet another potential candidate for a remodeler involved in nucleosome positioning around TSSs. To test this, as described for Snf21, the Ino80 ATPase could be fused to the AID-tag and nucleosome occupancy could be mapped upon depletion of Ino80.

As several data suggest a role for RNA-Polymerase II assembly or elongation in nucleosome positioning, this possible connection should be investigated in more detail in *S. pombe*. So far, we employed a mutant strain carrying a temperature-sensitive allele for the Pol II subunit Rpb7 in order to map nucleosome occupancy in a system deficient for transcription. Rpb7 couples transcription to RNA processing [271] and depletion of Rpb7 led to decreased transcription at many loci. However, depletion of the largest Pol II subunit Rpb1 that contains the carboxyl-terminal domain (CTD) should be even more effective in ceasing transcription. In *S. cerevisiae*, a shift of the nucleosomal array was observed upon depletion of Rpb1 [208]. Thus, a *S. pombe* strain carrying an Rpb1-AID allele could be generated and nucleosome occupancy could be mapped after induction of Rpb1 degradation.

In *S. cerevisiae*, *in-vivo*-like nucleosome positions could be reconstituted in an *in vitro* system lacking transcription [2]. Thus, in *S. cerevisiae* nucleosome positioning must be largely independent of transcription. For *S. pombe*, the corresponding *in vitro* system should be established in order to gain insights into the role of transcription in nucleosome positioning in *S. pombe*, a species that is far evolutionary divergent from *S. cerevisiae*.

Furthermore, once the *in vitro* reconstitution system is established in *S. pombe*, the role of remodelers and other factors in nucleosome positioning could be investigated in more detail using mutant extracts and/or purified factors for reconstitution.

4.9.2 Histone exchange

In *S. cerevisiae*, elevated histone exchange over gene bodies and increased cryptic transcription were shown for Isw1, Chd1, Set2 and Rpd3s complex mutants. The authors concluded that ISWI and CHD1 remodelers, Set2 and the Rpd3S complex act together to prevent histone exchange and thereby initiation of cryptic transcription. However, as we could show in *S. pombe* that nucleosome positions are changed in CHD1 remodeler mutants, but not in Set2 or Clr6 mutants, we suppose that CHD1 and/or ISWI remodelers and Set2-Clr6/Rpd3S act in different pathways in order to prevent initiation of cryptic transcription. In *S. pombe*, it has not been shown yet if the respective mutants show also elevated histone turnover. For this purpose a *S. pombe* strain carrying tagged histones in addition to the respective deletions or mutations could be generated. The strain could be designed corresponding to the *S. cerevisiae* strain used for histone turnover experiments and harbour a Myc-tagged histone H3 driven by the endogenous promoter and a Flag-tagged histone H3 driven by an inducible promoter, e.g. the tetracycline-regulated promoter constructed by Zilio et al. [272]. Histone turnover could be assigned via calculation of the ratio of Myc-tagged and Flag-tagged histone H3 [202].

4.9.3 Transcriptome mapping by CAGE and annotation of TSSs

In preliminary experiments in wildtype we could map a subset of transcripts by CAGE and assign TSSs to the respective transcripts. Aligning nucleosome occupancy data at those TSSs resulted in stereotypic nucleosome occupancy pattern with high peak-trough ratios and made us conclude that the CAGE approach allows confidential mapping of 5’ ends. Therefore, transcripts will be mapped genome-wide for wildtype by CAGE and TSSs will be annotated. In addition, transcriptomes of an exosome mutant (*rrp6Δ*) will be generated in order to map transcripts that would be rapidly degraded in the presence of functional exosomes.

4.9.4 Annotation of bidirectional and tandem promoters

Comparison of nucleosome occupancy patterns at promoters in *S. cerevisiae* and *S. pombe* revealed a clear difference: While in *S. cerevisiae* a distinct nucleosomal array is not only present downstream but also upstream of the TSS, in *S. pombe* mostly a distinct downstream array is present [8]. In *S. cerevisiae*, transcription is quite pervasive [217] and we could show that upstream nucleosomal arrays arise mainly at bidirectional and tandem promoters. We annotated bidirectional and 3’ tandem promoters for *S. pombe* and could demonstrate that bidirectional promoters also exhibit upstream nucleosomal arrays but are less abundant than in *S. cerevisiae*. Therefore, bidirectional promoters contribute less to all genes-overlay patterns, which may explain the apparent lack of regular upstream arrays. However, the transcriptome data we used for promoter-type annotation were not complete and thus, annotations will be repeated by employing the CAGE transcriptome data.

References

1. Sun, M., et al., *Comparative dynamic transcriptome analysis (cDTA) reveals mutual feedback between mRNA synthesis and degradation.* Genome Res, 2012. **22**(7): p. 1350-9.
2. Zhang, Z., et al., *A packing mechanism for nucleosome organization reconstituted across a eukaryotic genome.* Science, 2011. **332**(6032): p. 977-80.
3. Shimanuki, M., et al., *Two-step, extensive alterations in the transcriptome from G0 arrest to cell division in Schizosaccharomyces pombe.* Genes Cells, 2007. **12**(5): p. 677-92.
4. Kaplan, N., et al., *The DNA-encoded nucleosome organization of a eukaryotic genome.* Nature, 2009. **458**(7236): p. 362-6.
5. Clapier, C.R. and B.R. Cairns, *The biology of chromatin remodeling complexes.* Annu Rev Biochem, 2009. **78**: p. 273-304.
6. Jiang, C. and B.F. Pugh, *Nucleosome positioning and gene regulation: advances through genomics.* Nat Rev Genet, 2009. **10**(3): p. 161-72.
7. Maeshima, K., S. Hihara, and M. Eltsov, *Chromatin structure: does the 30-nm fibre exist in vivo?* Curr Opin Cell Biol, 2010. **22**(3): p. 291-7.
8. Lantermann, A.B., et al., *Schizosaccharomyces pombe genome-wide nucleosome mapping reveals positioning mechanisms distinct from those of Saccharomyces cerevisiae.* Nat Struct Mol Biol, 2010. **17**(2): p. 251-7.
9. Rhind, N., et al., *Comparative functional genomics of the fission yeasts.* Science, 2011. **332**(6032): p. 930-6.
10. Joti, Y., et al., *Chromosomes without a 30-nm chromatin fiber.* Nucleus, 2012. **3**(5): p. 404-10.
11. Flaus, A., et al., *Identification of multiple distinct Snf2 subfamilies with conserved structural motifs.* Nucleic Acids Res, 2006. **34**(10): p. 2887-905.
12. Hewish, D.R. and L.A. Burgoyne, *Chromatin sub-structure. The digestion of chromatin DNA at regularly spaced sites by a nuclear deoxyribonuclease.* Biochem Biophys Res Commun, 1973. **52**(2): p. 504-10.
13. Olins, A.L. and D.E. Olins, *Spheroid chromatin units (v bodies).* Science, 1974. **183**(4122): p. 330-2.
14. Oudet, P., M. Gross-Bellard, and P. Chambon, *Electron microscopic and biochemical evidence that chromatin structure is a repeating unit.* Cell, 1975. **4**(4): p. 281-300.
15. Finch, J.T., et al., *Structure of nucleosome core particles of chromatin.* Nature, 1977. **269**(5623): p. 29-36.
16. Arents, G., et al., *The nucleosomal core histone octamer at 3.1 A resolution: a tripartite protein assembly and a left-handed superhelix.* Proc Natl Acad Sci U S A, 1991. **88**(22): p. 10148-52.

17. Luger, K., et al., *Crystal structure of the nucleosome core particle at 2.8 A resolution.* Nature, 1997. **389**(6648): p. 251-60.
18. Davey, C.A., et al., *Solvent mediated interactions in the structure of the nucleosome core particle at 1.9 a resolution.* J Mol Biol, 2002. **319**(5): p. 1097-113.
19. Kaplan, N., et al., *Contribution of histone sequence preferences to nucleosome organization: proposed definitions and methodology.* Genome Biol, 2010. **11**(11): p. 140.
20. Valouev, A., et al., *Determinants of nucleosome organization in primary human cells.* Nature, 2011. **474**(7352): p. 516-20.
21. Van Holde, K.E., *Chromatin.* Springer-Verlag, New York, 1988.
22. Godde, J.S. and J. Widom, *Chromatin structure of Schizosaccharomyces pombe. A nucleosome repeat length that is shorter than the chromatosomal DNA length.* J Mol Biol, 1992. **226**(4): p. 1009-25.
23. Tsankov, A., et al., *Evolutionary divergence of intrinsic and trans-regulated nucleosome positioning sequences reveals plastic rules for chromatin organization.* Genome Res, 2011. **21**(11): p. 1851-62.
24. Givens, R.M., et al., *Chromatin architectures at fission yeast transcriptional promoters and replication origins.* Nucleic Acids Res, 2012. **40**(15): p. 7176-89.
25. Kowalski, A. and J. Palyga, *Linker histone subtypes and their allelic variants.* Cell Biol Int, 2012. **36**(11): p. 981-96.
26. Rupp, R.A. and P.B. Becker, *Gene regulation by histone H1: new links to DNA methylation.* Cell, 2005. **123**(7): p. 1178-9.
27. Finch, J.T. and A. Klug, *Solenoidal model for superstructure in chromatin.* Proc Natl Acad Sci U S A, 1976. **73**(6): p. 1897-901.
28. Horowitz, R.A., et al., *The three-dimensional architecture of chromatin in situ: electron tomography reveals fibers composed of a continuously variable zig-zag nucleosomal ribbon.* J Cell Biol, 1994. **125**(1): p. 1-10.
29. Nishino, Y., et al., *Human mitotic chromosomes consist predominantly of irregularly folded nucleosome fibres without a 30-nm chromatin structure.* EMBO J, 2012. **31**(7): p. 1644-53.
30. Dorigo, B., et al., *Nucleosome arrays reveal the two-start organization of the chromatin fiber.* Science, 2004. **306**(5701): p. 1571-3.
31. Robinson, P.J., et al., *EM measurements define the dimensions of the "30-nm" chromatin fiber: evidence for a compact, interdigitated structure.* Proc Natl Acad Sci U S A, 2006. **103**(17): p. 6506-11.
32. Schalch, T., et al., *X-ray structure of a tetranucleosome and its implications for the chromatin fibre.* Nature, 2005. **436**(7047): p. 138-41.
33. Fussner, E., R.W. Ching, and D.P. Bazett-Jones, *Living without 30nm chromatin fibers.* Trends Biochem Sci, 2011. **36**(1): p. 1-6.
34. Worcel, A., S. Strogatz, and D. Riley, *Structure of chromatin and the linking number of DNA.* Proc Natl Acad Sci U S A, 1981. **78**(3): p. 1461-5.

35. Woodcock, C.L., L.L. Frado, and J.B. Rattner, *The higher-order structure of chromatin: evidence for a helical ribbon arrangement.* J Cell Biol, 1984. **99**(1 Pt 1): p. 42-52.

36. Kruithof, M., et al., *Single-molecule force spectroscopy reveals a highly compliant helical folding for the 30-nm chromatin fiber.* Nat Struct Mol Biol, 2009. **16**(5): p. 534-40.

37. Hansen, J.C., *Human mitotic chromosome structure: what happened to the 30-nm fibre?* EMBO J, 2012. **31**(7): p. 1621-3.

38. Lieberman-Aiden, E., et al., *Comprehensive mapping of long-range interactions reveals folding principles of the human genome.* Science, 2009. **326**(5950): p. 289-93.

39. Mirny, L.A., *The fractal globule as a model of chromatin architecture in the cell.* Chromosome Res, 2011. **19**(1): p. 37-51.

40. Bonisch, C., et al., *Chromatin proteomics and epigenetic regulatory circuits.* Expert Rev Proteomics, 2008. **5**(1): p. 105-19.

41. Yuan, G. and B. Zhu, *Histone variants and epigenetic inheritance.* Biochim Biophys Acta, 2012. **1819**(3-4): p. 222-9.

42. Bonisch, C. and S.B. Hake, *Histone H2A variants in nucleosomes and chromatin: more or less stable?* Nucleic Acids Res, 2012. **40**(21): p. 10719-41.

43. Bernstein, E. and S.B. Hake, *The nucleosome: a little variation goes a long way.* Biochem Cell Biol, 2006. **84**(4): p. 505-17.

44. Hake, S.B. and C.D. Allis, *Histone H3 variants and their potential role in indexing mammalian genomes: the "H3 barcode hypothesis".* Proc Natl Acad Sci U S A, 2006. **103**(17): p. 6428-35.

45. Okada, M., et al., *CENP-H-containing complex facilitates centromere deposition of CENP-A in cooperation with FACT and CHD1.* Mol Biol Cell, 2009. **20**(18): p. 3986-95.

46. Krogan, N.J., et al., *A Snf2 family ATPase complex required for recruitment of the histone H2A variant Htz1.* Mol Cell, 2003. **12**(6): p. 1565-76.

47. Kobor, M.S., et al., *A protein complex containing the conserved Swi2/Snf2-related ATPase Swr1p deposits histone variant H2A.Z into euchromatin.* PLoS Biol, 2004. **2**(5): p. E131.

48. Mizuguchi, G., et al., *ATP-driven exchange of histone H2AZ variant catalyzed by SWR1 chromatin remodeling complex.* Science, 2004. **303**(5656): p. 343-8.

49. Buchanan, L., et al., *The Schizosaccharomyces pombe JmjC-protein, Msc1, prevents H2A.Z localization in centromeric and subtelomeric chromatin domains.* PLoS Genet, 2009. **5**(11): p. e1000726.

50. Kouzarides, T., *Chromatin modifications and their function.* Cell, 2007. **128**(4): p. 693-705.

51. Glozak, M.A., et al., *Acetylation and deacetylation of non-histone proteins.* Gene, 2005. **363**: p. 15-23.

52. Huang, J. and S.L. Berger, *The emerging field of dynamic lysine methylation of non-histone proteins.* Curr Opin Genet Dev, 2008. **18**(2): p. 152-8.

53. Tropberger, P., et al., *Regulation of transcription through acetylation of H3K122 on the lateral surface of the histone octamer.* Cell, 2013. **152**(4): p. 859-72.

54. Liu, Y., et al., *Influence of histone tails and H4 tail acetylations on nucleosome-nucleosome interactions.* J Mol Biol, 2011. **414**(5): p. 749-64.

55. Strahl, B.D. and C.D. Allis, *The language of covalent histone modifications.* Nature, 2000. **403**(6765): p. 41-5.

56. Shogren-Knaak, M., et al., *Histone H4-K16 acetylation controls chromatin structure and protein interactions.* Science, 2006. **311**(5762): p. 844-7.

57. Dhalluin, C., et al., *Structure and ligand of a histone acetyltransferase bromodomain.* Nature, 1999. **399**(6735): p. 491-6.

58. Rando, O.J., *Combinatorial complexity in chromatin structure and function: revisiting the histone code.* Curr Opin Genet Dev, 2012. **22**(2): p. 148-55.

59. Filion, G.J., et al., *Systematic protein location mapping reveals five principal chromatin types in Drosophila cells.* Cell, 2010. **143**(2): p. 212-24.

60. Jones, P.A., *Functions of DNA methylation: islands, start sites, gene bodies and beyond.* Nat Rev Genet, 2012. **13**(7): p. 484-92.

61. Branco, M.R., G. Ficz, and W. Reik, *Uncovering the role of 5-hydroxymethylcytosine in the epigenome.* Nat Rev Genet, 2012. **13**(1): p. 7-13.

62. Eberharter, A. and P.B. Becker, *ATP-dependent nucleosome remodelling: factors and functions.* J Cell Sci, 2004. **117**(Pt 17): p. 3707-11.

63. Becker, P.B. and W. Horz, *ATP-dependent nucleosome remodeling.* Annu Rev Biochem, 2002. **71**: p. 247-73.

64. Erdel, F., et al., *Targeting chromatin remodelers: signals and search mechanisms.* Biochim Biophys Acta, 2011. **1809**(9): p. 497-508.

65. Eisen, J.A., K.S. Sweder, and P.C. Hanawalt, *Evolution of the SNF2 family of proteins: subfamilies with distinct sequences and functions.* Nucleic Acids Res, 1995. **23**(14): p. 2715-23.

66. Pointner, J., et al., *CHD1 remodelers regulate nucleosome spacing in vitro and align nucleosomal arrays over gene coding regions in S. pombe.* EMBO J, 2012. **31**(23): p. 4388-403.

67. Erdel, F., et al., *Human ISWI chromatin-remodeling complexes sample nucleosomes via transient binding reactions and become immobilized at active sites.* Proc Natl Acad Sci U S A, 2010. **107**(46): p. 19873-8.

68. Badis, G., et al., *A library of yeast transcription factor motifs reveals a widespread function for Rsc3 in targeting nucleosome exclusion at promoters.* Mol Cell, 2008. **32**(6): p. 878-87.

69. Hassan, A.H., et al., *Function and selectivity of bromodomains in anchoring chromatin-modifying complexes to promoter nucleosomes.* Cell, 2002. **111**(3): p. 369-79.

70. Kasten, M., et al., *Tandem bromodomains in the chromatin remodeler RSC recognize acetylated histone H3 Lys14.* EMBO J, 2004. **23**(6): p. 1348-59.

71. Gottschalk, A.J., et al., *Poly(ADP-ribosyl)ation directs recruitment and activation of an ATP-dependent chromatin remodeler.* Proc Natl Acad Sci U S A, 2009. **106**(33): p. 13770-4.

72. Gottschalk, A.J., et al., *Activation of the SNF2 family ATPase ALC1 by poly(ADP-ribose) in a stable ALC1.PARP1.nucleosome intermediate.* J Biol Chem, 2012. **287**(52): p. 43527-32.

73. Papamichos-Chronakis, M., et al., *Global regulation of H2A.Z localization by the INO80 chromatin-remodeling enzyme is essential for genome integrity.* Cell, 2011. **144**(2): p. 200-13.

74. Gutierrez, J.L., et al., *Activation domains drive nucleosome eviction by SWI/SNF.* EMBO J, 2007. **26**(3): p. 730-40.

75. Lee, W., et al., *A high-resolution atlas of nucleosome occupancy in yeast.* Nat Genet, 2007. **39**(10): p. 1235-44.

76. Yuan, G.C., et al., *Genome-scale identification of nucleosome positions in S. cerevisiae.* Science, 2005. **309**(5734): p. 626-30.

77. Valouev, A., et al., *A high-resolution, nucleosome position map of C. elegans reveals a lack of universal sequence-dictated positioning.* Genome Res, 2008. **18**(7): p. 1051-63.

78. Mavrich, T.N., et al., *Nucleosome organization in the Drosophila genome.* Nature, 2008. **453**(7193): p. 358-62.

79. Schones, D.E., et al., *Dynamic regulation of nucleosome positioning in the human genome.* Cell, 2008. **132**(5): p. 887-98.

80. Segal, E. and J. Widom, *What controls nucleosome positions?* Trends Genet, 2009. **25**(8): p. 335-43.

81. Weintraub, H. and M. Groudine, *Chromosomal subunits in active genes have an altered conformation.* Science, 1976. **193**(4256): p. 848-56.

82. Wu, C., *The 5' ends of Drosophila heat shock genes in chromatin are hypersensitive to DNase I.* Nature, 1980. **286**(5776): p. 854-60.

83. Wu, C., *Analysis of hypersensitive sites in chromatin.* Methods Enzymol, 1989. **170**: p. 269-89.

84. Livingstone-Zatchej, M. and F. Thoma, *Mapping of nucleosome positions in yeast.* Methods Mol Biol, 1999. **119**: p. 363-78.

85. Gregory, P.D. and W. Horz, *Mapping chromatin structure in yeast.* Methods Enzymol, 1999. **304**: p. 365-76.

86. Albert, I., et al., *Translational and rotational settings of H2A.Z nucleosomes across the Saccharomyces cerevisiae genome.* Nature, 2007. **446**(7135): p. 572-6.

87. Barski, A., et al., *High-resolution profiling of histone methylations in the human genome.* Cell, 2007. **129**(4): p. 823-37.

88. Chodavarapu, R.K., et al., *Relationship between nucleosome positioning and DNA methylation.* Nature, 2010. **466**(7304): p. 388-92.

89. Li, Z., et al., *The nucleosome map of the mammalian liver.* Nat Struct Mol Biol, 2011. **18**(6): p. 742-6.

90. McGhee, J.D. and G. Felsenfeld, *Another potential artifact in the study of nucleosome phasing by chromatin digestion with micrococcal nuclease.* Cell, 1983. **32**(4): p. 1205-15.

91. Chung, H.R., et al., *The effect of micrococcal nuclease digestion on nucleosome positioning data.* PLoS One, 2010. **5**(12): p. e15754.

92. Allan, J., et al., *Micrococcal nuclease does not substantially bias nucleosome mapping.* J Mol Biol, 2012. **417**(3): p. 152-64.

93. Flaus, A. and T.J. Richmond, *Base-pair resolution mapping of nucleosome positions using site-directed hydroxy radicals.* Methods Enzymol, 1999. **304**: p. 251-63.

94. Brogaard, K., et al., *A map of nucleosome positions in yeast at base-pair resolution.* Nature, 2012. **486**(7404): p. 496-501.

95. Travers, A., et al., *Nucleosome positioning--what do we really know?* Mol Biosyst, 2009. **5**(12): p. 1582-92.

96. Zhang, Y., et al., *Intrinsic histone-DNA interactions are not the major determinant of nucleosome positions in vivo.* Nat Struct Mol Biol, 2009. **16**(8): p. 847-52.

97. Segal, E., et al., *A genomic code for nucleosome positioning.* Nature, 2006. **442**(7104): p. 772-8.

98. Satchwell, S.C., H.R. Drew, and A.A. Travers, *Sequence periodicities in chicken nucleosome core DNA.* J Mol Biol, 1986. **191**(4): p. 659-75.

99. Field, Y., et al., *Distinct modes of regulation by chromatin encoded through nucleosome positioning signals.* PLoS Comput Biol, 2008. **4**(11): p. e1000216.

100. Stein, A., T.E. Takasuka, and C.K. Collings, *Are nucleosome positions in vivo primarily determined by histone-DNA sequence preferences?* Nucleic Acids Res, 2010. **38**(3): p. 709-19.

101. Peckham, H.E., et al., *Nucleosome positioning signals in genomic DNA.* Genome Res, 2007. **17**(8): p. 1170-7.

102. Yuan, G.C. and J.S. Liu, *Genomic sequence is highly predictive of local nucleosome depletion.* PLoS Comput Biol, 2008. **4**(1): p. e13.

103. Miele, V., et al., *DNA physical properties determine nucleosome occupancy from yeast to fly.* Nucleic Acids Res, 2008. **36**(11): p. 3746-56.

104. Gupta, S., et al., *Predicting human nucleosome occupancy from primary sequence.* PLoS Comput Biol, 2008. **4**(8): p. e1000134.

105. Ioshikhes, I.P., et al., *Nucleosome positions predicted through comparative genomics.* Nat Genet, 2006. **38**(10): p. 1210-5.

106. Ganapathi, M., et al., *Extensive role of the general regulatory factors, Abf1 and Rap1, in determining genome-wide chromatin structure in budding yeast.* Nucleic Acids Res, 2011. **39**(6): p. 2032-44.

107. Hartley, P.D. and H.D. Madhani, *Mechanisms that specify promoter nucleosome location and identity.* Cell, 2009. **137**(3): p. 445-58.

108. Koerber, R.T., et al., *Interaction of transcriptional regulators with specific nucleosomes across the Saccharomyces genome.* Mol Cell, 2009. **35**(6): p. 889-902.

109. Rhee, H.S. and B.F. Pugh, *Comprehensive genome-wide protein-DNA interactions detected at single-nucleotide resolution.* Cell, 2011. **147**(6): p. 1408-19.

110. Raisner, R.M., et al., *Histone variant H2A.Z marks the 5' ends of both active and inactive genes in euchromatin.* Cell, 2005. **123**(2): p. 233-48.

111. Langst, G., P.B. Becker, and I. Grummt, *TTF-I determines the chromatin architecture of the active rDNA promoter.* EMBO J, 1998. **17**(11): p. 3135-45.

112. Nemeth, A., et al., *Epigenetic regulation of TTF-I-mediated promoter-terminator interactions of rRNA genes.* EMBO J, 2008. **27**(8): p. 1255-65.

113. Fu, Y., et al., *The insulator binding protein CTCF positions 20 nucleosomes around its binding sites across the human genome.* PLoS Genet, 2008. **4**(7): p. e1000138.

114. Cuddapah, S., et al., *Global analysis of the insulator binding protein CTCF in chromatin barrier regions reveals demarcation of active and repressive domains.* Genome Res, 2009. **19**(1): p. 24-32.

115. Monahan, B.J., et al., *Fission yeast SWI/SNF and RSC complexes show compositional and functional differences from budding yeast.* Nat Struct Mol Biol, 2008. **15**(8): p. 873-80.

116. Gkikopoulos, T., et al., *SWI/SNF and Asf1p cooperate to displace histones during induction of the saccharomyces cerevisiae HO promoter.* Mol Cell Biol, 2009. **29**(15): p. 4057-66.

117. Schwabish, M.A. and K. Struhl, *The Swi/Snf complex is important for histone eviction during transcriptional activation and RNA polymerase II elongation in vivo.* Mol Cell Biol, 2007. **27**(20): p. 6987-95.

118. Takahata, S., Y. Yu, and D.J. Stillman, *FACT and Asf1 regulate nucleosome dynamics and coactivator binding at the HO promoter.* Mol Cell, 2009. **34**(4): p. 405-15.

119. Sudarsanam, P., et al., *Whole-genome expression analysis of snf/swi mutants of Saccharomyces cerevisiae.* Proc Natl Acad Sci U S A, 2000. **97**(7): p. 3364-9.

120. Shivaswamy, S. and V.R. Iyer, *Stress-dependent dynamics of global chromatin remodeling in yeast: dual role for SWI/SNF in the heat shock stress response.* Mol Cell Biol, 2008. **28**(7): p. 2221-34.

121. Gregory, P.D., et al., *Chromatin remodelling at the PHO8 promoter requires SWI-SNF and SAGA at a step subsequent to activator binding.* EMBO J, 1999. **18**(22): p. 6407-14.

122. Neef, D.W. and M.P. Kladde, *Polyphosphate loss promotes SNF/SWI- and Gcn5-dependent mitotic induction of PHO5.* Mol Cell Biol, 2003. **23**(11): p. 3788-97.

123. Barbaric, S., et al., *Redundancy of chromatin remodeling pathways for the induction of the yeast PHO5 promoter in vivo.* J Biol Chem, 2007. **282**(38): p. 27610-21.

124. Wippo, C.J., et al., *Differential cofactor requirements for histone eviction from two nucleosomes at the yeast PHO84 promoter are determined by intrinsic nucleosome stability.* Mol Cell Biol, 2009. **29**(11): p. 2960-81.

125. Bernal, G. and E. Maldonado, *Isolation of a novel complex of the SWI/SNF family from Schizosaccharomyces pombe and its effects on in vitro transcription in nucleosome arrays.* Mol Cell Biochem, 2007. **303**(1-2): p. 131-9.

126. Wilson, B.G. and C.W. Roberts, *SWI/SNF nucleosome remodellers and cancer.* Nat Rev Cancer, 2011. **11**(7): p. 481-92.

127. Montel, F., et al., *RSC remodeling of oligo-nucleosomes: an atomic force microscopy study.* Nucleic Acids Res, 2011. **39**(7): p. 2571-9.

128. van Vugt, J.J., et al., *Multiple aspects of ATP-dependent nucleosome translocation by RSC and Mi-2 are directed by the underlying DNA sequence.* PLoS One, 2009. **4**(7): p. e6345.

129. Parnell, T.J., J.T. Huff, and B.R. Cairns, *RSC regulates nucleosome positioning at Pol II genes and density at Pol III genes.* EMBO J, 2008. **27**(1): p. 100-10.

130. Yen, K., et al., *Genome-wide nucleosome specificity and directionality of chromatin remodelers.* Cell, 2012. **149**(7): p. 1461-73.

131. Boeger, H., et al., *Removal of promoter nucleosomes by disassembly rather than sliding in vivo.* Mol Cell, 2004. **14**(5): p. 667-73.

132. Reinke, H. and W. Horz, *Histones are first hyperacetylated and then lose contact with the activated PHO5 promoter.* Mol Cell, 2003. **11**(6): p. 1599-607.

133. Lorch, Y., B. Maier-Davis, and R.D. Kornberg, *Chromatin remodeling by nucleosome disassembly in vitro.* Proc Natl Acad Sci U S A, 2006. **103**(9): p. 3090-3.

134. Cao, Y., et al., *Sfh1p, a component of a novel chromatin-remodeling complex, is required for cell cycle progression.* Mol Cell Biol, 1997. **17**(6): p. 3323-34.

135. Hsu, J.M., et al., *The yeast RSC chromatin-remodeling complex is required for kinetochore function in chromosome segregation.* Mol Cell Biol, 2003. **23**(9): p. 3202-15.

136. Yamada, K., et al., *Essential roles of Snf21, a Swi2/Snf2 family chromatin remodeler, in fission yeast mitosis.* Genes Genet Syst, 2008. **83**(5): p. 361-72.

137. Garcia, J.F., et al., *Combinatorial, site-specific requirement for heterochromatic silencing factors in the elimination of nucleosome-free regions.* Genes Dev, 2010. **24**(16): p. 1758-71.

138. Elfring, L.K., et al., *Identification and characterization of Drosophila relatives of the yeast transcriptional activator SNF2/SWI2.* Mol Cell Biol, 1994. **14**(4): p. 2225-34.

139. Tsukiyama, T. and C. Wu, *Purification and properties of an ATP-dependent nucleosome remodeling factor.* Cell, 1995. **83**(6): p. 1011-20.

140. Varga-Weisz, P.D., et al., *Chromatin-remodelling factor CHRAC contains the ATPases ISWI and topoisomerase II.* Nature, 1997. **388**(6642): p. 598-602.

141. Ito, T., et al., *ACF, an ISWI-containing and ATP-utilizing chromatin assembly and remodeling factor.* Cell, 1997. **90**(1): p. 145-55.

142. Corona, D.F. and J.W. Tamkun, *Multiple roles for ISWI in transcription, chromosome organization and DNA replication.* Biochim Biophys Acta, 2004. **1677**(1-3): p. 113-9.

143. Tsukiyama, T., et al., *Characterization of the imitation switch subfamily of ATP-dependent chromatin-remodeling factors in Saccharomyces cerevisiae.* Genes Dev, 1999. **13**(6): p. 686-97.

144. Vary, J.C., Jr., et al., *Yeast Isw1p forms two separable complexes in vivo.* Mol Cell Biol, 2003. **23**(1): p. 80-91.

145. Langst, G. and P.B. Becker, *Nucleosome mobilization and positioning by ISWI-containing chromatin-remodeling factors.* J Cell Sci, 2001. **114**(Pt 14): p. 2561-8.

146. Langst, G., et al., *Nucleosome movement by CHRAC and ISWI without disruption or trans-displacement of the histone octamer.* Cell, 1999. **97**(7): p. 843-52.

147. Eberharter, A., et al., *Acf1, the largest subunit of CHRAC, regulates ISWI-induced nucleosome remodelling.* EMBO J, 2001. **20**(14): p. 3781-8.

148. Hamiche, A., et al., *ATP-dependent histone octamer sliding mediated by the chromatin remodeling complex NURF.* Cell, 1999. **97**(7): p. 833-42.

149. Gangaraju, V.K. and B. Bartholomew, *Dependency of ISW1a chromatin remodeling on extranucleosomal DNA.* Mol Cell Biol, 2007. **27**(8): p. 3217-25.

150. Stockdale, C., et al., *Analysis of nucleosome repositioning by yeast ISWI and Chd1 chromatin remodeling complexes.* J Biol Chem, 2006. **281**(24): p. 16279-88.

151. Zofall, M., J. Persinger, and B. Bartholomew, *Functional role of extranucleosomal DNA and the entry site of the nucleosome in chromatin remodeling by ISW2.* Mol Cell Biol, 2004. **24**(22): p. 10047-57.

152. Dang, W., M.N. Kagalwala, and B. Bartholomew, *Regulation of ISW2 by concerted action of histone H4 tail and extranucleosomal DNA.* Mol Cell Biol, 2006. **26**(20): p. 7388-96.

153. Hota, S.K., et al., *Nucleosome mobilization by ISW2 requires the concerted action of the ATPase and SLIDE domains.* Nat Struct Mol Biol, 2013. **20**(2): p. 222-9.

154. Yang, J.G., et al., *The chromatin-remodeling enzyme ACF is an ATP-dependent DNA length sensor that regulates nucleosome spacing.* Nat Struct Mol Biol, 2006. **13**(12): p. 1078-83.

155. Racki, L.R., et al., *The chromatin remodeller ACF acts as a dimeric motor to space nucleosomes.* Nature, 2009. **462**(7276): p. 1016-21.

156. Goldmark, J.P., et al., *The Isw2 chromatin remodeling complex represses early meiotic genes upon recruitment by Ume6p.* Cell, 2000. **103**(3): p. 423-33.

157. Whitehouse, I., et al., *Chromatin remodelling at promoters suppresses antisense transcription.* Nature, 2007. **450**(7172): p. 1031-5.

158. Tirosh, I., N. Sigal, and N. Barkai, *Widespread remodeling of mid-coding sequence nucleosomes by Isw1.* Genome Biol, 2010. **11**(5): p. R49.

159. Morillon, A., et al., *Isw1 chromatin remodeling ATPase coordinates transcription elongation and termination by RNA polymerase II.* Cell, 2003. **115**(4): p. 425-35.

160. Gkikopoulos, T., et al., *A role for Snf2-related nucleosome-spacing enzymes in genome-wide nucleosome organization.* Science, 2011. **333**(6050): p. 1758-60.

161. Mizuguchi, G., et al., *Role of nucleosome remodeling factor NURF in transcriptional activation of chromatin.* Mol Cell, 1997. **1**(1): p. 141-50.

162. Deuring, R., et al., *The ISWI chromatin-remodeling protein is required for gene expression and the maintenance of higher order chromatin structure in vivo.* Mol Cell, 2000. **5**(2): p. 355-65.

163. Liu, Y.I., et al., *The chromatin remodelers ISWI and ACF1 directly repress Wingless transcriptional targets.* Dev Biol, 2008. **323**(1): p. 41-52.

164. Delmas, V., D.G. Stokes, and R.P. Perry, *A mammalian DNA-binding protein that contains a chromodomain and an SNF2/SWI2-like helicase domain.* Proc Natl Acad Sci U S A, 1993. **90**(6): p. 2414-8.

165. Woodage, T., et al., *Characterization of the CHD family of proteins.* Proc Natl Acad Sci U S A, 1997. **94**(21): p. 11472-7.

166. Alen, C., et al., *A role for chromatin remodeling in transcriptional termination by RNA polymerase II.* Mol Cell, 2002. **10**(6): p. 1441-52.

167. Jae Yoo, E., et al., *Hrp3, a chromodomain helicase/ATPase DNA binding protein, is required for heterochromatin silencing in fission yeast.* Biochem Biophys Res Commun, 2002. **295**(4): p. 970-4.

168. McKnight, J.N., et al., *Extranucleosomal DNA binding directs nucleosome sliding by Chd1.* Mol Cell Biol, 2011. **31**(23): p. 4746-59.

169. Patel, A., et al., *Decoupling nucleosome recognition from DNA binding dramatically alters the properties of the Chd1 chromatin remodeler.* Nucleic Acids Res, 2013. **41**(3): p. 1637-48.

170. Lusser, A., D.L. Urwin, and J.T. Kadonaga, *Distinct activities of CHD1 and ACF in ATP-dependent chromatin assembly.* Nat Struct Mol Biol, 2005. **12**(2): p. 160-6.

171. Konev, A.Y., et al., *CHD1 motor protein is required for deposition of histone variant H3.3 into chromatin in vivo.* Science, 2007. **317**(5841): p. 1087-90.

172. Stokes, D.G., K.D. Tartof, and R.P. Perry, *CHD1 is concentrated in interbands and puffed regions of Drosophila polytene chromosomes.* Proc Natl Acad Sci U S A, 1996. **93**(14): p. 7137-42.

173. Simic, R., et al., *Chromatin remodeling protein Chd1 interacts with transcription elongation factors and localizes to transcribed genes.* EMBO J, 2003. **22**(8): p. 1846-56.

174. Walfridsson, J., et al., *A genome-wide role for CHD remodelling factors and Nap1 in nucleosome disassembly.* EMBO J, 2007. **26**(12): p. 2868-79.

175. Walfridsson, J., et al., *The CHD remodeling factor Hrp1 stimulates CENP-A loading to centromeres.* Nucleic Acids Res, 2005. **33**(9): p. 2868-79.

176. Yoo, E.J., et al., *Fission yeast hrp1, a chromodomain ATPase, is required for proper chromosome segregation and its overexpression interferes with chromatin condensation.* Nucleic Acids Res, 2000. **28**(9): p. 2004-11.

177. Sugiyama, T., et al., *SHREC, an effector complex for heterochromatic transcriptional silencing.* Cell, 2007. **128**(3): p. 491-504.

178. Allen, H.F., P.A. Wade, and T.G. Kutateladze, *The NuRD architecture.* Cell Mol Life Sci, 2013.

179. Ebbert, R., A. Birkmann, and H.J. Schuller, *The product of the SNF2/SWI2 paralogue INO80 of Saccharomyces cerevisiae required for efficient expression of various yeast structural genes is part of a high-molecular-weight protein complex.* Mol Microbiol, 1999. **32**(4): p. 741-51.

180. Jin, J., et al., *A mammalian chromatin remodeling complex with similarities to the yeast INO80 complex.* J Biol Chem, 2005. **280**(50): p. 41207-12.

181. Klymenko, T., et al., *A Polycomb group protein complex with sequence-specific DNA-binding and selective methyl-lysine-binding activities.* Genes Dev, 2006. **20**(9): p. 1110-22.

182. Morrison, A.J. and X. Shen, *Chromatin remodelling beyond transcription: the INO80 and SWR1 complexes.* Nat Rev Mol Cell Biol, 2009. **10**(6): p. 373-84.

183. Cai, Y., et al., *YY1 functions with INO80 to activate transcription.* Nat Struct Mol Biol, 2007. **14**(9): p. 872-4.

184. Hogan, C.J., et al., *Fission yeast Iec1-ino80-mediated nucleosome eviction regulates nucleotide and phosphate metabolism.* Mol Cell Biol, 2010. **30**(3): p. 657-74.

185. Watanabe, S., et al., *A histone acetylation switch regulates H2A.Z deposition by the SWR-C remodeling enzyme.* Science, 2013. **340**(6129): p. 195-9.

186. Udugama, M., A. Sabri, and B. Bartholomew, *The INO80 ATP-dependent chromatin remodeling complex is a nucleosome spacing factor.* Mol Cell Biol, 2011. **31**(4): p. 662-73.

187. Billon, P. and J. Cote, *Precise deposition of histone H2A.Z in chromatin for genome expression and maintenance.* Biochim Biophys Acta, 2012. **1819**(3-4): p. 290-302.

188. Suto, R.K., et al., *Crystal structure of a nucleosome core particle containing the variant histone H2A.Z.* Nat Struct Biol, 2000. **7**(12): p. 1121-4.

189. Zilberman, D., et al., *Histone H2A.Z and DNA methylation are mutually antagonistic chromatin marks.* Nature, 2008. **456**(7218): p. 125-9.

190. Mavrich, T.N., et al., *A barrier nucleosome model for statistical positioning of nucleosomes throughout the yeast genome.* Genome Res, 2008. **18**(7): p. 1073-83.

191. Guillemette, B., et al., *Variant histone H2A.Z is globally localized to the promoters of inactive yeast genes and regulates nucleosome positioning.* PLoS Biol, 2005. **3**(12): p. e384.

192. Fan, J.Y., et al., *The essential histone variant H2A.Z regulates the equilibrium between different chromatin conformational states.* Nat Struct Biol, 2002. **9**(3): p. 172-6.

193. Li, B., et al., *Preferential occupancy of histone variant H2AZ at inactive promoters influences local histone modifications and chromatin remodeling.* Proc Natl Acad Sci U S A, 2005. **102**(51): p. 18385-90.

194. Izban, M.G. and D.S. Luse, *Factor-stimulated RNA polymerase II transcribes at physiological elongation rates on naked DNA but very poorly on chromatin templates.* J Biol Chem, 1992. **267**(19): p. 13647-55.

195. LeRoy, G., et al., *Requirement of RSF and FACT for transcription of chromatin templates in vitro.* Science, 1998. **282**(5395): p. 1900-4.

196. Gaykalova, D.A., et al., *A polar barrier to transcription can be circumvented by remodeler-induced nucleosome translocation.* Nucleic Acids Res, 2011. **39**(9): p. 3520-8.

197. Orphanides, G., et al., *FACT, a factor that facilitates transcript elongation through nucleosomes.* Cell, 1998. **92**(1): p. 105-16.

198. Li, G., et al., *Rapid spontaneous accessibility of nucleosomal DNA.* Nat Struct Mol Biol, 2005. **12**(1): p. 46-53.

199. Bohm, V., et al., *Nucleosome accessibility governed by the dimer/tetramer interface.* Nucleic Acids Res, 2011. **39**(8): p. 3093-102.

200. Petesch, S.J. and J.T. Lis, *Overcoming the nucleosome barrier during transcript elongation.* Trends Genet, 2012. **28**(6): p. 285-94.

201. Kulaeva, O.I., F.K. Hsieh, and V.M. Studitsky, *RNA polymerase complexes cooperate to relieve the nucleosomal barrier and evict histones.* Proc Natl Acad Sci U S A, 2010. **107**(25): p. 11325-30.

202. Dion, M.F., et al., *Dynamics of replication-independent histone turnover in budding yeast.* Science, 2007. **315**(5817): p. 1405-8.

203. Jamai, A., R.M. Imoberdorf, and M. Strubin, *Continuous histone H2B and transcription-dependent histone H3 exchange in yeast cells outside of replication.* Mol Cell, 2007. **25**(3): p. 345-55.

204. Kulaeva, O.I., et al., *Mechanism of chromatin remodeling and recovery during passage of RNA polymerase II.* Nat Struct Mol Biol, 2009. **16**(12): p. 1272-8.

205. Hodges, C., et al., *Nucleosomal fluctuations govern the transcription dynamics of RNA polymerase II.* Science, 2009. **325**(5940): p. 626-8.

206. Bintu, L., et al., *The elongation rate of RNA polymerase determines the fate of transcribed nucleosomes.* Nat Struct Mol Biol, 2011. **18**(12): p. 1394-9.

207. Fenouil, R., et al., *CpG islands and GC content dictate nucleosome depletion in a transcription-independent manner at mammalian promoters.* Genome Res, 2012. **22**(12): p. 2399-408.

208. Weiner, A., et al., *High-resolution nucleosome mapping reveals transcription-dependent promoter packaging.* Genome Res, 2010. **20**(1): p. 90-100.

209. Hughes, A.L., et al., *A functional evolutionary approach to identify determinants of nucleosome positioning: a unifying model for establishing the genome-wide pattern.* Mol Cell, 2012. **48**(1): p. 5-15.

210. Bjerling, P., et al., *Functional divergence between histone deacetylases in fission yeast by distinct cellular localization and in vivo specificity.* Mol Cell Biol, 2002. **22**(7): p. 2170-81.

211. Lantermann, A., et al., *Genome-wide mapping of nucleosome positions in Schizosaccharomyces pombe.* Methods, 2009. **48**(3): p. 218-25.

212. Wal, M. and B.F. Pugh, *Genome-wide mapping of nucleosome positions in yeast using high-resolution MNase ChIP-Seq.* Methods Enzymol, 2012. **513**: p. 233-50.

213. Krietenstein, N., et al., *Genome-wide in vitro reconstitution of yeast chromatin with in vivo-like nucleosome positioning.* Methods Enzymol, 2012. **513**: p. 205-32.

214. Price, P.A., *Characterization of Ca ++ and Mg ++ binding to bovine pancreatic deoxyribonuclease A.* J Biol Chem, 1972. **247**(9): p. 2895-9.

215. Henikoff, S., et al., *Genome-wide profiling of salt fractions maps physical properties of chromatin.* Genome Res, 2009. **19**(3): p. 460-9.

216. Jin, C., et al., *H3.3/H2A.Z double variant-containing nucleosomes mark 'nucleosome-free regions' of active promoters and other regulatory regions.* Nat Genet, 2009. **41**(8): p. 941-5.

217. Xu, Z., et al., *Bidirectional promoters generate pervasive transcription in yeast.* Nature, 2009. **457**(7232): p. 1033-7.

218. Wilhelm, B.T., et al., *Dynamic repertoire of a eukaryotic transcriptome surveyed at single-nucleotide resolution.* Nature, 2008. **453**(7199): p. 1239-43.

219. Zofall, M., et al., *Histone H2A.Z cooperates with RNAi and heterochromatin factors to suppress antisense RNAs.* Nature, 2009. **461**(7262): p. 419-22.

220. Chlebowski, A., et al., *RNA decay machines: The exosome.* Biochim Biophys Acta, 2013.

221. Dutrow, N., et al., *Dynamic transcriptome of Schizosaccharomyces pombe shown by RNA-DNA hybrid mapping.* Nat Genet, 2008. **40**(8): p. 977-86.

222. Halley, J.E., et al., *Roles for H2A.Z and its acetylation in GAL1 transcription and gene induction, but not GAL1-transcriptional memory.* PLoS Biol, 2010. **8**(6): p. e1000401.

223. Perocchi, F., et al., *Antisense artifacts in transcriptome microarray experiments are resolved by actinomycin D.* Nucleic Acids Res, 2007. **35**(19): p. e128.

224. Nicolas, E., et al., *Distinct roles of HDAC complexes in promoter silencing, antisense suppression and DNA damage protection.* Nat Struct Mol Biol, 2007. **14**(5): p. 372-80.

225. Morris, S.A., et al., *Histone H3 K36 methylation is associated with transcription elongation in Schizosaccharomyces pombe.* Eukaryot Cell, 2005. **4**(8): p. 1446-54.

226. Carrozza, M.J., et al., *Histone H3 methylation by Set2 directs deacetylation of coding regions by Rpd3S to suppress spurious intragenic transcription.* Cell, 2005. **123**(4): p. 581-92.

227. Govind, C.K., et al., *Phosphorylated Pol II CTD recruits multiple HDACs, including Rpd3C(S), for methylation-dependent deacetylation of ORF nucleosomes.* Mol Cell, 2010. **39**(2): p. 234-46.

228. Radman-Livaja, M., et al., *A key role for Chd1 in histone H3 dynamics at the 3' ends of long genes in yeast.* PLoS Genet, 2012. **8**(7): p. e1002811.

229. Smolle, M., et al., *Chromatin remodelers Isw1 and Chd1 maintain chromatin structure during transcription by preventing histone exchange.* Nat Struct Mol Biol, 2012. **19**(9): p. 884-92.

230. Venkatesh, S., et al., *Set2 methylation of histone H3 lysine 36 suppresses histone exchange on transcribed genes.* Nature, 2012. **489**(7416): p. 452-5.

231. Sinha, I., et al., *Genome-wide mapping of histone modifications and mass spectrometry reveal H4 acetylation bias and H3K36 methylation at gene promoters in fission yeast.* Epigenomics, 2010. **2**(3): p. 377-93.

232. Lee, C.K., et al., *Evidence for nucleosome depletion at active regulatory regions genome-wide.* Nat Genet, 2004. **36**(8): p. 900-5.

233. Zawadzki, K.A., A.V. Morozov, and J.R. Broach, *Chromatin-dependent transcription factor accessibility rather than nucleosome remodeling predominates during global transcriptional restructuring in Saccharomyces cerevisiae.* Mol Biol Cell, 2009. **20**(15): p. 3503-13.

234. Kaplan, N., et al., *Nucleosome sequence preferences influence in vivo nucleosome organization.* Nat Struct Mol Biol, 2010. **17**(8): p. 918-20; author reply 920-2.

235. Sekinger, E.A., Z. Moqtaderi, and K. Struhl, *Intrinsic histone-DNA interactions and low nucleosome density are important for preferential accessibility of promoter regions in yeast.* Mol Cell, 2005. **18**(6): p. 735-48.

236. Iyer, V. and K. Struhl, *Poly(dA:dT), a ubiquitous promoter element that stimulates transcription via its intrinsic DNA structure.* EMBO J, 1995. **14**(11): p. 2570-9.

237. Sadeghi, L., et al., *Podbat: a novel genomic tool reveals Swr1-independent H2A.Z incorporation at gene coding sequences through epigenetic meta-analysis.* PLoS Comput Biol, 2011. **7**(8): p. e1002163.

238. Allis, C.D., et al., *Histone variants specific to the transcriptionally active, amitotically dividing macronucleus of the unicellular eucaryote, Tetrahymena thermophila.* Cell, 1980. **20**(3): p. 609-17.

239. Santisteban, M.S., T. Kalashnikova, and M.M. Smith, *Histone H2A.Z regulats transcription and is partially redundant with nucleosome remodeling complexes.* Cell, 2000. **103**(3): p. 411-22.

240. Zhang, H., D.N. Roberts, and B.R. Cairns, *Genome-wide dynamics of Htz1, a histone H2A variant that poises repressed/basal promoters for activation through histone loss.* Cell, 2005. **123**(2): p. 219-31.

241. Millar, C.B., et al., *Acetylation of H2AZ Lys 14 is associated with genome-wide gene activity in yeast.* Genes Dev, 2006. **20**(6): p. 711-22.

242. Keogh, M.C., et al., *The Saccharomyces cerevisiae histone H2A variant Htz1 is acetylated by NuA4.* Genes Dev, 2006. **20**(6): p. 660-5.

243. Galarneau, L., et al., *Multiple links between the NuA4 histone acetyltransferase complex and epigenetic control of transcription.* Mol Cell, 2000. **5**(6): p. 927-37.

244. Durant, M. and B.F. Pugh, *NuA4-directed chromatin transactions throughout the Saccharomyces cerevisiae genome.* Mol Cell Biol, 2007. **27**(15): p. 5327-35.

245. Matangkasombut, O., et al., *Bromodomain factor 1 corresponds to a missing piece of yeast TFIID.* Genes Dev, 2000. **14**(8): p. 951-62.

246. Auger, A., et al., *Eaf1 is the platform for NuA4 molecular assembly that evolutionarily links chromatin acetylation to ATP-dependent exchange of histone H2A variants.* Mol Cell Biol, 2008. **28**(7): p. 2257-70.

247. Hardy, S., et al., *The euchromatic and heterochromatic landscapes are shaped by antagonizing effects of transcription on H2A.Z deposition.* PLoS Genet, 2009. **5**(10): p. e1000687.

248. Bargaje, R., et al., *Proximity of H2A.Z containing nucleosome to the transcription start site influences gene expression levels in the mammalian liver and brain.* Nucleic Acids Res, 2012. **40**(18): p. 8965-78.

249. Wippo, C.J., et al., *The RSC chromatin remodelling enzyme has a unique role in directing the accurate positioning of nucleosomes.* EMBO J, 2011. **30**(7): p. 1277-88.

250. Shen, X., et al., *Involvement of actin-related proteins in ATP-dependent chromatin remodeling.* Mol Cell, 2003. **12**(1): p. 147-55.

251. Hennig, B.P., et al., *Chd1 chromatin remodelers maintain nucleosome organization and repress cryptic transcription.* EMBO Rep, 2012. **13**(11): p. 997-1003.

252. Shim, Y.S., et al., *Hrp3 controls nucleosome positioning to suppress non-coding transcription in eu- and heterochromatin.* EMBO J, 2012. **31**(23): p. 4375-87.

253. van Bakel, H., et al., *A compendium of nucleosome and transcript profiles reveals determinants of chromatin architecture and transcription.* PLoS Genet, 2013. **9**(5): p. e1003479.

254. Gossett, A.J. and J.D. Lieb, *In vivo effects of histone H3 depletion on nucleosome occupancy and position in Saccharomyces cerevisiae.* PLoS Genet, 2012. **8**(6): p. e1002771.

255. Adelman, K. and J.T. Lis, *Promoter-proximal pausing of RNA polymerase II: emerging roles in metazoans.* Nat Rev Genet, 2012. **13**(10): p. 720-31.

256. Rhee, H.S. and B.F. Pugh, *Genome-wide structure and organization of eukaryotic pre-initiation complexes.* Nature, 2012. **483**(7389): p. 295-301.

257. Quan, T.K. and G.A. Hartzog, *Histone H3K4 and K36 methylation, Chd1 and Rpd3S oppose the functions of Saccharomyces cerevisiae Spt4-Spt5 in transcription.* Genetics, 2010. **184**(2): p. 321-34.

258. Cheung, V., et al., *Chromatin- and transcription-related factors repress transcription from within coding regions throughout the Saccharomyces cerevisiae genome.* PLoS Biol, 2008. **6**(11): p. e277.

259. Kaplan, C.D., L. Laprade, and F. Winston, *Transcription elongation factors repress transcription initiation from cryptic sites.* Science, 2003. **301**(5636): p. 1096-9.

260. Celona, B., et al., *Substantial histone reduction modulates genomewide nucleosomal occupancy and global transcriptional output.* PLoS Biol, 2011. **9**(6): p. e1001086.

261. Belotserkovskaya, R., et al., *FACT facilitates transcription-dependent nucleosome alteration.* Science, 2003. **301**(5636): p. 1090-3.

262. Strahl, B.D., et al., *Set2 is a nucleosomal histone H3-selective methyltransferase that mediates transcriptional repression.* Mol Cell Biol, 2002. **22**(5): p. 1298-306.

263. Xie, L., et al., *KDM5B regulates embryonic stem cell self-renewal and represses cryptic intragenic transcription.* EMBO J, 2011. **30**(8): p. 1473-84.

264. Raveh-Sadka, T., et al., *Manipulating nucleosome disfavoring sequences allows fine-tune regulation of gene expression in yeast.* Nat Genet, 2012. **44**(7): p. 743-50.

265. Kornberg, R.D. and L. Stryer, *Statistical distributions of nucleosomes: nonrandom locations by a stochastic mechanism.* Nucleic Acids Res, 1988. **16**(14A): p. 6677-90.

266. Mobius, W., et al., *Toward a unified physical model of nucleosome patterns flanking transcription start sites.* Proc Natl Acad Sci U S A, 2013. **110**(14): p. 5719-24.

267. Fascher, K.D., J. Schmitz, and W. Horz, *Structural and functional requirements for the chromatin transition at the PHO5 promoter in Saccharomyces cerevisiae upon PHO5 activation.* J Mol Biol, 1993. **231**(3): p. 658-67.

268. Zaugg, J.B. and N.M. Luscombe, *A genomic model of condition-specific nucleosome behavior explains transcriptional activity in yeast.* Genome Res, 2012. **22**(1): p. 84-94.

269. Nishimura, K., et al., *An auxin-based degron system for the rapid depletion of proteins in nonplant cells.* Nat Methods, 2009. **6**(12): p. 917-22.

270. Kanke, M., et al., *Auxin-inducible protein depletion system in fission yeast.* BMC Cell Biol, 2011. **12**: p. 8.

271. Mitsuzawa, H., E. Kanda, and A. Ishihama, *Rpb7 subunit of RNA polymerase II interacts with an RNA-binding protein involved in processing of transcripts.* Nucleic Acids Res, 2003. **31**(16): p. 4696-701.

272. Zilio, N., S. Wehrkamp-Richter, and M.N. Boddy, *A new versatile system for rapid control of gene expression in the fission yeast Schizosaccharomyces pombe.* Yeast, 2012. **29**(10): p. 425-34.

Abbreviations

5hmc	5-hydroxymethylcytosine
5mc	5-methylcytosine
AFM	Atomic force microscopy
AID	Auxin-inducible degron
ATP	Adenosintriphosphate
bp	Base pair
BSA	Bovine serum albumine
Ca^{2+}	Calcium
CAD	Caspase-activated DNase
CAGE	Cap analysis gene expression
CDS	Coding sequence
C. elegans	*Caenorhabditis elegans*
CENP-A	Centromere protein A
CHD	Chromodomain-helicase-DNA-binding
ChIP	Chromatin immunoprecipitation
CGI	CpG island
CK	Creatine kinase
CP	Creatine phosphate
CpG	Cytosine (followed by) guanine
CUT	Cryptic unstable transcript
DMSO	Dimethylsulfoxide
DNA	Deoxyribonucleic acid
DNase I	Deoxyribonuclease I
DNMT	DNA methyltransferase
dNTP	Deoxyribonucleotidetriphosphate

D. melanogaster	*Drosophila melanogaster*
DTT	Dithiothreitol
E. coli	*Escherichia coli*
EDTA	Ethylendiamintetraacetate
EGTA	Ethylenglycol-bis(2-aminoethyl)-N,N,N’,N’-tetraacetic acid
EM	Electron microscopy
EMM	Edinburgh minimal medium
EtOH	Ethanol
FRET	Fluorescence resonance energy transfer
h	Hour
H1/H2A/H2B/H3/H4	Histone proteins
HAT	Histone acetyltransferase
HDAC	Histone deacetylase
HEPES	N-(2-Hydroxyethyl)piperazine-H’-2-ethanesulfonic acid
HJURP	Holliday Junction-Recognizing Protein
HMT	Histone methyltransferase
IAC	Isoamylalcohol/chloroform
ICRE	Inositol/choline response element
INO80	Inositol auxotroph 80
ISWI	Imitation switch (*D. melanogaster*)
KMT	Lysine methyltransferase
IGR	Intergenic region
ISW1a/ISW1b/ISW2	Imitation switch (*S. cerevisiae*)
l	Liter
M	Molar
Mg^{2+}	Magnesium
min	Minute(s)
ml	Milli liter

mM	Milli molar
MNase	Micrococcal Nuclease
MWCO	Molecular weight cut off
NDR	Nucleosome depleted region
nm	Nano meter
nt	nucleotides
NRL	Nucleosome repeat length
OD	Optical density
O/N	over night
ORF	Open reading frame
PCR	Polymerase chain reaction
PIC	Preinitiation complex
PMSF	Phenylmethylsulphonylfluoride
Pol II	RNA-Polymerase II
PTM	Posttranslational modification
RNA	Ribonucleic acid
RNAi	RNA interference
RNase A	Ribonuclease A
RSC	Remodels the structure of chromatin
rpm	Revolutions per minute
RT	Room temperature
SAXS	Small-angle X-ray scattering
S. cerevisiae	*Saccharomyces cerevisiae*
SDS	Sodium dodecyl sulfate
S. pombe	*Schizosaccharomyces pombe*
Sth1	Snf two homologous 1
SWI/SNF	Switch/sucrose non-fermenting
SWR1	Swi2/Snf2-related 1
TAE	Tris acetate EDTA buffer

TET	Ten-eleven translocation
TdT	Terminal deoxynucleotidyl transferase
Tris	Tris(hydroxymethyl)aminomethane
ts	Temperature-sensitive
TSS	Transcription start site
TTS	Transcription termination site
U	Unit
USAXS	Ultrasmall-angle X-ray scattering
UV	Ultraviolet
v/v	Volume per volume
WGD	Whole genome duplication
wt	Wildtype
w/v	Weight per volume
YAC	Yeast artificial chromosome

Curriculum vitae

Julia Pointner

Birth name:	Jakubsche
Date of birth:	November 12th 1983
Place of birth:	München

Education

03/2010 - present	**PhD thesis at the Ludwig-Maximilians-University of Munich, Prof. Dr. Peter Becker, Group of Dr. Philipp Korber** Project: Genome-wide identification of nucleosome positioning determinants in *Schizosaccharomyces pombe*
04/2009 – 12/2009	**Diploma thesis at the University of Edinburgh, Wellcome Trust Centre for Cell Biology, Group of Prof. Dr. William C. Earnshaw** Project: Manipulating the chromatin state of the centromere of a human artificial chromosome
10/2006 – 12/2009	**Studies of Biology at the Ludwig-Maximilians-University of Munich** Hauptstudium
10/2004 – 09/2006	**Studies of Biology at the University of Regensburg** Grundstudium
09/1994 – 06/2003	**Secondary school: Ernst-Mach-Gymnasium Haar** Abitur

Publications

Pointner J., Persson J., Prasad P., Norman-Axelsson U., Stralfors A., Khorosjutina O., Krietenstein N., Svensson J.P., Ekwall K., Korber P. 2012. CHD1 remodelers regulate nucleosome spacing in vitro and align nucleosomal arrays over gene coding regions in *S. pombe*. *EMBO J.*, 31(23):4388-403

Bergmann J.H., **Jakubsche J.N.**, Martins N.M., Kagansky A., Nakano M., Kimura H., Kelly D.A., Turner B.M., Masumoto H., Larivonov V., Earnshaw W.C. 2012. Epigenetic engineering: histone H3K9 acetylation is compatible with kinetochore structure and function. *J Cell Sci*, 125(Pt2):411-21